Supplement of Atmos. Chem. Phys., 24, 9459–9473, 2024
https://doi.org/10.5194/acp-24-9459-2024-supplement


Atmospheric Chemistry and Physics
Open Access

*Supplement of*

# Formation and temperature dependence of highly oxygenated organic molecules (HOMs) from $\Delta^3$-carene ozonolysis

**Yuanyuan Luo et al.**

*Correspondence to:* Yuanyuan Luo (yuanyuan.luo@helsinki.fi) and Mikael Ehn (mikael.ehn@helsinki.fi)

**S1. Details for chamber facilities**

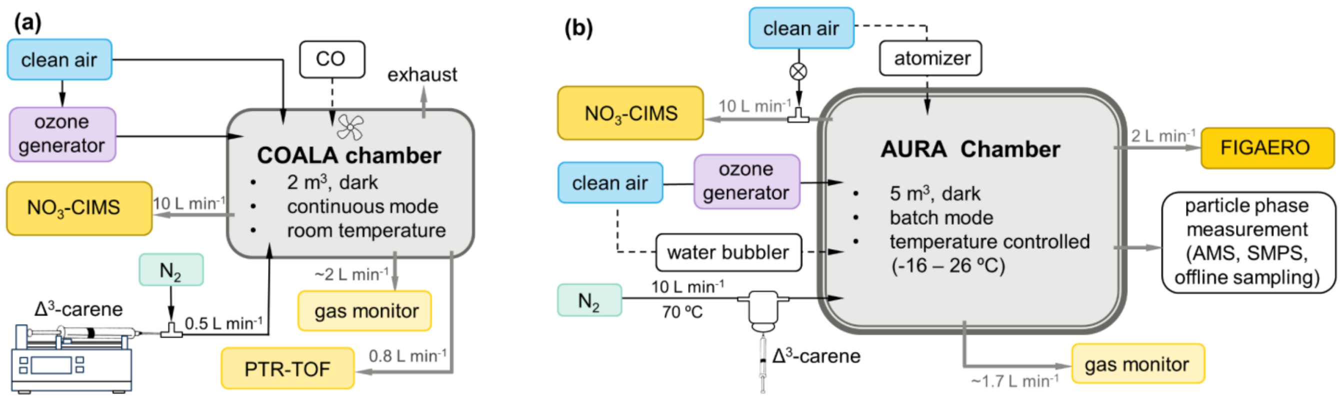


**Figure S1. Experimental set-ups. The set-up of experiments conducted in the COALA chamber is shown in panel (a), while the set-up in the AURA chamber is shown in panel (b). The dashed lines represent injections only used for specific experiments.**

**COALA chamber**

The COALA chamber is a 2 $m^3$ Teflon reactor, which is maintained at room temperature (25 ± 1℃) and under dry conditions with RH < 1%. To prevent contamination from external sources, the chamber was operated at a slightly elevated pressure (~3 Pa). More details of the COALA chamber can be found in Riva et al. (2019). During this campaign, the chamber was run in continuous mode with a total inflow of 40 L $min^{-1}$ (average residence time: ~50 min). Each experiment ran for a minimum of 140 minutes, allowing the chamber to reach a steady state. For a more in-depth discussion about the dynamics of our continuous mode "steady-state" chamber, see Peräkylä et al. (2020). Purified dry air was injected into the chamber as the main inflow, while ozone was generated and injected by passing 5 L $min^{-1}$ purified air through a Dasibi 1008-PC ozone generator. $\Delta^3$-carene or α-pinene (for comparison) was introduced using a syringe pump with a 0.5 L $min^{-1}$ nitrogen flow as the carrier gas. The injection rate of VOC or the strength of the ozone generator was adjusted to achieve different oxidation conditions in the chamber. In some experiments (Table S1), approximately 200 ppm of CO from a gas bottle was introduced to the chamber as an OH scavenger. The majority of the outflow from the chamber was sampled by instruments, while the remaining flow was flushed out as exhaust. A schematic of the COALA chamber setup is shown in Figure S1(a).

Measurements of temperature, RH, and pressure inside the chamber were obtained using a Vaisala temperature and humidity probe (INTERCAP® HMP60) and a differential pressure sensor (Sensirion SDP1000-L025). To monitor the precursors and oxidation products of $\Delta^3$-carene ozonolysis, two state-of-the-art mass spectrometers were utilized. A proton transfer reaction time-of-flight mass spectrometer (PTR-TOF 8000, Ionicon Analytik GmbH) was deployed to measure VOC concentrations, calibrated before the experiments directly with a mixture of VOCs, including monoterpenes. A chemical ionization atmospheric pressure interface time-of-flight mass analyser (CIMS, Tofwerk AG/Aerodyne Research, Inc.) was employed to probe oxygenated products from $\Delta^3$-carene ozonolysis, with a primary focus on HOMs. Nitric acid ($HNO_3$) and an X-ray source were used to produce nitrate reagent ions ($NO_3^-$) for the CI inlet. The equipped long TOF analyser enables the measurement of ions within the HOM region (m/z 300 – 600 Th) with a mass resolving power of ~8000 Th. During the experiments, the $NO_3$-CIMS continuously sampled chamber flow at a rate of 10 L min$^{-1}$ and recorded averaged mass spectra every 10 s. The data from both PTR-TOF and $NO_3$-CIMS were pre-processed using the tofTools MATLAB package (version 612). Chamber background was determined during the period before VOC injection in each experiment. All data collected in the COALA chamber, unless specified otherwise, were subtracted with chamber background and averaged to 10 min resolution. Further technical details and instrument specifications have been presented by Jordan et al. (2009) and Jokinen et al. (2012) for PTR-TOF and $NO_3$-CIMS, respectively.

**Table S1. Experimental conditions for $\Delta^3$-carene (a) and α-pinene (b) ozonolysis conducted in the COALA chamber. For all experiments, the chamber was run in continuous mode at room temperature (25 ± 1°C) and under dry conditions (RH < 1%).**

| (a) | Date | Experiment | injected $\Delta^3$-carene (ppb) | injected $O_3$ (ppb) | injected CO (ppm) |
|---|---|---|---|---|---|
| | 2023-2-9 | 1 | 10±1 | 30±2 | |
| | | 2 | 20±2 | 30±2 | |
| | | 3 | 20±2 | 30±2 | ~200 |
| | | 4 | 30±2 | 30±2 | ~200 |
| | | 5 | 30±2 | 30±2 | |
| | 2023-2-10 | 6 | 10±1 | 30±2 | |
| | | 7 | 30±2 | 30±2 | |
| | | 8 | 30±2 | 50±3 | |
| | 2023-2-11* | 9 | 30→0 | 30±2 | |
| | 2023-2-13 | 10 | 20±2 | 30±2 | |
| | 2023-2-14 | 11 | 20±2 | 30±2 | ~200 |

| (b) | Date | Experiment | injected α-pinene (ppb) | injected $O_3$ (ppb) | injected CO (ppm) |
|---|---|---|---|---|---|
| | 2023-2-6 | 12 | 20±2 | 30±2 | |
| | | 13 | 25±1 | 45±1 | |
| | 2023-2-7 | 14 | 50±2 | 60±1 | |
| | | 15 | 50±2 | 60±1 | |
| | 2023-2-8 | 16 | 45±2 | 13±1 | |
| | | 17 | 45±2 | 13±1 | ~200 |
| | | 18 | 45±2 | 13±1 | |
| | 2023-2-14 | 19 | 20±2 | 30±2 | |
| | | 20 | 20±2 | 30±2 | ~200 |

* The $\Delta^3$-carene in the syringe ran out at around 10:40 am, causing the injection of $\Delta^3$-carene decreased from ~30 ppb to 0 ppb gradually afterwards.

## AURA chamber

**Table S2. Experimental conditions for Δ$^3$-carene ozonolysis experiments conducted in the AURA chamber. Δ$^3$-carene and $O_3$ are the starting concentrations of VOC and $O_3$ at experiment time = 0 min, respectively.**

| Date | Experiment | Δ$^3$-carene (ppb) | $O_3$ (ppb) | T (°C) | RH (%) | NO$_3$-CIMS condition: flow from chamber* (L min$^{-1}$) | NO$_3$-CIMS condition: Setting# |
|---|---|---|---|---|---|---|---|
| 2022-1-11 | 20A | 10±5 | 181±15 | 20.2±0.1 | 0±0 | 5 | 1 |
| 2022-1-13 | 10A | 10±5 | 174±15 | 10.1±0.1 | 0±0 | 5 | 1 |
| 2022-1-24 | 10D | 10±5 | 174±15 | 10.2±0.1 | 78±2 | 10 | 2 |
| 2022-1-31 | 10E | 20±5 | 169±15 | 10.2±0.1 | 76±1 | 10 | 2 |
| 2022-2-2 | 0A | 10±5 | 159±15 | 0.1±0.1 | 1.6±1.6 | 10 | 3 |
| 2022-2-4 | 10B | 10±5 | 171±15 | 10.1±0.1 | 0.4±0.8 | 10 | 3 |
| 2022-2-5 | 20B | 10±5 | 181±15 | 20.2±0.1 | 0±0 | 10 | 3 |

* The total inlet flow of $NO_3$-CIMS was 10 L min$^{-1}$ for all experiments, and the flow from chamber shows the proportion of the total inlet flow sampled directly from the chamber.

# During the AURA chamber campaign, the settings of $NO_3$-CIMS was modified three times. Setting 1 was the original setting. In Setting 2, the TofDaq setting was kept the same as in Setting 1, but the TPS setting was adjusted. In Setting 3, the TPS setting remained the same as in Setting 2, while the ToFDaq setting was altered. By rapidly switching between Setting 2 and Setting 3 at some point during the experiments, a correction factor of 2.43 was determined for Setting 2 to enable comparability of the data collected using this setting with that obtained using Setting 3.

The AURA chamber is a 5 m$^3$ Teflon chamber situated in a temperature-controlled room (temperature range: -16 – 26 °C). A detailed description of the AURA chamber can be found in Kristensen et al. (2017). The setup of the AURA chamber is illustrated in Figure S1(b). Throughout the campaign, the AURA chamber was run in batch mode, meaning the sources and sinks for products were progressively accumulated from the beginning of each experiment. For each experiment, the chamber was first filled with purified air, and a specific amount of water vapour and $O_3$ were injected to achieve the desired RH and $O_3$ levels. The experiment commenced with the introduction of 10 or 20 ppb Δ$^3$-carene into the chamber, marking the time as experiment time = 0 min. The conditions of the ozonolysis experiments conducted in the AURA chamber are briefly summarized in Table S2, while a comprehensive description of the experiments can be found in Thomsen et al. (2024). In general, the HOM formation of Δ$^3$-carene ozonolysis was examined under dry conditions (RH < 15%) at 20 °C (20A & B), 10 °C (10A & B), and 0 °C (0A), and twice under humid conditions (RH = 80%) at 10 °C with two different Δ$^3$-carene loadings (10D: 10 ppb and 10E: 20 ppb).

As shown in Figure S1(b), instruments for both gas-phase and particle-phase measurements were utilized. Particle size distributions were determined using a scanning mobility particle sizer (SMPS, TSI Incorporated), while the chemical composition of the aerosols was analysed with a high-resolution time-of-flight aerosol mass spectrometer (AMS, Aerodyne Research, Inc., DeCarlo et al. (2006)), and a filter-inlet for gases and aerosols chemical ionization mass spectrometer (FIGAERO, Lopez-Hilfiker et al. (2014)). Additionally, particles were continuously collected with a sequential spot sampler (Series 110 A, Aerosol Devices, Eiguren Fernandez et al. (2014); Eiguren-Fernandez et al. (2014)) for detailed offline analysis using an ultra-high-performance liquid chromatography (UHPLC) coupled with a quadrupole time-of-flight mass spectrometry (QTOF-MS, Compact, Bruker). For HOM measurement, a $NO_3$-CIMS with a long TOF analyser (Tofwerk AG/Aerodyne Research, Inc.) was employed (Jokinen et al., 2012). The inlet flow rate of the $NO_3$-CIMS was 10 L $min^{-1}$ for all experiments listed in Table S2. However, for 20A and 10A experiments, a dilution flow of purified air (5 L $min^{-1}$) was added to the sample flow from the chamber (5 L $min^{-1}$), while the total 10 L $min^{-1}$ of the inlet flow was from the chamber for the remaining experiments. Due to unknown instrumental issues causing a dramatic decrease in sensitivity, certain voltage and acquisition settings of the $NO_3$-CIMS had to be manually adjusted during the campaign to improve the signal strengths. This adds additional uncertainties to our ability to compare different experiments. Some key parameters of the instrument in each experiment are shown in Figure S2. By rapidly switching between Setting 2 and 3 at certain points during the experiments, a correction factor of 2.43 was estimated for scaling data collected with Setting 2 to data collected with Setting 3 (Figure S3). The $NO_3$-CIMS data were pre-processed with the tofTools MATLAB package (version 612). Chamber background was determined during the period before VOC injection in each experiment, and the all $NO_3$-CIMS data were after background subtraction.

This study is exclusively concentrated on the formation of HOMs from $\Delta^3$-carene ozonolysis in the gas phase. For further insights into particle phase properties and composition, detailed analyses using AMS, SMPS, and UHPLC-QTOF-MS are provided in the work of Thomsen et al. (2024). Additionally, research on the partitioning of volatile organic compounds, employing the FIGAERO, is extensively discussed in the study by Li et al. (2024).

**Continuous vs. batch-mode chamber**

Continuous and batch modes are commonly employed in environmental chamber studies to investigate atmospheric processes. In continuous mode, exemplified by the COALA chamber in our study, there is a constant inflow of air with steady concentrations of reactants, matched by an equal total outflow. The balance between sources and sinks allows the chamber to reach a steady state, characterized by consistent concentrations of precursors and products. The duration to achieve steady state primarily depends on the total inflow rate

In contrast, the batch mode, as demonstrated by the AURA chamber in this study, involves introducing a fixed amount of reactants into a clean chamber all at once, with no additional inflow during the experiment. This leads to a high initial concentration of precursors that diminishes over time due to chemical reactions and physical processes, with product concentrations accumulating progressively. As the instrument continued sampling, the volume of the Teflon bag decreased throughout the experiment. The estimated volume fraction used in the chamber bag was 50% for each experiment. Batch mode, however, requires careful consideration of mixing to prevent the formation of local hot spots and ensure homogeneity.

Continuous mode offers the advantage of studying reaction dynamics under stable conditions, reducing the effects of local concentration disparities and ensuring a uniform reaction environment over time, while batch mode effectively simulates abrupt atmospheric events and allows for the examination of the aging process over longer periods.

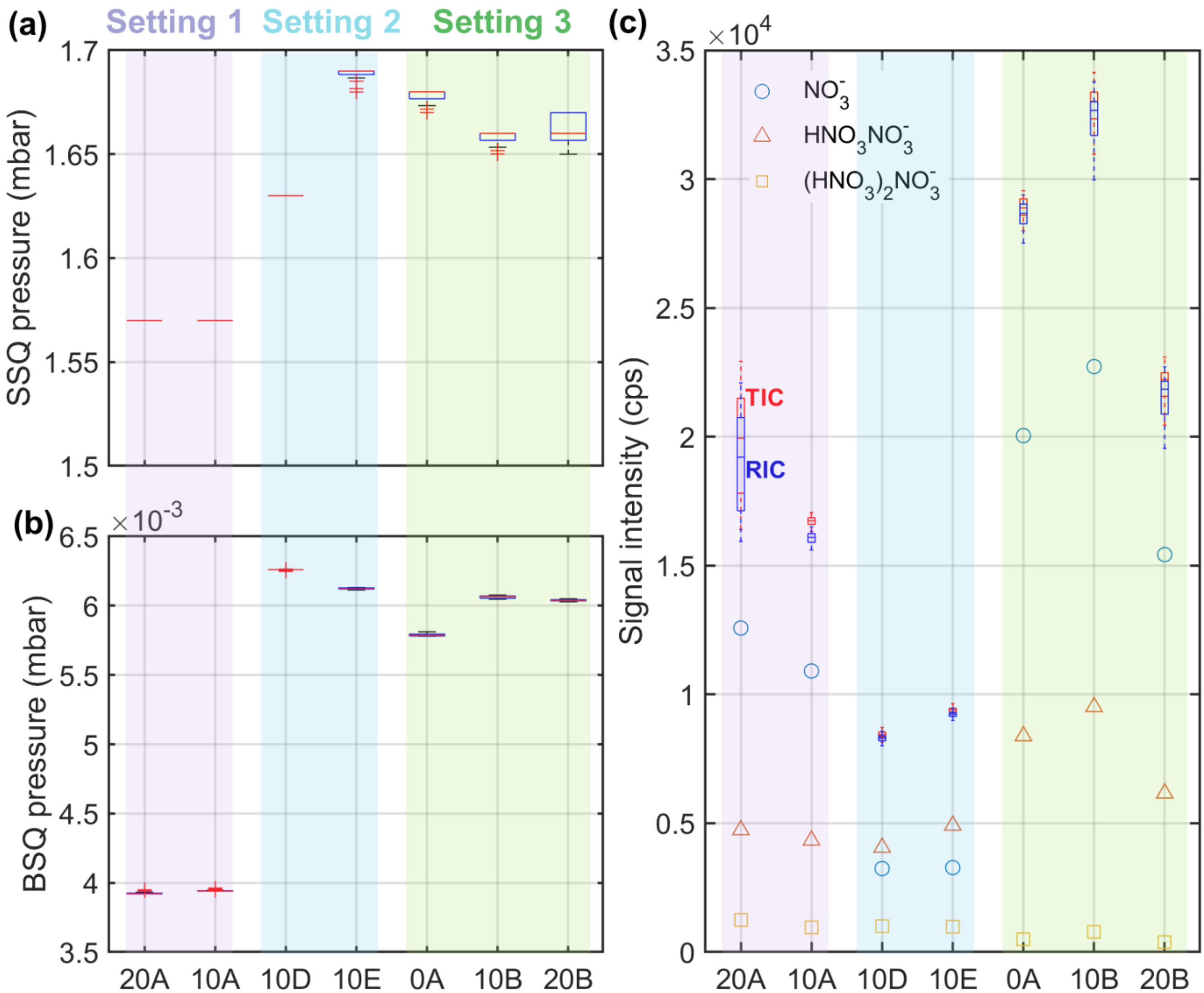


**Figure S2. $NO_3$-CIMS pressures in the (a) SSQ and (b) BSQ chambers, and (c) signal counts of different experiments conducted in the AURA chamber. Box plots in panel (c) show averages of the sum of all ion signals (TIC: red) and the sum of all reagent ion signals (RIC: blue). Signal intensities of reagent ions are also shown separately with different markers in panel (c). The colours of shaded areas in all panels represent different settings of $NO_3$-CIMS.**

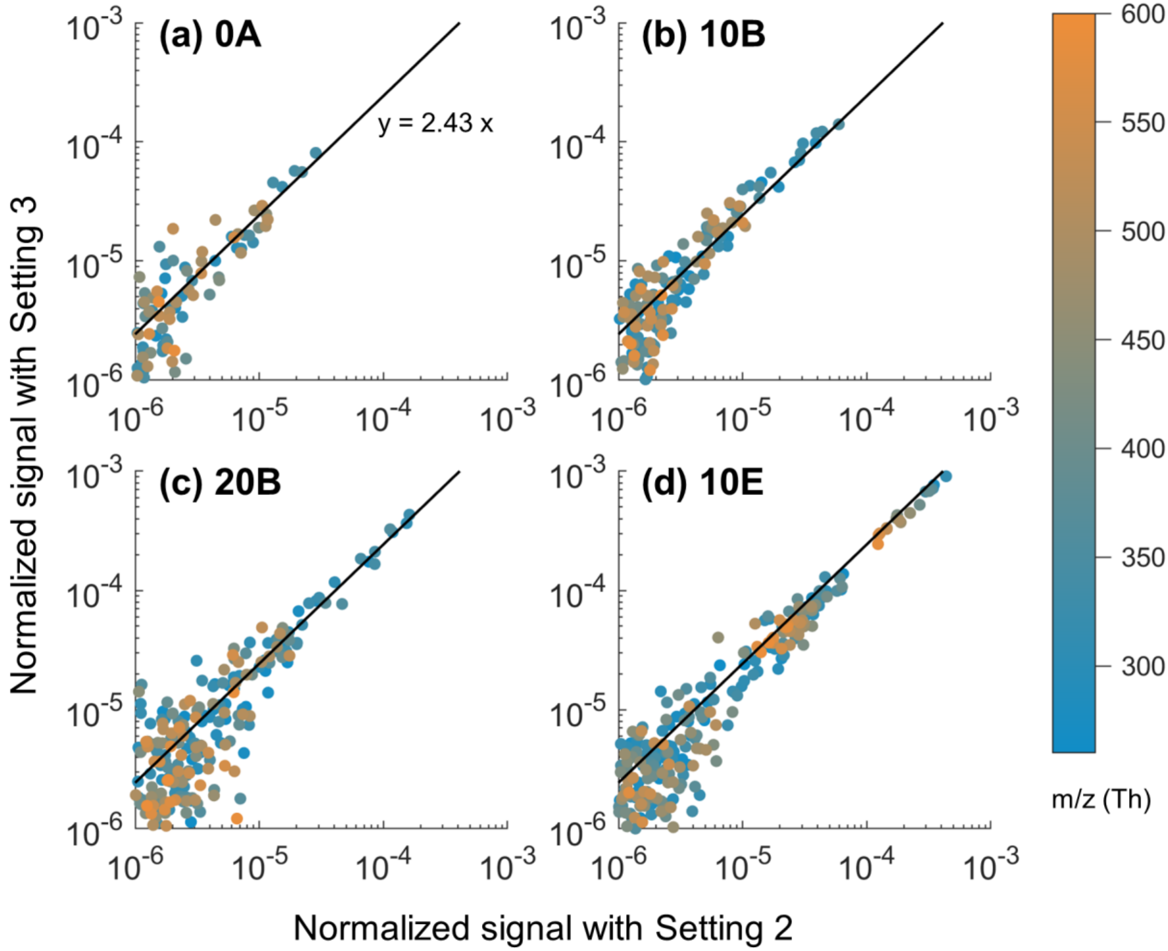


**Figure S3. Scatter plot of the normalized signal intensity with Setting 2 and Setting 3. The colour shows the mass-to-charge ratio in the spectra where the compound was identified. The black solid lines indicate y : x=2.43. For experiments 0A, 10B, 20B and 10E in the AURA chamber, after the experiments had been running for around 70-80 min, the TofDaq settings of the instrument were quickly switched to the another (Setting 3 to 2 for 0A, 10B, and 20B; Setting 2 to 3 for 10E) to collect data for 5-10 minutes. As the change of the products was slow at that time, the difference in the signal intensities was mainly caused by the change of the setting. We estimated a factor of 2.43 to convert the data collected with Setting 2 to Setting 3 based on the averaged slope of the linear fit.**

**S2. HOM dynamics and yield estimates**

The rate of change in HOM concentration within a chamber can be expressed as:

$$\frac{d[HOM]}{dt} = Production_{HOM} - Loss_{HOM} \quad (S1)$$

Where $Production_{HOM}$ and $Loss_{HOM}$ are the total production and loss rates of HOMs, respectively. [HOM] is the concentration of HOMs in the chamber, which can be estimated as:

$$[HOM] = C \times \frac{\sum_i HOM_i \cdot NO_3^-}{NO_3^- + HNO_3NO_3^- + (HNO_3)_2NO_3^-} \quad (S2)$$

Here, C is a calibration factor, and in this study, a value of $C=1\times10^{10}$ $cm^{-3}$ was used based on typical values reported earlier (Ehn et al., 2014; Jokinen et al., 2012; Jokinen et al., 2014). $HOM_i \cdot NO_3^-$ is the signal intensity of a cluster of HOM species with $NO_3^-$, and $(HNO_3)_jNO_3^-$ (j=0,1,2) is the signal intensity of reagent ions measured by $NO_3$-CIMS. Note that the $NO_3$-CIMS was not calibrated in this study, and therefore quantification of HOMs has a very large uncertainty, estimated to be at least a factor of 3. The ionization of HOMs with the $NO_3$-CIMS is expected to be collision-limited, i.e. HOMs collide with $NO_3^-$ forming clusters irreversibly, which is why we can roughly estimate the instrument sensitivity even without a direct calibration (Ehn et al., 2014). Nevertheless, the large uncertainty must always be kept in mind when interpreting the data.

For HOM formation during $\Delta^3$-carene ozonolysis, the production rate of HOMs can be written as $k_1\gamma[carene][O_3]$, where $k_1$ is the carene-$O_3$ reaction rate coefficient, $\gamma$ is the HOM molar yield, [carene] is the $\Delta^3$-carene concentration, and $[O_3]$ is the ozone concentration. The losses of HOMs arise from condensation on the chamber walls and particles, and flush-out from the chamber (in the case of a continuous-mode chamber). The total loss rate of HOMs can be represented as $k_{loss}[HOM]$, where $k_{loss}$ is the total loss rate of HOMs.

The COALA chamber was operated in continuous mode, meaning that the inflow of all gases and VOCs was constant. When the chamber reached a steady state, the concentrations of all reactants and products should be constant as well. Therefore, the Equation S1 can be written as:

$$\frac{d[HOM]}{dt} = k_1\gamma[carene][O_3] - k_{loss}[HOM] = 0 \quad (S3)$$

$$\Rightarrow \gamma = \frac{k_{loss}[HOM]}{k_1[carene][O_3]} \quad (S4)$$

Since no seed particles were injected in the COALA chamber, and the dataset suggested none or only a negligible amount of particles were formed, the total loss rate of HOMs was mainly driven by loss to the walls and flush-out. The $k_{loss}$ was determined to be ~ 0.0025 $s^{-1}$ in the COALA chamber. This determination was achieved by modelling the decay of HOMs using a simple box model after the removal of $O_3$ and $\Delta^3$-carene injection at the end of experiment 11. The $k_1$ was reported to be $3.7\times10^{-17} cm^3 s^{-1}$ at room temperature by Chen et al. (2015).

The AURA chamber was operated in batch mode, meaning that the concentrations of products depended on the cumulative sources and sinks within the chamber. The temporal change in HOM concentrations was not zero, therefore Equation S1 can be written as:

$$\gamma = \frac{k_{loss}[HOM] + \frac{d[HOM]}{dt}}{k_1[carene][O_3]} \tag{S5}$$

We observed particle formation for all experiments in the AURA chamber, and thus the loss of HOMs ($k_{loss}$) also included the condensation on particles (CS) in addition to the chamber walls ($k_{wall}$). We used the method reported by Tuovinen et al. (2021) to estimate CS for HOM monomers and dimers separately for each experiment, and the loss rate to the chamber wall $k_{wall}$ is constant across one experiment and assumed to less than the order of $10^{-3} s^{-1}$ (Quéléver et al., 2019). The time series of typical CS for HOM monomers and dimers and wall loss across one experiment are shown in Figure S4. Since the temperature-dependent reaction rate of $\Delta^3$-carene ozonolysis has not yet been experimentally determined, in this study, we assumed that the temperature dependence of $k_1$ is the same as that for α-pinene in MCM: $3.7\times10^{-16} \exp\left(-\frac{640}{T}\right) cm^3 s^{-1}$, where T represents the chamber temperature. The estimated $k_1$ at 300 K aligns with the measured value reported by Hantschke et al. (2021). With Equation S5, the molar yield of HOMs can be derived as the slope of a linear fit when we plot $k_1[carene][O_3]$ on the x axis and $k_{loss}[HOM] + \frac{d[HOM]}{dt}$ on the y axis. The period we used for HOM estimation is from experiment time = ~20 min to 180 min.

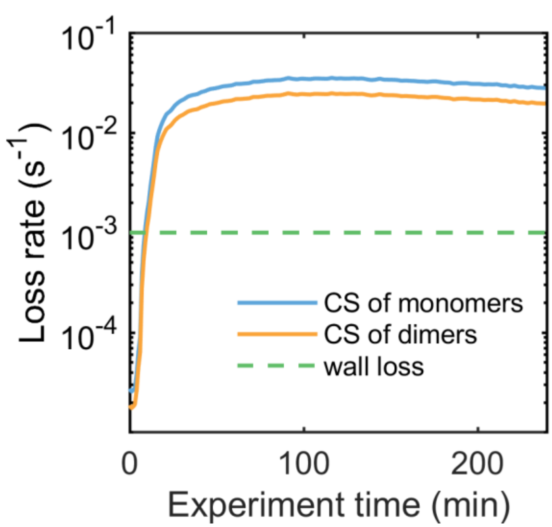


**Figure S4. Estimated condensation sink from particles and wall loss rate for HOMs in the 20B experiment in the AURA chamber.**

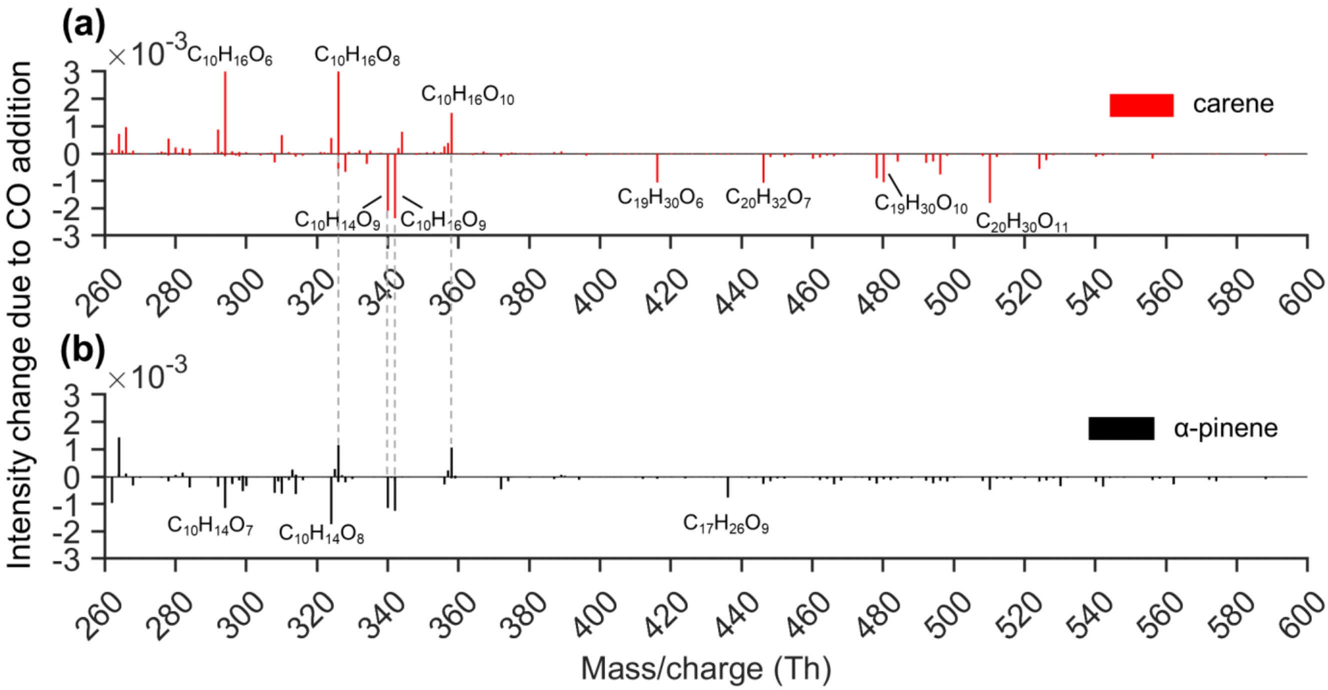


**Figure S5. Differential spectrum (diff-spectrum) of (a) carene ozonolysis and (b) α-pinene ozonolysis after CO injection (diff-spectrum = spectrum with CO presence – spectrum before CO injection). The high resolution (HR) the mass spectra from carene and α-pinene ozonolysis were collected under the same conditions (VOC = 20 ppb, $O_3$ = 30 ppb). All peaks labelled here were detected as a cluster with $NO_3^-$. Grey dashed lines mark some of the products with the same formulas detected in carene and α-pinene ozonolysis experiments.**

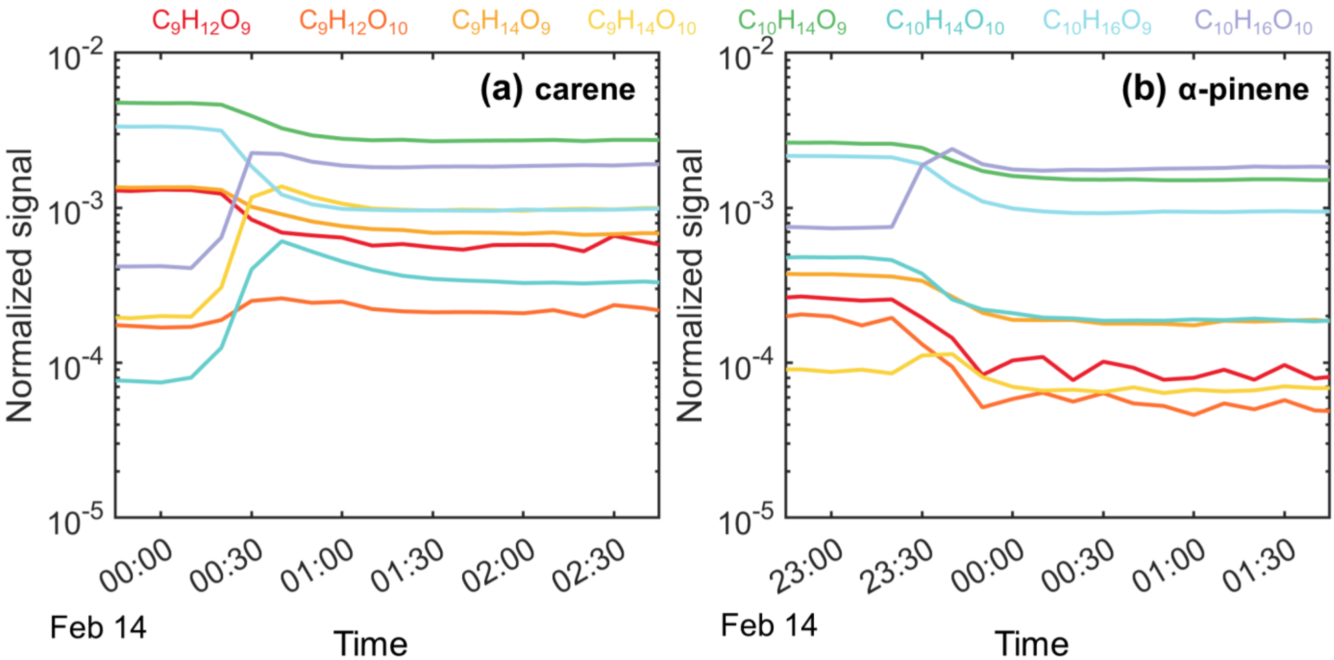


**Figure S6. Time series of the selected HOMs after injecting CO into (a) the carene ozonolysis system and (b) the α-pinene ozonolysis system in the COALA chamber.**

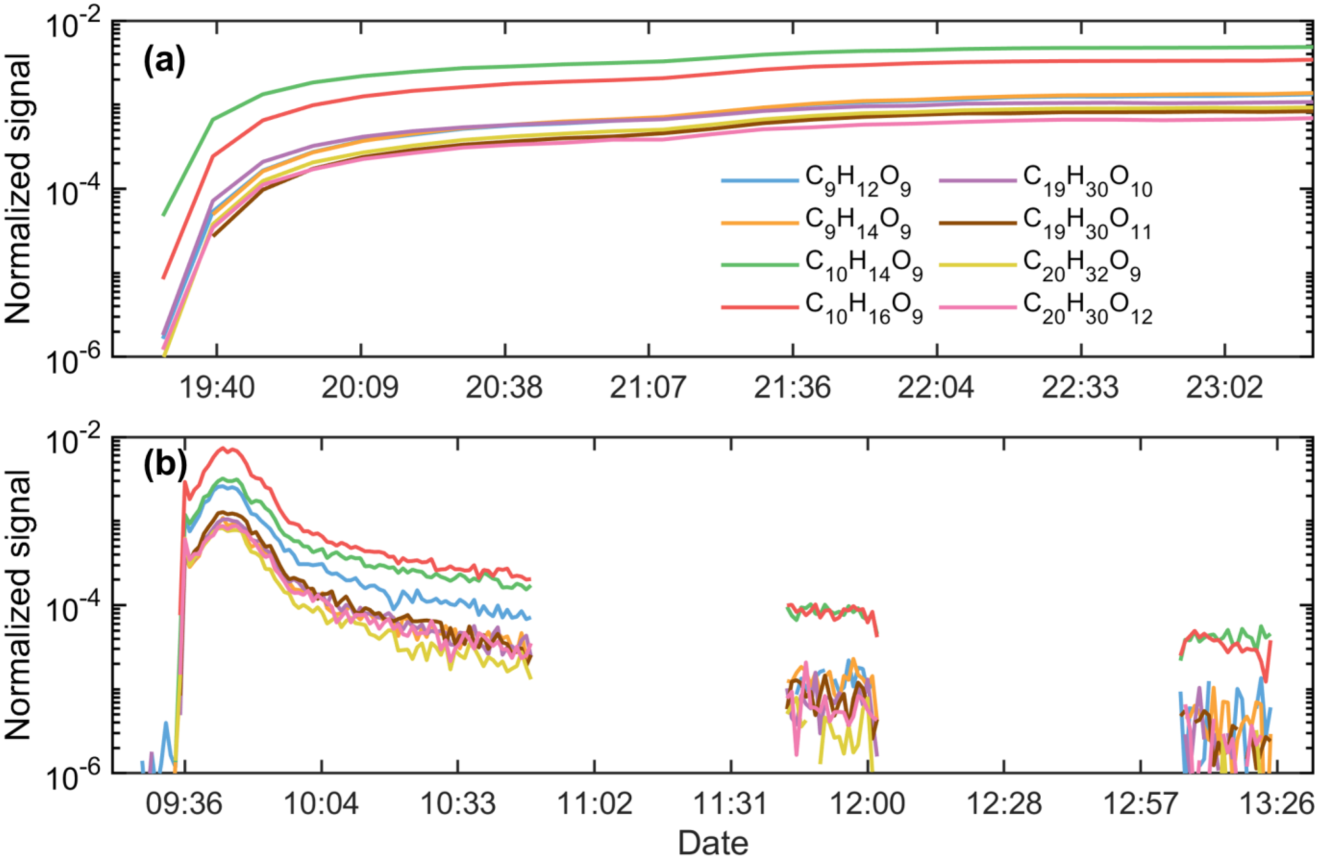


**Figure S7. Time series of the selected HOMs in (a) the COALA chamber (Experiment 10) and (b) the AURA chamber (20B).**

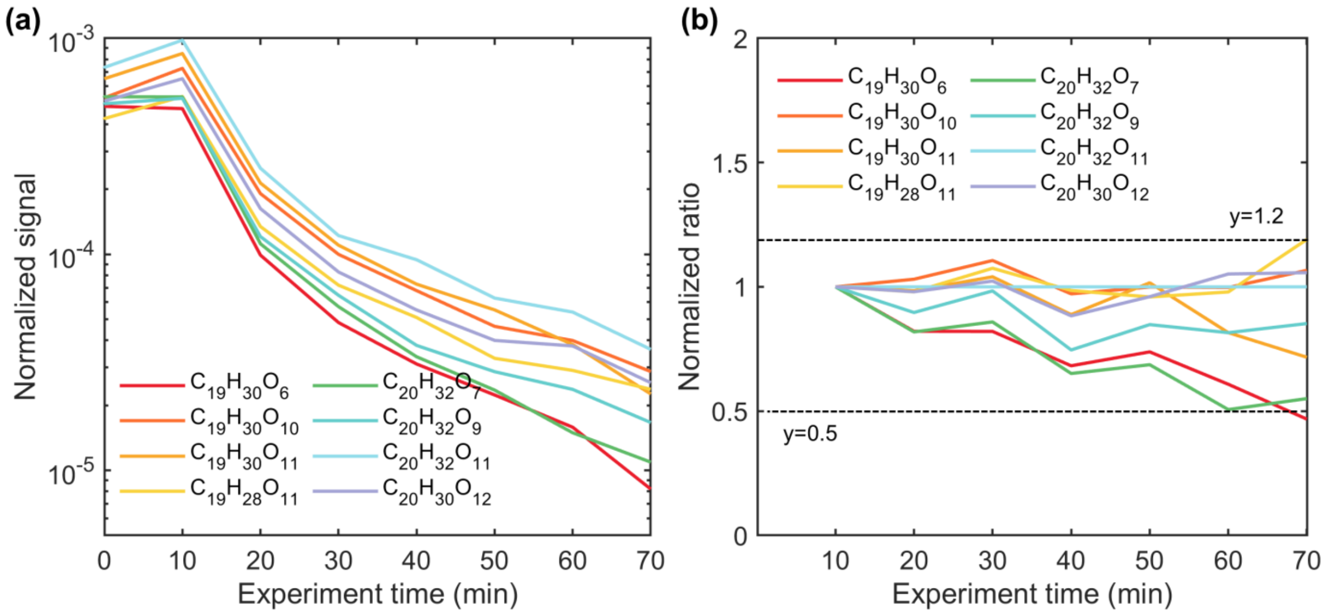


**Figure S8. (a) Normalized signal intensity of the largest 8 HOM dimers and (b) the temporal behaviours of the normalized ratios of these dimers (M) to the reference dimer ($C_{20}H_{32}O_{11}$) during the 20B experiment in the AURA chamber. The "normalized ratio" on the y-axis was determined by first calculating the ratio M:$C_{20}H_{32}O_{11}$ at each time point, and this ratio was then normalized by dividing it by the ratio value at experiment time = 10 min.**

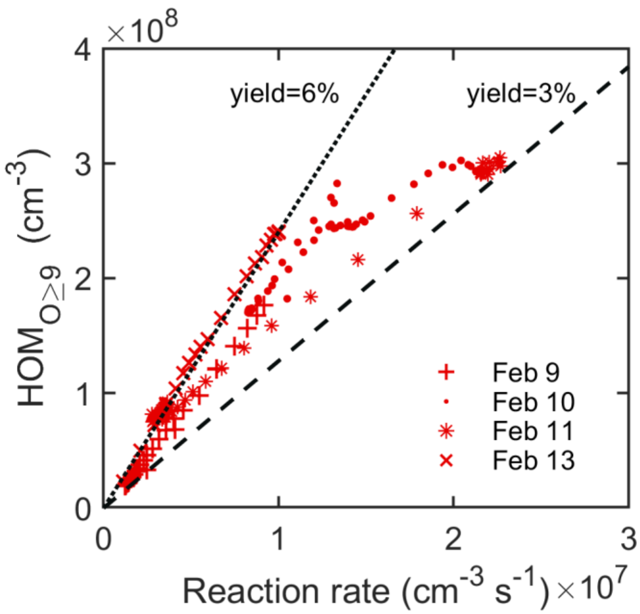


**Figure S9. Molar yield of $HOM_{O\geq9}$ (the sum of HOM monomers with no fewer than 9 O-atoms and all HOM dimers (O-atoms ≥ 6)) from Δ[3]-carene ozonolysis in the COALA chamber at room temperature. Dotted and dashed lines represent the upper and lower limits of the estimated $HOM_{O\geq9}$ yields.**

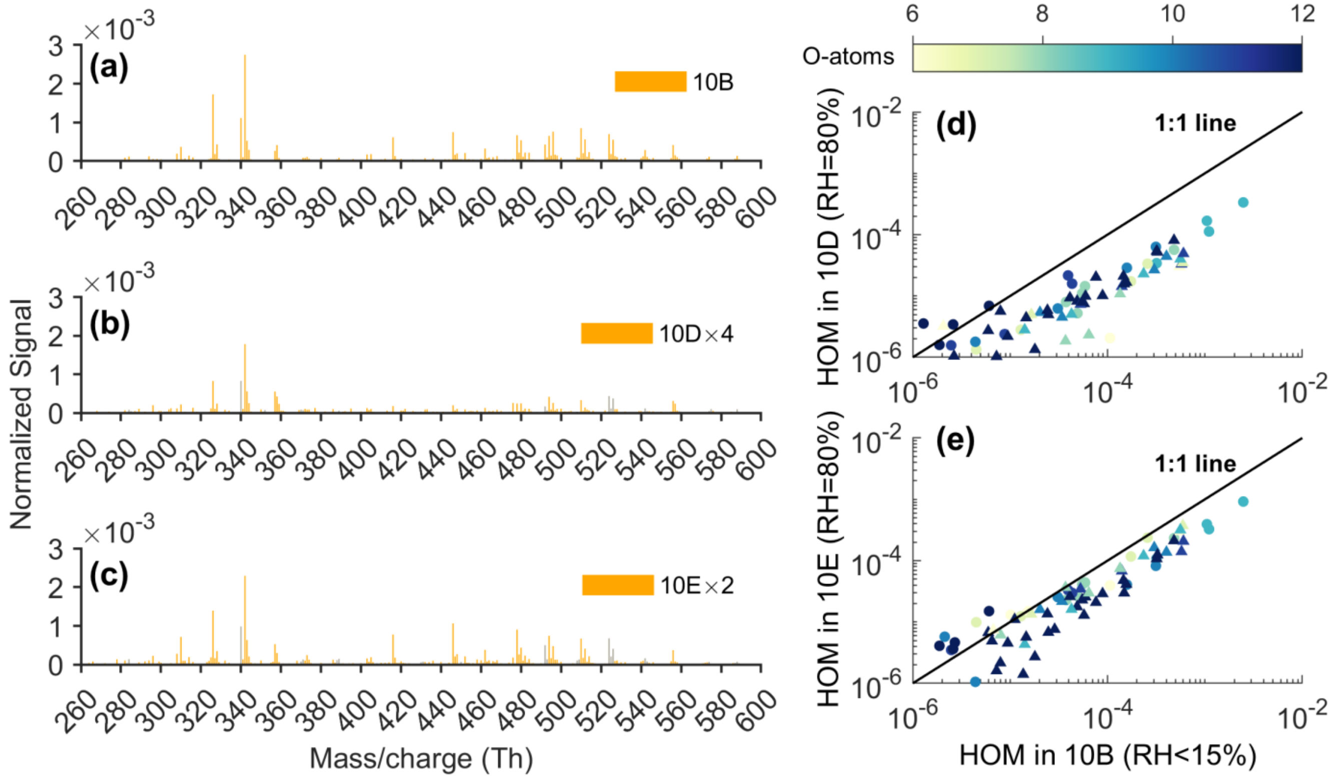


**Figure S10. Panels (a)-(c): UMR (unit-mass resolution) mass spectra from 10B (RH < 15%), 10D, and 10 E (RH = 80%) carene ozonolysis experiments in the AURA chamber. The grey bars are the water clusters. Panels (d)-(e): Scatter plot of the normalized HOM signal intensity from the dry condition experiment (10B) and two high humidty experiments (10D and 10E). The signal intensities were multiplied by 4 and 2 in panels (b) and (c), respectively. The circles represent HOM monomers, and the triangles represent HOM dimers. The colour indicates the O-atom content in the identified species.**

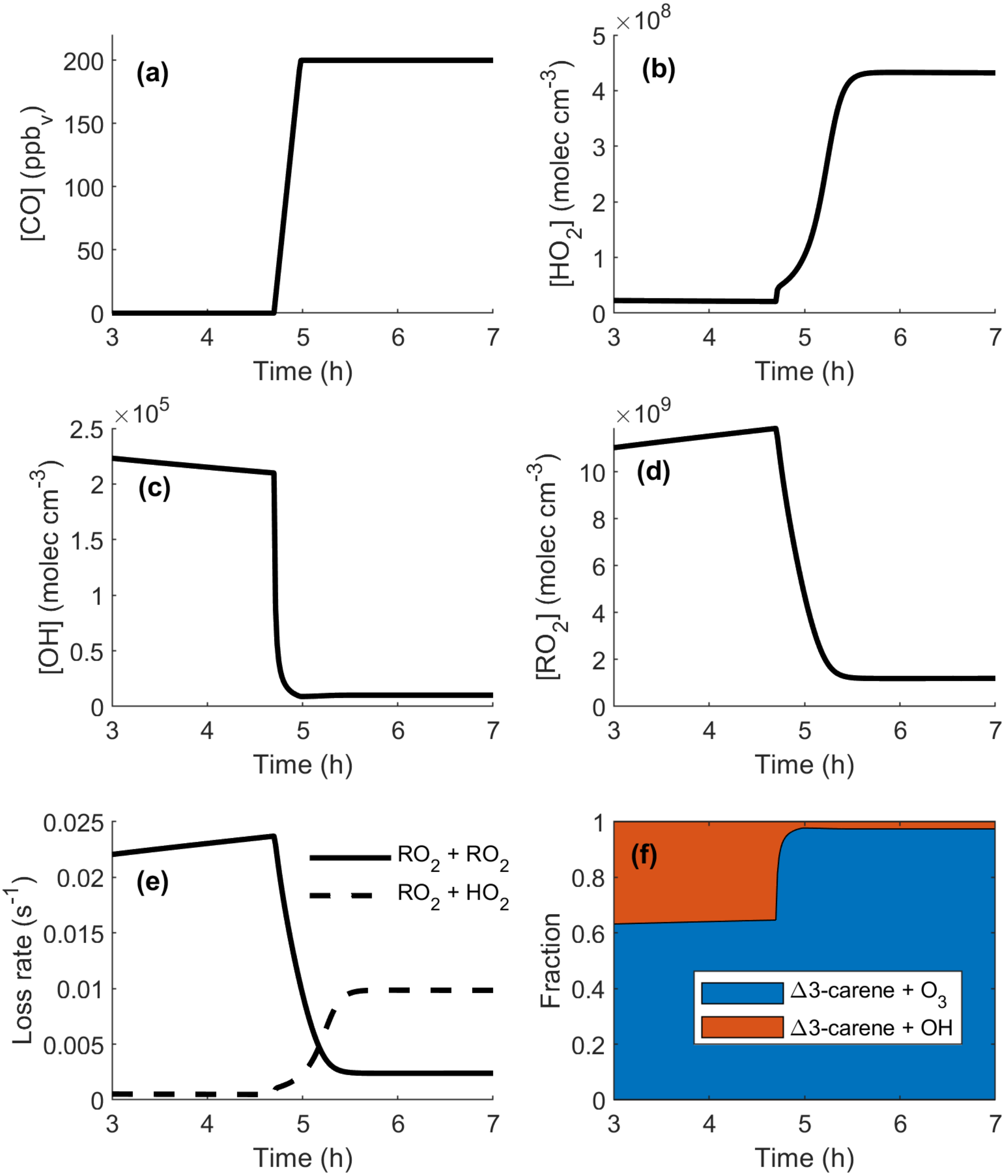


**Figure S11. Modelled CO, $HO_2$, OH, and total $RO_2$ concentrations during the COALA $\Delta^3$-carene ozonolysis experiment with CO addition after ~5 hours (Experiment 10 and 11). Panel (e) shows the modelled loss rate of PRAM $RO_2$ species due to reactions with $RO_2$ and $HO_2$ respectively. Panel (f) shows the modelled fraction of $\Delta^3$-carene that react with ozone and OH, respectively.**

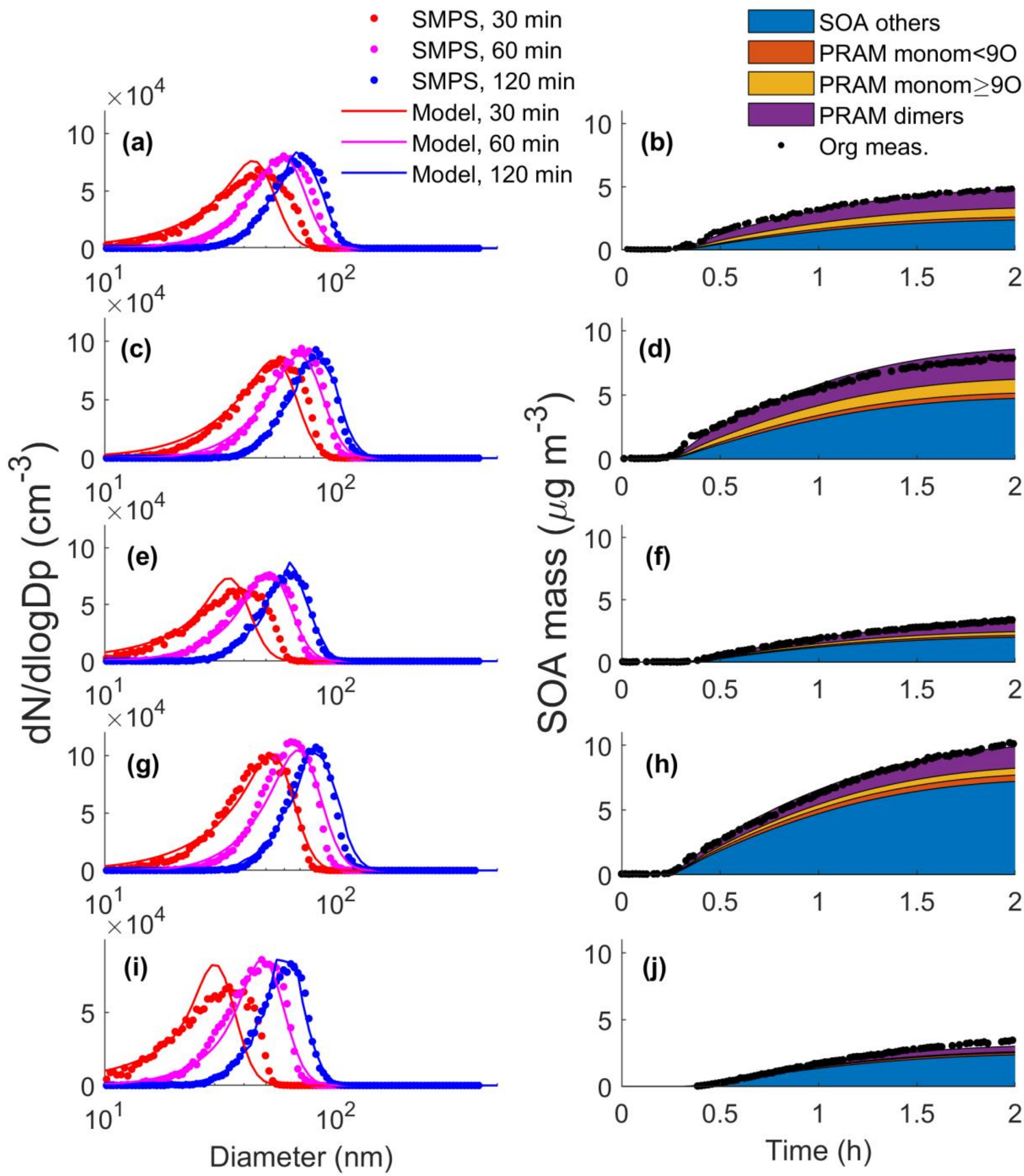


**Figure S12. Modelled and measured particle number size distributions and SOA mass concentrations for five different AURA experiments. Panels (a)–(b) show results from exp. 20A (T = 20 °C, estimated initial [$\Delta^3$-carene] = 9 ppb), panels (c)–(d) results from exp. 20B (T = 20 °C, estimated initial [$\Delta^3$-carene] = 13.5 ppb), panels (e)–(f) results from exp. 10A (T = 10 °C, estimated initial [$\Delta^3$-**

**carene] = 6.5 ppb), panels (g)–(h) results from exp. 10B (T = 10 °C, estimated initial [Δ$^3$-carene] = 13.5 ppb) and panels (i)–(j) results from exp. 0A (T = 0 °C, estimated initial [Δ$^3$-carene] = 5.5 ppb).**

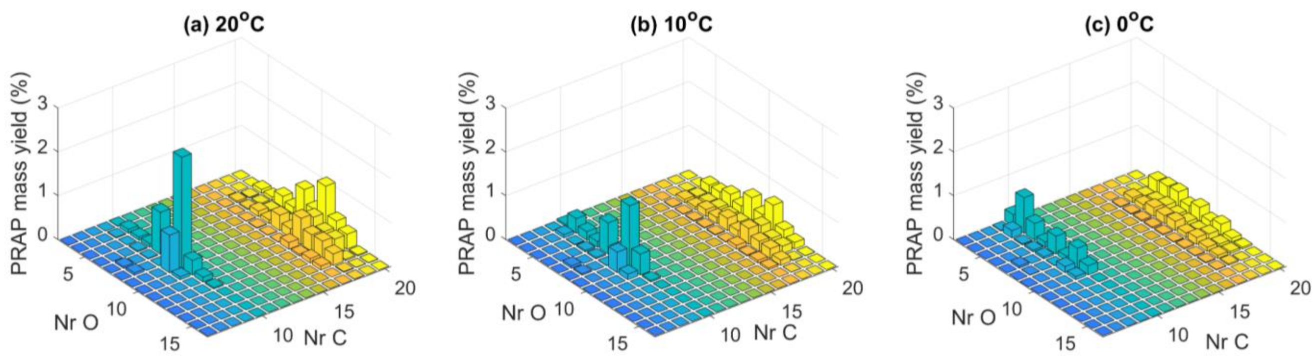


**Figure S13. Modelled Peroxy Radical Autoxidation Products (PRAP) SOA yield distribution on a 2-dimensional molecular oxygen and carbon atoms domain for AURA experiment (a2) 0A (a), (b) 10A, and (c) 0A. The colours represent the number of carbon atoms. The monomer distribution (number of C ≤ 10) and dimers (number of C ≥ 17) can be clearly distinguished. The number of oxygen atoms in the PRAP species distribution decreases when the temperature is lowered. This is both a result of slower autoxidation rates and lower saturation vapour pressures at low temperatures.**

**Tabel S3. Molar yield of initial peroxy radical ($RO_2$) products that can undergo autoxidation.**

| Name | Total molar yield after Δ$^3$-carene + $O_3$ |
|---|---|
| D3CO2_O4i1 | 2.75% |
| D3CO2_O4i2 | 0.605% |
| D3CO2_O4i3 | 1.925% |
| D3CO2_C9_O4 | Maximum ~1.2% if all D3C109O2 react with NO or $RO_2$ |

**Table S4. Δ$^3$-carene ozone oxidation chemistry based on proposed initial oxidation steps by Wang et al. (2019), with slight modifications to achieve a 65% OH yield from the initial ozonolysis reaction of Δ$^3$-carene in accordance with Hantschke et al. (2021). The subsequent multigeneration oxidation mechanism is adopted from the α-pinene mechanism in MCMv3.3.1**.

| Reactions | Rate constants ($cm^3s^{-1}$) | Notes |
|---|---|---|
| D3CARENE + O3 → D3COOA | 3.7E-16*EXP(-640/TEMP)*0.5 | Criegee intermediate conformer Z-CI1 in Wang et al. (2019) |
| D3CARENE + O3 → D3COOB | 3.7E-16*EXP(-640/TEMP)*0.2 | Criegee intermediate conformer Z-CI2 in Wang et al. (2019) |
| D3CARENE + O3 → D3COOC | 3.7E-16*EXP(-640/TEMP)*0.3 | Criegee intermediate conformer E-CI1 in Wang et al. (2019) |
| D3COOA → D3CSOZ | 0.5*KDEC | Secondary ozonoide (SOZ) formation based on Wang et al. (2019) |

| | | |
|---|---|---|
| D3COOA → D3CVHP1 | 0.5*KDEC | Vinyl hydroperoxide (VHP) product 1, VHP1 in Wang et al. (2019), Schemes 1 and 4 |
| D3COOB → D3CSOZ | 0.5*KDEC | Secondary ozonoide (SOZ) formation based on Wang et al. (2019) |
| D3COOB → D3CVHP2 | 0.5*KDEC | Vinyl hydroperoxide (VHP) product 2, VHP2 in Wang et al. (2019), Scheme 1 |
| D3COOC → D3CVHP1 | KDEC | Vinyl hydroperoxide (VHP) product 1, VHP1 in Wang et al. (2019), Schemes 1 and 4 |
| D3CSOZ → D3CONIC | KDEC | cis-3-caronic acid formation, 35 % production yield |
| D3CONIC + OH → D3C96O2 + CO + OH | 6.65E-12 | |
| D3CVHP1 → D3C109O2 + OH | KDEC*0.904 | D3C109O2 analogous to MCMv3.3.1 α-pinene ozonolysis product C109O2 |
| D3CVHP1 → D3CO2_O4i1 + OH | KDEC*0.05 | Reaction leading to $C_{10}$ $RO_2$ autoxidation products |
| D3CVHP1 → D3CO2_O4i2 + OH | KDEC*0.011 | Reaction leading to $C_{10}$ $RO_2$ autoxidation products |
| D3CVHP1 → D3CO2_O4i3 + OH | KDEC*0.035 | Reaction leading to $C_{10}$ $RO_2$ autoxidation products |
| D3CVHP2 → D3C107O2 + OH | KDEC | |
| **Continued multigeneration oxidation chemistry analogous to MCMv3.3.1 a-pinene C109O2 product reaction pathway** | | |
| D3C109O2 + HO2 → D3C109OOH | KRO2HO2*0.914 | |
| D3C109O2 + NO → D3C109O + NO2 | KRO2NO | |
| D3C109O2 + NO3 → D3C109O + NO2 | KRO2NO3 | |
| D3C109O2 → D3C109CO | 1.00E-11*RO2*0.05 | |
| D3C109O2 → D3C109O | 1.00E-11*RO2*0.95 | |
| D3C109O2 → D3C109OH | 1.00E-11*RO2*0.05*0.0 | |
| D3C109O → D3C89CO3 + HCHO | KDEC*0.88 | |
| D3C109O → D3C920CO3 | KDEC*0.1 | |
| D3C109O → D3CO2_C9_O4 + HCHO | KDEC*0.02 | Reaction leading to $C_9$ $RO_2$ autoxidation products |
| D3C109OOH + OH → D3C109CO + OH | 5.47E-11 | |
| D3C109OOH → D3C109O + OH | J(41)+J(15) | Photolysis reaction |
| D3C109OOH → D3C89CO3 + HCHO + OH | J(22) | Photolysis reaction |
| D3C109CO + OH → D3C89CO3 + CO | 5.47E-11 | |
| D3C109CO → D3C89CO3 + CO + HO2 | J(34)+J(15) | Photolysis reaction |
| D3C109OH + OH → D3C109CO + HO2 | 4.45E-11 | |
| D3C109OH → D3C89CO3 + HCHO + HO2 | J(22) | Photolysis reaction |
| D3C109OH → D3C920O2 + CO + HO2 | J(15) | Photolysis reaction |
| D3C89CO3 + HO2 → D3C89CO2 + OH | KAPHO2*0.44 | |
| D3C89CO3 + HO2 → D3C89CO2H + O3 | KAPHO2*0.15 | |
| D3C89CO3 + HO2 → D3C89CO3H | KAPHO2*0.41 | |

| | | |
|---|---|---|
| D3C89CO3 + NO → D3C89CO2 + NO2 | KAPNO | |
| D3C89CO3 + NO2 → D3C89PAN | KFPAN | |
| D3C89CO3 + NO3 → D3C89CO2 + NO2 | KRO2NO3*1.74 | |
| D3C89CO3 → D3C89CO2 | 1.00E-11*RO2*0.7 | |
| D3C89CO3 → D3C89CO2H | 1.00E-11*RO2*0.3 | |
| D3C89CO2 → D3C811CO3 | KDEC*0.8000 | |
| D3C89CO2 → D3C89O2 | KDEC*0.2000 | |
| D3C89CO2H + OH → D3C89CO2 | 2.69E-11 | |
| D3C89CO2H → D3C89CO2 + HO2 | J(15) | Photolysis reaction |
| D3C89CO3H + OH → D3C89CO3 | 3.00E-11 | |
| D3C89CO3H → D3C89CO2 + OH | J(41)+J(15) | Photolysis reaction |
| D3C89PAN + OH → CH3COCH3 + CO13C4CHO + CO + NO2 | 2.52E-11 | |
| D3C89PAN → D3C89CO3 + NO2 | KBPAN | |
| D3C89O2 + HO2 → D3C89OOH | KRO2HO2*0.859 | |
| D3C89O2 + NO → D3C89NO3 | KRO2NO*0.104 | |
| D3C89O2 + NO → D3C89O + NO2 | KRO2NO*0.896 | |
| D3C89O2 + NO3 → D3C89O + NO2 | KRO2NO3 | |
| D3C89O2 → D3C89O | 6.70E-15*RO2*0.7 | |
| D3C89O2 → D3C89OH | 6.70E-15*RO2*0.3 | |
| D3C89OOH + OH → D3C89O2 | 3.61E-11 | |
| D3C89OOH → D3C89O + OH | J(41)+J(15) | Photolysis reaction |
| D3C89NO3 + OH → CH3COCH3 + CO13C4CHO + NO2 | 2.56E-11 | |
| D3C89NO3 → D3C89O + NO2 | J(55)+J(15) | Photolysis reaction |
| D3C89O → D3C810O2 | 2.70D+14*EXP(-6643/TEMP) | |
| D3C89OH + OH → D3C89O | 2.86E-11 | |
| D3C89OH → D3C89O + HO2 | J(15) | Photolysis reaction |
| D3C920CO3 + HO2 → D3C920CO3H | KAPHO2*0.41 | |
| D3C920CO3 + HO2 → D3C920O2 + OH | KAPHO2*0.44 | |
| D3C920CO3 + HO2 → HOD3CONIC + O3 | KAPHO2*0.15 | OH-3-caronic acid formation |
| D3C920CO3 + NO → D3C920O2 + NO2 | KAPNO | |
| D3C920CO3 + NO2 → D3C920PAN | KFPAN | |
| D3C920CO3 + NO3 → D3C920O2 + NO2 | KRO2NO3*1.74 | |
| D3C920CO3 → D3C920O2 | 1.00E-11*RO2*0.70 | |
| D3C920CO3 → HOD3CONIC | 1.00E-11*RO2*0.30 | OH-3-caronic acid formation |
| D3C920O2 + HO2 → D3C920OOH | KRO2HO2*0.890 | |
| D3C920O2 + NO → D3C920O + NO2 | KRO2NO | |
| D3C920O2 + NO3 → D3C920O + NO2 | KRO2NO3 | |
| D3C920O2 → D3C920O | 1.30E-12*RO2 | |
| D3C920CO3H + OH → D3C920CO3 | 9.16E-12 | |

| | | |
|---|---|---|
| D3C920CO3H → D3C920O2 + OH | J(41)+J(22) | Photolysis reaction |
| D3C920PAN + OH → D3C109OH + CO + NO2 | 5.56E-12 | |
| D3C920PAN → D3C920CO3 + NO2 | KBPAN | |
| D3C920OOH + OH → D3C920O2 | 2.36E-11 | |
| D3C920OOH → D3C920O + OH | J(41)+J(22) | Photolysis reaction |
| D3C920O → D3C921O2 | 4.20D+10*EXP(-3523/TEMP) | |
| D3C811CO3 + HO2 → D3C811CO3H | KAPHO2*0.4100 | |
| D3C811CO3 + HO2 → D3C811O2 + OH | KAPHO2*0.4400 | |
| D3C811CO3 + HO2 → D3CIC + O3 | KAPHO2*0.1500 | cis-3-caric acid formation |
| D3C811CO3 + NO → D3C811O2 + NO2 | KAPNO | |
| D3C811CO3 + NO2 → D3C811PAN | KFPAN | |
| D3C811CO3 + NO3 → D3C811O2 + NO2 | KRO2NO3*1.74 | |
| D3C811CO3 → D3C811O2 | 1.0001E-11*RO2*0.70 | |
| D3C811CO3 → D3CIC | 1.0001E-11*RO2*0.30 | cis-3-caric acid formation |
| D3C811CO3H + OH → D3C811CO3 | 1.04E-11 | |
| D3C811CO3H → D3C811O2 + OH | J(41) | Photolysis reaction |
| D3C811O2 + HO2 → D3C811OOH | KRO2HO2*0.859 | |
| D3C811O2 + NO → D3C811NO3 | KRO2NO*0.138 | |
| D3C811O2 + NO → D3C811O + NO2 | KRO2NO*0.862 | |
| D3C811O2 + NO3 → D3C811O + NO2 | KRO2NO3 | |
| D3C811O2 → D3C721CHO | 1.30E-12*RO2*0.2 | |
| D3C811O2 → D3C811O | 1.30E-12*RO2*0.6 | |
| D3C811O2 → D3C811OH | 1.30E-12*RO2*0.2 | |
| D3CIC + OH → D3C811O2 | 7.29E-12 | |
| D3C811PAN + OH → D3C721CHO + CO + NO2 | 6.77E-12 | |
| D3C811PAN → D3C811CO3 + NO2 | KBPAN | |
| D3C811OOH + OH → D3C721CHO + OH | 1.70E-11 | |
| D3C811OOH → D3C811O + OH | J(41) | Photolysis reaction |
| D3C811NO3 + OH → D3C721CHO + NO2 | 3.29E-12 | |
| D3C811NO3 → D3C811O + NO2 | J(53) | Photolysis reaction |
| D3C811O → D3C812O2 | KDEC | |
| D3C811OH + OH → D3C721CHO + HO2 | 7.89E-12 | |
| D3C810O2 + HO2 → D3C810OOH | KRO2HO2*0.914 | |
| D3C810O2 + NO → D3C810NO3 | KRO2NO*0.104 | |
| D3C810O2 + NO → D3C810O + NO2 | KRO2NO*0.896 | |
| D3C810O2 + NO3 → D3C810O + NO2 | KRO2NO3 | |
| D3C810O2 → D3C810O | 6.70E-15*RO2*0.7 | |
| D3C810O2 → D3C810OH | 6.70E-15*RO2*0.3 | |
| D3C810OOH + OH → D3C810O2 | 8.35E-11 | |
| D3C810OOH → D3C810O + OH | J(41)+J(15) | Photolysis reaction |

| | | |
|---|---|---|
| D3C810NO3 + OH → CH3COCH3 + CO13C4CHO + NO2 | 4.96E-11 | |
| D3C810NO3 → D3C810O + NO2 | J(55)+J(15) | Photolysis reaction |
| D3C810O → CH3COCH3 + C514O2 | 2.70D+14*EXP(-6643/TEMP) | |
| D3C810OH + OH → D3C810O | 8.00E-11 | |
| D3C810OH → D3C810O + HO2 | J(15) | Photolysis reaction |
| D3C812O2 + HO2 → D3C812OOH | KRO2HO2*0.859 | |
| D3C812O2 + NO → D3C812O + NO2 | KRO2NO | |
| D3C812O2 + NO3 → D3C812O + NO2 | KRO2NO3 | |
| D3C812O2 → D3C812O | 9.20E-14*RO2*0.7 | |
| D3C812O2 → D3C812OH | 9.20E-14*RO2*0.3 | |
| D3C812OOH + OH → D3C812O2 | 1.09E-11 | |
| D3C812OOH → D3C812O + OH | J(41) | Photolysis reaction |
| D3C812O → D3C813O2 | KDEC | |
| D3C812OH + OH → D3C812O | 7.42E-12 | |
| D3C813O2 + HO2 → D3C813OOH | KRO2HO2*0.859 | |
| D3C813O2 + NO → D3C813NO3 | KRO2NO*0.104 | |
| D3C813O2 + NO → D3C813O + NO2 | KRO2NO*0.896 | |
| D3C813O2 + NO3 → D3C813O + NO2 | KRO2NO3 | |
| D3C813O2 → D3C813O | 6.70E-15*RO2*0.7 | |
| D3C813O2 → D3C813OH | 6.70E-15*RO2*0.3 | |
| D3C813OOH + OH → D3C813O2 | 1.86E-11 | |
| D3C813OOH → D3C813O + OH | J(41)+J(34) | Photolysis reaction |
| D3C813NO3 + OH → CH3COCH3 + CO13C3CO2H + HCHO + NO2 | 7.82E-12 | |
| D3C813NO3 → D3C813O + NO2 | J(55)+J(34) | Photolysis reaction |
| D3C813O → CH3COCH3 + C516O2 | KDEC | |
| D3C813OH + OH → D3C813O | 1.75E-11 | |
| D3C813OH → D3C813O + HO2 | J(34) | Photolysis reaction |
| D3C921O2 + HO2 → D3C921OOH | KRO2HO2*0.890 | |
| D3C921O2 + NO → D3C921O + NO2 | KRO2NO | |
| D3C921O2 + NO3 → D3C921O + NO2 | KRO2NO3 | |
| D3C921O2 → D3C921O | 6.70E-15*RO2 | |
| D3C921OOH + OH → D3C921O2 | 1.29E-11 | |
| D3C921OOH → D3C921O + OH | J(41)+J(22) | Photolysis reaction |
| D3C921O → D3C922O2 | KDEC | |
| D3C922O2 + HO2 → D3C922OOH | KRO2HO2*0.890 | |
| D3C922O2 + NO → D3C922O + NO2 | KRO2NO | |
| D3C922O2 + NO3 → D3C922O + NO2 | KRO2NO3 | |
| D3C922O2 → D3C922O | 6.70E-15*RO2 | |
| D3C922OOH + OH → D3C922O2 | 1.51E-11 | |

| | | |
|---|---|---|
| D3C922OOH → D3C922O + OH | J(41)+J(22) | Photolysis reaction |
| D3C922O → CH3COCH3 + C621O2 | KDEC | |
| D3C96O2 + HO2 → D3C96OOH | KRO2HO2*0.890 | |
| D3C96O2 + NO → D3C96NO3 | KRO2NO*0.157 | |
| D3C96O2 + NO → D3C96O + NO2 | KRO2NO*0.843 | |
| D3C96O2 + NO3 → D3C96O + NO2 | KRO2NO3 | |
| D3C96O2 → D3C96O | 1.30E-12*0.6*RO2 | |
| D3C96O2 → D3C96OH | 1.30E-12*0.2*RO2 | |
| D3C96O2 → NORD3CAL | 1.30E-12*0.2*RO2 | |
| D3C96CO3 + HO2 → D3C96O2 + OH | KAPHO2*0.44 | |
| D3C96CO3 + HO2 → PERD3CONIC | KAPHO2*0.41 | |
| D3C96CO3 + HO2 → D3CONIC + O3 | KAPHO2*0.15 | cis-3-caronic acid formation |
| D3C96CO3 + NO → D3C96O2 + NO2 | KAPNO | |
| D3C96CO3 + NO2 → D3CPAN | KFPAN | |
| D3C96CO3 + NO3 → D3C96O2 + NO2 | KRO2NO3*1.74 | |
| D3C96CO3 → D3C96O2 | 1.00E-11*0.7*RO2 | |
| D3C96CO3 → D3CONIC | 1.00E-11*0.3*RO2 | cis-3-caronic acid formation |
| D3C96OOH + OH → D3C96O2 | 1.90E-12*EXP(190/TEMP) | |
| D3C96OOH + OH → NORD3CAL + OH | 1.30E-11 | |
| D3C96OOH → D3C96O + OH | J(41)+J(22) | Photolysis reaction |
| D3C96NO3 + OH → NORD3CAL + NO2 | 2.88E-12 | |
| D3C96NO3 → D3C96O + NO2 | J(53)+J(22) | Photolysis reaction |
| D3C96O → D3C97O2 | 4.20D+10*EXP(-3523/TEMP) | |
| D3C96OH + OH → NORD3CAL + HO2 | 7.67E-12 | |
| D3C96OH → D3C96O + HO2 | J(22) | Photolysis reaction |
| D3CPAN + OH → NORD3CAL + CO + NO2 | 3.66E-12 | |
| D3CPAN → D3C96CO3 + NO2 | KBPAN | |
| PERCANONIC + OH → D3C96CO3 | 9.73E-12 | |
| PERCANONIC → D3C96O2 + OH | J(41)+J(22) | Photolysis reaction |
| NORD3CAL + NO3 → D3C85CO3 + HNO3 | KNO3AL*8.5 | |
| NORD3CAL + OH → D3C85CO3 | 2.64E-11 | |
| NORD3CAL → D3C85O2 + CO + HO2 | J(15) | Photolysis reaction |
| D3C85CO3 + HO2 → D3C85CO3H | KAPHO2*0.56 | |
| D3C85CO3 + HO2 → D3C85O2 + OH | KAPHO2*0.44 | |
| D3C85CO3 + NO → D3C85O2 + NO2 | KAPNO | |
| D3C85CO3 + NO2 → D3C9PAN | KFPAN | |
| D3C85CO3 + NO3 → D3C85O2 + NO2 | KRO2NO3*1.74 | |
| D3C85CO3 → D3C85O2 | 1.00E-11*RO2 | |
| D3C85O2 + HO2 → D3C85OOH | KRO2HO2*0.859 | |
| D3C85O2 + NO → D3C85O + NO2 | KRO2NO | |

| | | |
|---|---|---|
| D3C85O2 + NO3 → D3C85O + NO2 | KRO2NO3 | |
| D3C85O2 → D3C85O | 6.70E-15*RO2 | |
| D3C85CO3H + OH → D3C85CO3 | 1.02E-11 | |
| D3C85CO3H → D3C85O2 + OH | J(41)+J(22) | Photolysis reaction |
| D3C9PAN + OH → D3C85OOH + CO + NO2 | 6.60E-12 | |
| D3C9PAN → D3C85CO3 + NO2 | KBPAN | |
| D3C85OOH + OH → D3C85O2 | 1.29E-11 | |
| D3C85OOH → D3C85O + OH | J(41)+J(22) | Photolysis reaction |
| D3C85O → D3C86O2 | KDEC | |
| D3C86O2 + HO2 → D3C86OOH | KRO2HO2*0.859 | |
| D3C86O2 + NO → D3C86O + NO2 | KRO2NO | |
| D3C86O2 + NO3 → D3C86O + NO2 | KRO2NO3 | |
| D3C86O2 → D3C86O | 6.70E-15*RO2 | |
| D3C86OOH + OH → D3C86O2 | 3.45E-11 | |
| D3C86OOH → D3C86O + OH | J(41)+J(15) | Photolysis reaction |
| D3C86O → C511O2 + CH3COCH3 | KDEC | |
| **Chemistry based on MCM APINENE chemistry C107O2** | | |
| D3C107O2 + HO2 → D3C107OOH | KRO2HO2*0.914 | |
| D3C107O2 + NO → D3C107O + NO2 | KRO2NO | |
| D3C107O2 + NO3 → D3C107O + NO2 | KRO2NO3 | |
| D3C107O2 → D3C107O | 9.20E-14*0.7*RO2 | |
| D3C107O2 → D3C107OH | 9.20E-14*0.3*RO2 | |
| D3C107OOH + OH → D3C107O2 | 3.01E-11 | |
| D3C107OOH → D3C107O + OH | J(41)+J(15) | Photolysis reaction |
| D3C107O → D3C108O2 | KDEC | |
| D3C107OH + OH → D3C107O | 2.66E-11 | |
| D3C107OH → D3C107O + HO2 | J(15) | Photolysis reaction |
| D3C108O2 + HO2 → D3C108OOH | KRO2HO2*0.914 | |
| D3C108O2 + NO → D3C108NO3 | KRO2NO*0.125 | |
| D3C108O2 + NO → D3C108O + NO2 | KRO2NO*0.875 | |
| D3C108O2 + NO3 → D3C108O + NO2 | KRO2NO3 | |
| D3C108O2 → D3C108O | 6.70E-15*0.7*RO2 | |
| D3C108O2 → D3C108OH | 6.70E-15*0.3*RO2 | |
| D3C108OOH + OH → D3C108O2 | 6.28E-11 | |
| D3C108OOH → D3C108O + OH | J(41)+J(35) | Photolysis reaction |
| D3C108NO3 + OH → CO235C6CHO + CH3COCH3 + NO2 | 2.85E-11 | |
| D3C108NO3 → D3C108O + NO2 | J(55)+J(35) | Photolysis reaction |
| D3C108O → C717O2 + CH3COCH3 | KDEC | |
| D3C108OH + OH → D3C108O | 5.93E-11 | |
| D3C108OH → D3C108O + HO2 | J(35) | Photolysis reaction |

| | | |
|---|---|---|
| D3C97O2 + HO2 → D3C97OOH | KRO2HO2*0.890 | |
| D3C97O2 + NO → D3C97O + NO2 | KRO2NO | |
| D3C97O2 + NO3 → D3C97O + NO2 | KRO2NO3 | |
| D3C97O2 → D3C97O | 6.70E-15*0.7*RO2 | |
| D3C97O2 → D3C97OH | 6.70E-15*0.3*RO2 | |
| D3C97OOH + OH → D3C97O2 | 1.05E-11 | |
| D3C97OOH → D3C97O + OH | J(41)+J(22) | Photolysis reaction |
| D3C97O → D3C98O2 | KDEC | |
| D3C97OH + OH → D3C97O | 7.20E-12 | |
| D3C97OH → D3C97O + HO2 | J(22) | Photolysis reaction |
| D3C98O2 + HO2 → D3C98OOH | KRO2HO2*0.890 | |
| D3C98O2 + NO → D3C98NO3 | KRO2NO*0.118 | |
| D3C98O2 + NO → D3C98O + NO2 | KRO2NO*0.882 | |
| D3C98O2 + NO3 → D3C98O + NO2 | KRO2NO3 | |
| D3C98O2 → D3C98O | 6.70E-15*0.7*RO2 | |
| D3C98O2 → D3C98OH | 6.70E-15*0.3*RO2 | |
| D3C98OOH + OH → D3C98O2 | 2.05E-11 | |
| D3C98OOH → D3C98O + OH | J(41)+J(35) | Photolysis reaction |
| D3C98NO3 + OH → CH3COCH3 + C614CO + NO2 | 5.37E-12 | |
| D3C98NO3 → D3C98O + NO2 | J(55)+J(35) | Photolysis reaction |
| D3C98O → C614O2 + CH3COCH3 | KDEC | |
| D3C98OH + OH → D3C98O | 1.69E-11 | |
| D3C98OH → D3C98O + HO2 | J(35) | Photolysis reaction |
| D3C721CHO + NO3 → D3C721CO3 + HNO3 | KNO3AL*8.5 | |
| D3C721CHO + OH → D3C721CO3 | 2.63E-11 | |
| D3C721CHO → D3C721O2 + CO + HO2 | J(15) | Photolysis reaction |
| D3C721CO3 + HO2 → D3C721CO3H | KAPHO2*0.41 | |
| D3C721CO3 + HO2 → D3C721O2 + OH | KAPHO2*0.44 | |
| D3C721CO3 + HO2 → NORD3CIC + O3 | KAPHO2*0.15 | |
| D3C721CO3 + NO → D3C721O2 + NO2 | KAPNO | |
| D3C721CO3 + NO2 → D3C721PAN | KFPAN | |
| D3C721CO3 + NO3 → D3C721O2 + NO2 | KRO2NO3*1.74 | |
| D3C721CO3 → D3C721O2 | 1.00E-11*RO2*0.7 | |
| D3C721CO3 → NORD3CIC | 1.00E-11*RO2*0.3 | |
| D3C721O2 + HO2 → D3C721OOH | KRO2HO2*0.820 | |
| D3C721O2 + NO → D3C721O + NO2 | KRO2NO | |
| D3C721O2 + NO3 → D3C721O + NO2 | KRO2NO3 | |
| D3C721O2 → D3C721O | 1.30E-12*RO2 | |
| D3C721CO3H + OH → D3C721CO3 | 9.65E-12 | |
| D3C721CO3H → D3C721O2 + OH | J(41) | Photolysis reaction |

| | | |
|---|---|---|
| D3C721PAN + OH → D3C721OOH + CO + NO2 | 2.96E-12 | |
| D3C721PAN → D3C721CO3 + NO2 | KBPAN | |
| D3C721OOH + OH → D3C721O2 | 1.27E-11 | |
| D3C721OOH → D3C721O + OH | J(41) | Photolysis reaction |
| D3C721O → C722O2 | KDEC | |
| NORD3CIC + OH → D3C721O2 | 6.57E-12 | |

**Table S5. Δ$^3$-carene OH oxidation mechanism based on Hantschke et al. (2021) and analogous reactions as for α-pinene in MCMv3.3.1.**

| Reactions | Rate constants (cm$^3$s$^{-1}$) | Notes |
|---|---|---|
| D3CENE + OH → D3C1O2 | 0.6*2.48E-11*EXP(357./TEMP) | Absolute rate from Dillon et al. (2017) |
| D3CENE + OH → D3C2O2 | 0.4*2.48E-11*EXP(357./TEMP) | Absolute rate from Dillon et al. (2017) |
| D3C1O2 + NO → D3CO | 0.77*KRO2NO | Analogous to APINBO2 reactions in MCMv3.3.1 |
| D3C1O2 + NO → D3C1NO3 | 0.23*KRO2NO | Analogous to APINBO2 reactions in MCMv3.3.1 |
| D3C1O2 + HO2 → D3C1OOH | KRO2HO2*0.914 | Analogous to APINBO2 reactions in MCMv3.3.1 |
| D3C1O2 + NO3 → D3CO | KRO2NO3 | Analogous to APINBO2 reactions in MCMv3.3.1 |
| D3C1O2 → D3CO | 0.6*RO2*8.8E-13 | Analogous to APINBO2 reactions in MCMv3.3.1 |
| D3C1O2 → D3COH | 0.2*RO2*8.8E-13 | Analogous to APINBO2 reactions in MCMv3.3.1 |
| D3C1O2 → D3CCO | 0.2*RO2*8.8E-13 | Analogous to APINBO2 reactions in MCMv3.3.1 |
| D3C2O2 + NO → D3CO | 0.77*KRO2NO | Analogous to APINAO2 reactions in MCMv3.3.1 |
| D3C2O2 + NO → D3C2NO3 | 0.23*KRO2NO | Analogous to APINAO2 reactions in MCMv3.3.1 |
| D3C2O2 + HO2 → D3C2OOH | KRO2HO2*0.914 | Analogous to APINAO2 reactions in MCMv3.3.1 |
| D3C2O2 + NO3 → D3CO | KRO2NO3 | Analogous to APINAO2 reactions in MCMv3.3.1 |
| D3C2O2 → D3CO | 0.7*RO2*9.4E-14 | Analogous to APINAO2 reactions in MCMv3.3.1 |
| D3C2O2 → D3COH | 0.3*RO2*9.4E-14 | Analogous to APINAO2 reactions in MCMv3.3.1 |
| D3CO → D3CAL + HO2 | KDEC*0.997 | 3-caronaldehyde formation |
| D3CO → D3CO2_OH_O4i3 | KDEC*0.003 | |
| D3CAL + OH → D3C96CO3 | 0.772*4.1E-11 | Analogous to PINAL (pinonaldehyde) in MCMv3.3.1 |
| D3CAL + OH → D3CALO2 | 0.228*4.1E-11 | Analogous to PINAL (pinonaldehyde) in MCMv3.3.1 |
| D3CAL → D3C96O2 | J(15) | Analogous to PINAL (pinonaldehyde) in MCMv3.3.1 |
| D3COH + OH → D3CCO + HO2 | 1.49E-11 | |

| | | |
|---|---|---|
| D3C2OOH + OH → D3C2O2 | 1.83E-11 | |
| D3C2OOH → D3CO + OH | J(41) | Photolysis reaction |
| D3C1OOH + OH → D3CCO + OH | 3.28E-11 | |
| D3C1OOH → D3CO + OH | J(41) | Photolysis reaction |
| D3C1NO3 + OH → D3CCO + NO2 | 3.64E-12 | |
| D3C2NO3 + OH → D3CAL + NO2 | 5.5E-12 | |
| D3CCO + OH → D3C96CO3 | 8.18E-12 | |
| D3CALO2 + HO2 → D3CALOOH | KRO2HO2*0.914 | |
| D3CALO2 + NO → D3CALNO3 | KRO2NO*0.050 | |
| D3CALO2 + NO → D3CALO + NO2 | KRO2NO*0.950 | |
| D3CALO2 + NO3 → D3CALO + NO2 | KRO2NO3 | |
| D3CALO2 → D3CALO | 6.70E-15*0.7*RO2 | |
| D3CALO2 → D3CALOH | 6.70E-15*0.3*RO2 | |
| D3CALOOH + OH → D3CALO2 | 2.75E-11 | |
| D3CALOOH → D3CALO + OH | J(41)+J(15) | Photolysis reaction |
| D3CALNO3 + OH → CO235C6CHO + CH3COCH3 + NO2 | 2.25E-11 | |
| D3CALNO3 → D3CALO + NO2 | J(55)+J(15) | Photolysis reaction |
| D3CALO → D3C106O2 | KDEC | |
| D3CALOH + OH → D3CALO | 2.41E-11 | |
| D3CALOH → D3CALO + HO2 | J(22) | Photolysis reaction |
| D3C106O2 + HO2 → D3C106OOH | KRO2HO2*0.914 | |
| D3C106O2 + NO → D3C106NO3 | KRO2NO*0.125 | |
| D3C106O2 + NO → D3C106O + NO2 | KRO2NO*0.875 | |
| D3C106O2 + NO3 → D3C106O + NO2 | KRO2NO3 | |
| D3C106O2 → D3C106O | 6.70E-15*0.7*RO2 | |
| D3C106O2 → D3C106OH | 6.70E-15*0.3*RO2 | |
| D3C106OOH + OH → D3C106O2 | 8.01E-11 | |
| D3C106OOH → D3C106O + OH | J(41)+J(15) | Photolysis reaction |
| D3C106NO3 + OH → CO235C6CHO + CH3COCH3 + NO2 | 7.03E-11 | |
| D3C106NO3 → D3C106O + NO2 | J(55)+J(15) | Photolysis reaction |
| D3C106O → C716O2 + CH3COCH3 | KDEC | |
| D3C106OH + OH → D3C106O | 7.66E-11 | |
| D3C106OH → D3C106O + HO2 | J(15) | Photolysis reaction |

235 **Table S6. Peroxy radical autoxidation mechanism (PRAM), monomer production. Rx (e.g. R1) in the 'Reactions' and 'Notes' columns corresponds to the reactions numbered in the main text.**

| Reactions | Rate constants ($cm^3s^{-1}$) | Notes |
|---|---|---|
| D3CO2_O4i1 → D3CO2_O6i1 | 3E16*exp(-1.2077D4/TEMP) | 0.075 $s^{-1}$ at 298 K |
| D3CO2_O4i2 → D3CO2_O6i2 | 3E16*exp(-1.2077D4/TEMP) | 0.075 $s^{-1}$ at 298 K |

| | | |
|---|---|---|
| D3CO2_O4i3 → D3CO2_O6i3 | 3E16*exp(-1.2077D4/TEMP) | 0.075 $s^{-1}$ at 298 K |
| D3CO2_C9_O4 → D3CO2_C9_O6 | 3E16*exp(-1.2077D4/TEMP) | 0.075 $s^{-1}$ at 298 K |
| D3CO2_O5i1 → D3CO2_O7i1 | 1E16*exp(-1.2077D4/TEMP) | 0.025 $s^{-1}$ at 298 K |
| D3CO2_O5i2 → D3CO2_O7i2 | 1E16*exp(-1.2077D4/TEMP) | 0.025 $s^{-1}$ at 298 K |
| D3CO2_O5i3 → D3CO2_O7i3 | 1E16*exp(-1.2077D4/TEMP) | 0.025 $s^{-1}$ at 298 K |
| D3CO2_C9_O5 → D3CO2_C9_O7 | 1E16*exp(-1.2077D4/TEMP) | 0.025 $s^{-1}$ at 298 K |
| D3CO2_O6i1 → D3CO2_O8i1 | 1E18*exp(-1.2077D4/TEMP) | 2.5 $s^{-1}$ at 298 K |
| D3CO2_O6i3 → D3CO2_O8i3 | 1E18*exp(-1.2077D4/TEMP) | 2.5 $s^{-1}$ at 298 K |
| D3CO2_C9_O6 → D3CO2_C9_O8 | 1E18*exp(-1.2077D4/TEMP) | 2.5 $s^{-1}$ at 298 K |
| D3CO2_O7i1 → D3CO2_O9i1 | 1E17*exp(-1.2077D4/TEMP) | 0.25 $s^{-1}$ at 298 K |
| D3CO2_O7i3 → D3CO2_O9i3 | 1E17*exp(-1.2077D4/TEMP) | 0.25 $s^{-1}$ at 298 K |
| D3CO2_O8i1 → D3CO2_O10i1 | 1E18*exp(-1.2077D4/TEMP) | 2.5 $s^{-1}$ at 298 K |
| D3CO2_C9_O8 → D3CO2_C9_O10 | 1E18*exp(-1.2077D4/TEMP) | 2.5 $s^{-1}$ at 298 K |
| D3CO2_O9i1 → D3CO2_O11i1 | 1E17*exp(-1.2077D4/TEMP) | 0.25 $s^{-1}$ at 298 K |
| D3CO2_O10i1 → D3CO2_O12 | 1E15*exp(-1.2077D4/TEMP) | 0.0025 $s^{-1}$ at 298 K |
| **R1. Unimolecular termination $RO_2$ → R=O + OH** | | |
| D3CO2_O7i1 → D3CO6CBNiU1 + OH | 0.0 | R1 |
| D3CO2_O7i2 → D3CO6CBNiU2 + OH | 0.0 | R1 |
| D3CO2_O7i3 → D3CO6CBNiU3 + OH | 0.0 | R1 |
| D3CO2_O8i1 → D3CO7CBNiU1 + OH | 0.0 | R1 |
| D3CO2_O8i2 → D3CO7CBNiU2 + OH | 0.0 | R1 |
| D3CO2_O8i3 → D3CO7CBNiU3 + OH | 2E-2 | R1 Based on COALA exp. |
| D3CO2_O9i1 → D3CO8CBNiU1 + OH | 0.0 | R1 |
| D3CO2_O9i3 → D3CO8CBNiU3 + OH | 2E-2 | R1 Based on COALA exp. |
| D3CO2_O10i1 → D3CO9CBNiU1 + OH | 2E-2 | R1 Based on COALA exp. |
| D3CO2_O11i1 → D3CO10CBNiU1 + OH | 0.0 | R1 |
| D3CO2_O12 → D3CO11CBNiU1 + OH | 2E-2 | R1 Based on COALA exp. |
| **R11. Conversion of PRAM alkoxy radicals to peroxy radicals (RO + $O_2$ → $RO_2$)** | | |
| D3CO_O3i1 → D3CO2_O5i1 | KDEC | R11 |
| D3CO_O3i2 → D3CO2_O5i2 | KDEC | R11 |
| D3CO_O3i3 → D3CO2_O5i3 | KDEC | R11 |
| D3CO_C9_O3 → D3CO2_C9_O5 | KDEC | R11 |
| D3CO_O4i1 → D3CO2_O6i1 | KDEC | R11 |
| D3CO_O4i2 → D3CO2_O6i2 | KDEC | R11 |
| D3CO_O4i3 → D3CO2_O6i3 | KDEC | R11 |
| D3CO_C9_O4 → D3CO2_C9_O6 | KDEC | R11 |
| D3CO_O5i1 → D3CO2_O7i1 | KDEC | R11 |
| D3CO_O5i2 → D3CO2_O7i2 | KDEC | R11 |
| D3CO_O5i3 → D3CO2_O7i3 | KDEC | R11 |
| D3CO_C9_O5 → D3CO2_C9_O7 | KDEC | R11 |

| | | |
|---|---|---|
| D3CO_O6i1 → D3CO2_O8i1 | KDEC | R11 |
| D3CO_O6i2 → D3CO2_O8i2 | KDEC | R11 |
| D3CO_O6i3 → D3CO2_O8i3 | KDEC | R11 |
| D3CO_C9_O6 → D3CO2_C9_O8 | KDEC | R11 |
| D3CO_O7i1 → D3CO2_O9i1 | KDEC | R11 |
| D3CO_O7i2 → D3CO2_O9i2 | KDEC | R11 |
| D3CO_O7i3 → D3CO2_O9i3 | KDEC | R11 |
| D3CO_C9_O7 → D3CO2_C9_O9 | KDEC | R11 |
| D3CO_O8i1 → D3CO2_O10i1 | KDEC | R11 |
| D3CO_C9_O8 → D3CO2_C9_O10 | KDEC | R11 |
| D3CO_O9i1 → D3CO2_O11i1 | KDEC | R11 |
| D3CO_O9i2 → D3CO2_O11i2 | KDEC | R11 |
| D3CO_O9i3 → D3CO2_O11i2 | KDEC | R11 |
| **R6. $RO_2$ + $HO_2$ → ROOH + $O_2$** | | |
| D3CO2_O4i1 + HO2 → D3CO4iH1 | KRO2HO2 | R6 |
| D3CO2_O4i2 + HO2 → D3CO4iH2 | KRO2HO2 | R6 |
| D3CO2_O4i3 + HO2 → D3CO4iH3 | KRO2HO2 | R6 |
| D3CO2_C9_O4 + HO2 → D3C9O4 | KRO2HO2 | R6 |
| D3CO2_O5i1 + HO2 → D3CO5iH1 | KRO2HO2 | R6 |
| D3CO2_O5i2 + HO2 → D3CO5iH2 | KRO2HO2 | R6 |
| D3CO2_O5i3 + HO2 → D3CO5iH3 | KRO2HO2 | R6 |
| D3CO2_C9_O5 + HO2 → D3C9O5 | KRO2HO2 | R6 |
| D3CO2_O6i1 + HO2 → D3CO6iH1 | KRO2HO2 | R6 |
| D3CO2_O6i2 + HO2 → D3CO6iH2 | KRO2HO2 | R6 |
| D3CO2_O6i3 + HO2 → D3CO6iH3 | KRO2HO2 | R6 |
| D3CO2_C9_O6 + HO2 → D3C9O6 | KRO2HO2 | R6 |
| D3CO2_O7i1 + HO2 → D3CO7iH1 | KRO2HO2 | R6 |
| D3CO2_O7i2 + HO2 → D3CO7iH2 | KRO2HO2 | R6 |
| D3CO2_O7i3 + HO2 → D3CO7iH3 | KRO2HO2 | R6 |
| D3CO2_C9_O7 + HO2 → D3C9O7 | KRO2HO2 | R6 |
| D3CO2_O8i1 + HO2 → D3CO8iH1 | KRO2HO2 | R6 |
| D3CO2_O8i2 + HO2 → D3CO8iH2 | KRO2HO2 | R6 |
| D3CO2_O8i3 + HO2 → D3CO8iH3 | KRO2HO2 | R6 |
| D3CO2_C9_O8 + HO2 → D3C9O8 | KRO2HO2 | R6 |
| D3CO2_O9i1 + HO2 → D3CO9iH1 | KRO2HO2 | R6 |
| D3CO2_O9i2 + HO2 → D3CO9iH2 | KRO2HO2 | R6 |
| D3CO2_O9i3 + HO2 → D3CO9iH3 | KRO2HO2 | R6 |
| D3CO2_C9_O9 + HO2 → D3C9O9 | KRO2HO2 | R6 |
| D3CO2_O10i1 + HO2 → D3CO10iH1 | KRO2HO2*0.25 | R6 Based on COALA CO exp. |

| | | |
|---|---|---|
| D3CO2_O10i1 + HO2 → D3CO_O9iH1 + OH | KRO2HO2*0.75 | R8 Based on COALA CO exp. |
| D3CO_O9iH1 → C511OOH+ CH3CO3 + HCOCH2CHO | KDEC | R10 |
| D3CO2_C9_O10 + HO2 → D3C9O10 | KRO2HO2 | R6 |
| D3CO2_O11i1 + HO2 → D3CO11iH1 | KRO2HO2 | R6 |
| D3CO2_O11i2 + HO2 → D3CO11iH2 | KRO2HO2 | R6 |
| D3CO2_O12 + HO2 → D3CO12iH | KRO2HO2 | R6 |
| **R2, R3 & R5 $RO_2$ + $RO_2$ reactions leading to closed shell monomers and alkoxy radicals (RO)** | | |
| D3CO2_O4i1 → D3CO3CBNi1 | 1.2E-12*0.3*RO2 | R3 |
| D3CO2_O4i1 → D3CO_O3i1 | 1.2E-12*0.4*RO2 | R2 |
| D3CO2_O4i1 → D3CO3i1 | 1.2E-12*0.3*RO2 | R3 |
| D3CO2_O4i2 → D3CO3CBNi2 | 1.2E-12*0.3*RO2 | R3 |
| D3CO2_O4i2 → D3CO_O3i2 | 1.2E-12*0.4*RO2 | R2 |
| D3CO2_O4i2 → D3CO3i2 | 1.2E-12*0.3*RO2 | R3 |
| D3CO2_O4i3 → D3CO3CBNi3 | 1.2E-12*0.3*RO2 | R3 |
| D3CO2_O4i3 → D3CO_O3i3 | 1.2E-12*0.4*RO2 | R2 |
| D3CO2_O4i3 → D3CO3i3 | 1.2E-12*0.3*RO2 | R3 |
| D3CO2_C9_O4 → D3C9O3CBN | 1.2E-12*0.3*RO2 | R3 |
| D3CO2_C9_O4 → D3CO_C9_O3 | 1.2E-12*0.4*RO2 | R2 |
| D3CO2_C9_O4 → D3C9O3 | 1.2E-12*0.3*RO2 | R3 |
| D3CO2_O5i1 → D3CO4CBNi1 | 1.2E-12*0.3*RO2 | R3 |
| D3CO2_O5i1 → D3CO_O4i1 | 1.2E-12*0.3*RO2 | R2 |
| D3CO2_O5i1 → D3CO4i1 | 1.2E-12*0.3*RO2 | R3 |
| D3CO2_O5i2 → D3CO4CBNi2 | 1.2E-12*0.3*RO2 | R3 |
| D3CO2_O5i2 → D3CO_O4i2 | 1.2E-12*0.4*RO2 | R2 |
| D3CO2_O5i2 → D3CO4i2 | 1.2E-12*0.3*RO2 | R3 |
| D3CO2_O5i3 → D3CO4CBNi3 | 1.2E-12*0.3*RO2 | R3 |
| D3CO2_O5i3 → D3CO_O4i3 | 1.2E-12*0.4*RO2 | R2 |
| D3CO2_O5i3 → D3CO4i3 | 1.2E-12*0.3*RO2 | R3 |
| D3CO2_C9_O5 → D3C9O4CBN | 1.2E-12*0.3*RO2 | R3 |
| D3CO2_C9_O5 → D3CO_C9_O4 | 1.2E-12*0.4*RO2 | R2 |
| D3CO2_C9_O5 → D3C9O4 | 1.2E-12*0.3*RO2 | R3 |
| D3CO2_O6i1 → D3CO5CBNi1 | 1.6E-12*0.4*RO2 | R3 |
| D3CO2_O6i1 → D3CO_O5i1 | 1.6E-12*0.2*RO2 | R2 |
| D3CO2_O6i1 → D3CO5i1 | 1.6E-12*0.4*RO2 | R3 |
| D3CO2_O6i2 → D3CO5CBNi2 | 1.6E-12*0.4*RO2 | R3 |
| D3CO2_O6i2 → D3CO_O5i2 | 1.6E-12*0.2*RO2 | R2 |
| D3CO2_O6i2 → D3CO5i2 | 1.6E-12*0.4*RO2 | R3 |
| D3CO2_O6i3 → D3CO5CBNi3 | 1.6E-12*0.4*RO2 | R3 |
| D3CO2_O6i3 → D3CO_O5i3 | 1.6E-12*0.2*RO2 | R2 |

| | | |
|---|---|---|
| D3CO2_O6i3 → D3CO5i3 | 1.6E-12*0.4*RO2 | R3 |
| D3CO2_C9_O6 → D3C9O6CBN | 1.6E-12*0.4*RO2 | R3 |
| D3CO2_C9_O6 → D3CO_C9_O6 | 1.6E-12*0.2*RO2 | R2 |
| D3CO2_C9_O6 → D3C9O6 | 1.6E-12*0.4*RO2 | R3 |
| D3CO2_O7i1 → D3CO6CBNi1 | 2E-12*0.3*RO2 | R3 |
| D3CO2_O7i1 → D3CO_O6i1 | 2E-12*0.2*RO2 | R2 |
| D3CO2_O7i1 → D3CO6i1 | 2E-12*0.5*RO2 | R3 |
| D3CO2_O7i2 → D3CO6CBNi2 | 2E-12*0.3*RO2 | R3 |
| D3CO2_O7i2 → D3CO_O6i2 | 2E-12*0.2*RO2 | R2 |
| D3CO2_O7i2 → D3CO6i2 | 2E-12*0.5*RO2 | R3 |
| D3CO2_O7i3 → D3CO6CBNi3 | 2E-12*0.3*RO2 | R3 |
| D3CO2_O7i3 → D3CO_O6i3 | 2E-12*0.2*RO2 | R2 |
| D3CO2_O7i3 → D3CO6i3 | 2E-12*0.5*RO2 | R3 |
| D3CO2_C9_O7 → D3C9O6CBN | 2E-12*0.3*RO2 | R3 |
| D3CO2_C9_O7 → D3CO_C9_O6 | 2E-12*0.2*RO2 | R2 |
| D3CO2_C9_O7 → D3C9O6 | 2E-12*0.5*RO2 | R3 |
| D3CO2_O8i1 → D3CO7CBNi1 | 2E-12*0.5*RO2 | R3 |
| D3CO2_O8i1 → D3CO_O7i1 | 2E-12*0.2*RO2 | R2 |
| D3CO2_O8i1 → D3CC7H8O7 + CH3COCH3 | 2E-12*0.0*RO2 | R2 + R10 |
| D3CO2_O8i1 → D3CO7i1 | 2E-12*0.3*RO2 | R3 |
| D3CO2_O8i2 → D3CO7CBNi2 | 2E-12*0.5*RO2 | R3 |
| D3CO2_O8i2 → D3CO_O7i2 | 2E-12*0.2*RO2 | R2 |
| D3CO2_O8i2 → D3CC7H8O7 + CH3COCH3 | 2E-12*0.0*RO2 | R2 + R10 |
| D3CO2_O8i2 → D3CO7i2 | 2E-12*0.3*RO2 | R3 |
| D3CO2_O8i3 → D3CO7CBNi3 | 2E-12*0.27*RO2 | R3 Based on COALA exp |
| D3CO2_O8i3 → D3CO_O7i3 | 2E-12*0.2*RO2 | R2 |
| D3CO2_O8i3 → D3CC7H8O7 + CH3COCH3 | 2E-12*0.3*RO2 | R2 + R10 |
| D3CO2_O8i3 → D3CO7i3 | 2E-12*0.23*RO2 | Based on COALA exp |
| D3CO2_C9_O8 → D3C9O7CBN | 2E-12*0.5*RO2 | R3 |
| D3CO2_C9_O8 → D3CO_C9_O7 | 2E-12*0.2*RO2 | R2 |
| D3CO2_C9_O8 → D3C9O7 | 2E-12*0.3*RO2 | R3 |
| D3CO2_O9i1 → D3CO8CBNi1 | 2E-12*0.1*RO2 | R3 Based on COALA exp |
| D3CO2_O9i1 → D3CC7H8O8 + CH3COCH3 | 2E-12*0.1*RO2 | R2 + R10 |
| D3CO2_O9i1 → D3CO8i1 | 2E-12*0.8*RO2 | R3 Based on COALA exp |
| D3CO2_O9i2 → D3CO8CBNi2 | 2E-12*0.1*RO2 | R3 |
| D3CO2_O9i2 → D3CC7H8O8 + CH3COCH3 | 2E-12*0.1*RO2 | R2 + R10 |
| D3CO2_O9i2 → D3CO8i2 | 2E-12*0.8*RO2 | R3 |
| D3CO2_O9i3 → D3CO8CBNi3 | 2E-12*0.1*RO2 | R3 |
| D3CO2_O9i3 → D3CC7H8O8 + CH3COCH3 | 2E-12*0.1*RO2 | R2 + R10 |
| D3CO2_O9i3 → D3CO8i3 | 2E-12*0.8*RO2 | R3 |

| | | |
|---|---|---|
| D3CO2_C9_O9 → D3C9O8CBN | 2E-12*0.7*RO2 | R3 |
| D3CO2_C9_O9 → D3CO_C9_O8 | 2E-12*0.1*RO2 | R2 |
| D3CO2_C9_O9 → D3C9O8 | 2E-12*0.2*RO2 | R3 |
| D3CO2_O10i1 → D3CO9CBNi1 | 2E-12*0.55*RO2 | R3 Based on COALA exp |
| D3CO2_O10i1 → D3CC7H8O8 + CH3COCH3 | 2E-12*0.0*RO2 | R2 + R10 |
| D3CO2_O10i1 → D3CO9iR1 | 2E-12*0.45*RO2 | R3 Based on COALA exp |
| D3CO2_C9_O10 → D3C9O9CBN | 2E-12*0.5*RO2 | R3 Based on COALA exp |
| D3CO2_C9_O10 → D3C9O9 | 2E-12*0.5*RO2 | R3 Based on COALA exp |
| D3CO2_O11i1 → D3CO10CBNi1 | 2E-12*0.2*RO2 | R3 |
| D3CO2_O11i1 → D3CC7H8O8 + CH3COCH3 | 2E-12*0.6*RO2 | R2 + R10 |
| D3CO2_O11i1 → D3CO10i1 | 2E-12*0.2*RO2 | R3 |
| D3CO2_O12 → D3CO11CBN | 2E-12*0.8*RO2 | R3 |
| D3CO2_O12 → D3CC7H8O8 + CH3COCH3 | 2E-12*0.1*RO2 | R2 + R10 |
| D3CO2_O12 → D3CO11 | 2E-12*0.1*RO2 | R3 |
| **Functionalization of PRAM $RO_2$ when they react with NO ($RO_2$ + NO →RO + $NO_2$)** | | |
| D3CO2_O4i1 + NO → D3CO_O3i1 + NO2 | 0.8*KRO2NO | |
| D3CO2_O4i2 + NO → D3CO_O3i2 + NO2 | 0.8*KRO2NO | |
| D3CO2_O4i3 + NO → D3CO_O3i3 + NO2 | 0.8*KRO2NO | |
| D3CO2_C9_O4 + NO → D3CO_C9_O3 + NO2 | 0.8*KRO2NO | |
| D3CO2_O5i1 + NO → D3CO_O4i1 + NO2 | 0.6*KRO2NO | |
| D3CO2_O5i2 + NO → D3CO_O4i2 + NO2 | 0.6*KRO2NO | |
| D3CO2_O5i3 + NO → D3CO_O4i3 + NO2 | 0.6*KRO2NO | |
| D3CO2_C9_O5 + NO → D3CO_C9_O4 + NO2 | 0.6*KRO2NO | |
| D3CO2_O6i1 + NO → D3CO_O5i1 + NO2 | 0.4*KRO2NO | |
| D3CO2_O6i2 + NO → D3CO_O5i2 + NO2 | 0.4*KRO2NO | |
| D3CO2_O6i3 + NO → D3CO_O5i3 + NO2 | 0.4*KRO2NO | |
| D3CO2_C9_O6 + NO → D3CO_C9_O5 + NO2 | 0.4*KRO2NO | |
| D3CO2_O7i1 + NO → D3CO_O6i1 + NO2 | 0.2*KRO2NO | |
| D3CO2_O7i2 + NO → D3CO_O6i2 + NO2 | 0.2*KRO2NO | |
| D3CO2_O7i3 + NO → D3CO_O6i3 + NO2 | 0.2*KRO2NO | |
| D3CO2_C9_O7 + NO → D3CO_C9_O6 + NO2 | 0.2*KRO2NO | |
| **Fragmentation of $RO_2$ when they react with NO** | | |
| D3CO2_O4i1 + NO → C717O2 + CH3COCH3 + NO2 | 0.08*KRO2NO | |
| D3CO2_O4i2 + NO → C717O2 + CH3COCH3 + NO2 | 0.08*KRO2NO | |
| D3CO2_O4i3 + NO → C717O2 + CH3COCH3 + NO2 | 0.08*KRO2NO | |
| D3CO2_C9_O4 + NO → C717O2 + CH3CHO + NO2 | 0.08*KRO2NO | |
| D3CO2_O5i1 + NO → C717O2 + CH3COCH3+NO2 | 0.16*KRO2NO | |
| D3CO2_O5i2 + NO → C717O2 + CH3COCH3+NO2 | 0.16*KRO2NO | |
| D3CO2_O5i3 + NO → C717O2 + CH3COCH3+NO2 | 0.16*KRO2NO | |
| D3CO2_C9_O5 + NO → C717O2 + CH3CHO + NO2 | 0.16*KRO2NO | |

| | |
|---|---|
| D3CO2_O6i1 + NO → C717O2 + CH3COCH3 + NO2 | 0.24*KRO2NO |
| D3CO2_O6i2 + NO → C717O2 + CH3COCH3 + NO2 | 0.24*KRO2NO |
| D3CO2_O6i3 + NO → C717O2 + CH3COCH3 + NO2 | 0.24*KRO2NO |
| D3CO2_C9_O6 + NO → C717O2 + CH3CHO + NO2 | 0.24*KRO2NO |
| D3CO2_O7i1 + NO → C717O2 + CH3COCH3+NO2 | 0.32*KRO2NO |
| D3CO2_O7i2 + NO → C717O2 + CH3COCH3+NO2 | 0.32*KRO2NO |
| D3CO2_O7i3 + NO → C717O2 + CH3COCH3+NO2 | 0.32*KRO2NO |
| D3CO2_C9_O7 + NO → C717O2 + CH3CHO + NO2 | 0.32*KRO2NO |
| D3CO2_O8i1 + NO → D3CC7H8O7 + CH3COCH3+NO2 | 0.4*KRO2NO |
| D3CO2_O8i2 + NO → D3CC7H8O7 + CH3COCH3+NO2 | 0.4*KRO2NO |
| D3CO2_O8i3 + NO → D3CC7H8O7 + CH3COCH3+NO2 | 0.4*KRO2NO |
| D3CO2_C9_O8 + NO → D3CC7H8O7 + CH3CHO + NO2 | 0.4*KRO2NO |
| D3CO2_O9i1 + NO → R_C7H11O7 + MGLYOX+NO2 | 0.4*KRO2NO |
| D3CO2_O9i2 + NO → R_C7H11O7 + MGLYOX+NO2 | 0.4*KRO2NO |
| D3CO2_O9i3 + NO → R_C7H11O7 + MGLYOX+NO2 | 0.4*KRO2NO |
| D3CO2_C9_O9 + NO → R_C7H11O7 + GLYOX + NO2 | 0.4*KRO2NO |
| D3CO2_O10i1 + NO → R_C7H11O7 + CH3COCO2H+NO2 | 0.4*KRO2NO |
| D3CO2_C9_O10 + NO → R_C7H11O7 + GLYOX + NO2 | 0.4*KRO2NO |
| D3CO2_O11i1 + NO → D3CC7H8O8 + CH3COCH3+NO2 | 0.4*KRO2NO |
| D3CO2_O11i2 + NO → D3CC7H8O8 + CH3COCH3+NO2 | 0.4*KRO2NO |
| D3CO2_O12 + NO → D3CC7H8O8 + CH3COCH3+NO2 | 0.4*KRO2NO |
| R_C7H11O7 + NO → D3CC7NO3_O8 | KRO2NO |
| R_C7H11O7 → D3CC7H10O6 | 5.0E-12*RO2 |
| **$RO_2$ + NO → R→O + $NO_2$ + $HO_2$** | |
| D3CO2_O4i1 + NO → D3CO3CBNi1 + NO2 + HO2 | 0.06*KRO2NO |
| D3CO2_O4i2 + NO → D3CO3CBNi2 + NO2 + HO2 | 0.06*KRO2NO |
| D3CO2_O4i3 + NO → D3CO3CBNi3 + NO2 + HO2 | 0.06*KRO2NO |
| D3CO2_C9_O4 + NO → D3C9O3CBN + NO2 + HO2 | 0.06*KRO2NO |
| D3CO2_O5i1 + NO → D3CO4CBNi1 + NO2 + HO2 | 0.12*KRO2NO |
| D3CO2_O5i2 + NO → D3CO4CBNi2 + NO2 + HO2 | 0.12*KRO2NO |
| D3CO2_O5i3 + NO → D3CO4CBNi3 + NO2 + HO2 | 0.12*KRO2NO |
| D3CO2_C9_O5 + NO → D3C9O4CBN + NO2 + HO2 | 0.12*KRO2NO |
| D3CO2_O6i1 + NO → D3CO5CBNi1 + NO2 + HO2 | 0.18*KRO2NO |
| D3CO2_O6i2 + NO → D3CO5CBNi2 + NO2 + HO2 | 0.18*KRO2NO |
| D3CO2_O6i3 + NO → D3CO5CBNi3 + NO2 + HO2 | 0.18*KRO2NO |
| D3CO2_C9_O6 + NO → D3C9O5CBN + NO2 + HO2 | 0.18*KRO2NO |

| | |
|---|---|
| D3CO2_O7i1 + NO → D3CO6CBNi1 + NO2 + HO2 | 0.24*KRO2NO |
| D3CO2_O7i2 + NO → D3CO6CBNi2 + NO2 + HO2 | 0.24*KRO2NO |
| D3CO2_O7i3 + NO → D3CO6CBNi3 + NO2 + HO2 | 0.24*KRO2NO |
| D3CO2_C9_O7 + NO → D3C9O6CBN + NO2 + HO2 | 0.24*KRO2NO |
| D3CO2_O8i1 + NO → D3CO7CBNi1 + NO2 + HO2 | 0.3*KRO2NO |
| D3CO2_O8i2 + NO → D3CO7CBNi2 + NO2 + HO2 | 0.3*KRO2NO |
| D3CO2_O8i3 + NO → D3CO7CBNi3 + NO2 + HO2 | 0.3*KRO2NO |
| D3CO2_C9_O8 + NO → D3C9O7CBN + NO2 + HO2 | 0.3*KRO2NO |
| D3CO2_O9i1 + NO → D3CO8CBNi1 + NO2 + HO2 | 0.3*KRO2NO |
| D3CO2_O9i2 + NO → D3CO8CBNi2 + NO2 + HO2 | 0.3*KRO2NO |
| D3CO2_O9i3 + NO → D3CO8CBNi3 + NO2 + HO2 | 0.3*KRO2NO |
| D3CO2_C9_O9 + NO → D3C9O8CBN + NO2 + HO2 | 0.3*KRO2NO |
| D3CO2_O10i1 + NO → D3CO9CBNi1 + NO2 + HO2 | 0.3*KRO2NO |
| D3CO2_C9_O10 + NO → D3C9O9CBN + NO2 + HO2 | 0.3*KRO2NO |
| D3CO2_O11i1 + NO → D3CO10CBNi1 + NO2 + HO2 | 0.3*KRO2NO |
| D3CO2_O11i2 + NO → D3CO10CBNi2 + NO2 + HO2 | 0.3*KRO2NO |
| D3CO2_O12 + NO → D3CO11CBN + NO2 + HO2 | 0.3*KRO2NO |
| **$RO_2$ + NO → R-$NO_3$** | |
| D3CO2_O4i1 + NO → D3CNO5i1 | 0.06*KRO2NO |
| D3CO2_O4i2 + NO → D3CNO5i2 | 0.06*KRO2NO |
| D3CO2_O4i3 + NO → D3CNO5i3 | 0.06*KRO2NO |
| D3CO2_C9_O4 + NO → D3C9NO5 | 0.06*KRO2NO |
| D3CO2_O5i1 + NO → D3CNO6i1 | 0.12*KRO2NO |
| D3CO2_O5i2 + NO → D3CNO6i2 | 0.12*KRO2NO |
| D3CO2_O5i3 + NO → D3CNO6i3 | 0.12*KRO2NO |
| D3CO2_C9_O5 + NO → D3C9NO6 | 0.12*KRO2NO |
| D3CO2_O6i1 + NO → D3CNO7i1 | 0.18*KRO2NO |
| D3CO2_O6i2 + NO → D3CNO7i2 | 0.18*KRO2NO |
| D3CO2_O6i3 + NO → D3CNO7i3 | 0.18*KRO2NO |
| D3CO2_C9_O6 + NO → D3C9NO7 | 0.18*KRO2NO |
| D3CO2_O7i1 + NO → D3CNO8i1 | 0.24*KRO2NO |
| D3CO2_O7i2 + NO → D3CNO8i2 | 0.24*KRO2NO |
| D3CO2_O7i3 + NO → D3CNO8i3 | 0.24*KRO2NO |
| D3CO2_C9_O7 + NO → D3C9NO8 | 0.24*KRO2NO |
| D3CO2_O8i1 + NO → D3CNO9i1 | 0.3*KRO2NO |
| D3CO2_O8i2 + NO → D3CNO9i2 | 0.3*KRO2NO |
| D3CO2_O8i3 + NO → D3CNO9i3 | 0.3*KRO2NO |
| D3CO2_C9_O8 + NO → D3C9NO9 | 0.3*KRO2NO |
| D3CO2_O9i1 + NO → D3CNO10i1 | 0.3*KRO2NO |
| D3CO2_O9i2 + NO → D3CNO10i2 | 0.3*KRO2NO |

| | |
|---|---|
| D3CO2_O9i3 + NO → D3CNO10i3 | 0.3*KRO2NO |
| D3CO2_C9_O9 + NO → D3C9NO10 | 0.3*KRO2NO |
| D3CO2_O10i1 + NO → D3CNO11i1 | 0.3*KRO2NO |
| D3CO2_C9_O10 + NO → D3C9NO11 | 0.3*KRO2NO |
| D3CO2_O11i1 + NO → D3CNO12i1 | 0.3*KRO2NO |
| D3CO2_O11i2 + NO → D3CNO12i2 | 0.3*KRO2NO |
| D3CO2_O12 + NO → D3CNO13 | 0.3*KRO2NO |

**Table S7. Peroxy radical autoxidation mechanism (PRAM), dimer production. Rx (e.g., R1) in the 'Notes' column corresponds to the reactions numbered in the main text.**

| Reactions | Rate constants ($cm^3s^{-1}$) | Notes |
|---|---|---|
| D3C1O2+D3CO2_O4i1 → D3C20H32_O5 | 1E-13 | R4 |
| D3C2O2+D3CO2_O4i1 → D3C20H32_O5 | 1E-13 | R4 |
| D3C96CO3+D3CO2_O4i1 → D3C20H30_O6 | 1E-13 | R4 |
| D3CALO2+D3CO2_O4i1 → D3C20H30_O6 | 1E-13 | R4 |
| D3C106O2+D3CO2_O4i1 → D3C20H30_O7 | 1E-13 | R4 |
| D3C107O2+D3CO2_O4i1 → D3C20H30_O6 | 1E-13 | R4 |
| D3C108O2+D3CO2_O4i1 → D3C20H30_O7 | 1E-13 | R4 |
| D3C109O2+D3CO2_O4i1 → D3C20H30_O6 | 1E-13 | R4 |
| D3C920CO3+D3CO2_O4i1 → D3C20H30_O7 | 1E-13 | R4 |
| D3C96O2+D3CO2_O4i1 → D3C19H30_O5 | 1E-13 | R4 |
| D3C89CO3+D3CO2_O4i1 → D3C19H28_O6 | 1E-13 | R4 |
| D3C920O2+D3CO2_O4i1 → D3C19H30_O6 | 1E-13 | R4 |
| D3C811CO3+D3CO2_O4i1 → D3C19H28_O7 | 1E-13 | R4 |
| D3C921O2+D3CO2_O4i1 → D3C19H30_O7 | 1E-13 | R4 |
| D3C922O2+D3CO2_O4i1 → D3C19H30_O8 | 1E-13 | R4 |
| D3C97O2+D3CO2_O4i1 → D3C19H30_O6 | 1E-13 | R4 |
| D3C98O2+D3CO2_O4i1 → D3C19H30_O7 | 1E-13 | R4 |
| D3C89O2+D3CO2_O4i1 → D3C18H28_O5 | 1E-13 | R4 |
| D3C810O2+D3CO2_O4i1 → D3C18H28_O6 | 1E-13 | R4 |
| D3C811O2+D3CO2_O4i1 → D3C18H28_O6 | 1E-13 | R4 |
| D3C812O2+D3CO2_O4i1 → D3C18H28_O7 | 1E-13 | R4 |
| D3C813O2+D3CO2_O4i1 → D3C18H28_O8 | 1E-13 | R4 |
| D3C85O2+D3CO2_O4i1 → D3C18H28_O5 | 1E-13 | R4 |
| D3C86O2+D3CO2_O4i1 → D3C18H28_O6 | 1E-13 | R4 |
| D3C721CO3+D3CO2_O4i1 → D3C18H26_O7 | 1E-13 | R4 |
| | | |
| D3C1O2+D3CO2_O4i2 → D3C20H30_O5 | 1E-13 | R4 |
| D3C2O2+D3CO2_O4i2 → D3C20H30_O5 | 1E-13 | R4 |

| | | |
|---|---|---|
| D3C96CO3+D3CO2_O4i2 → D3C20H30_O6 | 1E-13 | R4 |
| D3CALO2+D3CO2_O4i2 → D3C20H30_O6 | 1E-13 | R4 |
| D3C106O2+D3CO2_O4i2 → D3C20H30_O7 | 1E-13 | R4 |
| D3C107O2+D3CO2_O4i2 → D3C20H30_O6 | 1E-13 | R4 |
| D3C108O2+D3CO2_O4i2 → D3C20H30_O7 | 1E-13 | R4 |
| D3C109O2+D3CO2_O4i2 → D3C20H30_O6 | 1E-13 | R4 |
| D3C920CO3+D3CO2_O4i2 → D3C20H30_O7 | 1E-13 | R4 |
| D3C96O2+D3CO2_O4i2 → D3C19H30_O5 | 1E-13 | R4 |
| D3C89CO3+D3CO2_O4i2 → D3C19H28_O6 | 1E-13 | R4 |
| D3C920O2+D3CO2_O4i2 → D3C19H30_O6 | 1E-13 | R4 |
| D3C811CO3+D3CO2_O4i2 → D3C19H28_O7 | 1E-13 | R4 |
| D3C921O2+D3CO2_O4i2 → D3C19H30_O7 | 1E-13 | R4 |
| D3C922O2+D3CO2_O4i2 → D3C19H30_O8 | 1E-13 | R4 |
| D3C97O2+D3CO2_O4i2 → D3C19H30_O6 | 1E-13 | R4 |
| D3C98O2+D3CO2_O4i2 → D3C19H30_O7 | 1E-13 | R4 |
| D3C89O2+D3CO2_O4i2 → D3C18H28_O5 | 1E-13 | R4 |
| D3C810O2+D3CO2_O4i2 → D3C18H28_O6 | 1E-13 | R4 |
| D3C811O2+D3CO2_O4i2 → D3C18H28_O6 | 1E-13 | R4 |
| D3C812O2+D3CO2_O4i2 → D3C18H28_O7 | 1E-13 | R4 |
| D3C813O2+D3CO2_O4i2 → D3C18H28_O8 | 1E-13 | R4 |
| D3C85O2+D3CO2_O4i2 → D3C18H28_O5 | 1E-13 | R4 |
| D3C86O2+D3CO2_O4i2 → D3C18H28_O6 | 1E-13 | R4 |
| D3C721CO3+D3CO2_O4i2 → D3C18H26_O7 | 1E-13 | R4 |
| | | |
| D3C1O2+D3CO2_O4i3 → D3C20H32_O5 | 1E-13 | R4 |
| D3C2O2+D3CO2_O4i3 → D3C20H32_O5 | 1E-13 | R4 |
| D3C96CO3+D3CO2_O4i3 → D3C20H30_O6 | 1E-13 | R4 |
| D3CALO2+D3CO2_O4i3 → D3C20H30_O6 | 1E-13 | R4 |
| D3C106O2+D3CO2_O4i3 → D3C20H30_O7 | 1E-13 | R4 |
| D3C107O2+D3CO2_O4i3 → D3C20H30_O6 | 1E-13 | R4 |
| D3C108O2+D3CO2_O4i3 → D3C20H30_O7 | 1E-13 | R4 |
| D3C109O2+D3CO2_O4i3 → D3C20H30_O6 | 1E-13 | R4 |
| D3C920CO3+D3CO2_O4i3 → D3C20H30_O7 | 1E-13 | R4 |
| D3C96O2+D3CO2_O4i3 → D3C19H30_O5 | 1E-13 | R4 |
| D3C89CO3+D3CO2_O4i3 → D3C19H28_O6 | 1E-13 | R4 |
| D3C920O2+D3CO2_O4i3 → D3C19H30_O6 | 1E-13 | R4 |
| D3C811CO3+D3CO2_O4i3 → D3C19H28_O7 | 1E-13 | R4 |
| D3C921O2+D3CO2_O4i3 → D3C19H30_O7 | 1E-13 | R4 |
| D3C922O2+D3CO2_O4i3 → D3C19H30_O8 | 1E-13 | R4 |
| D3C97O2+D3CO2_O4i3 → D3C19H30_O6 | 1E-13 | R4 |

| | | |
|---|---|---|
| D3C98O2+D3CO2_O4i3 → D3C19H30_O7 | 1E-13 | R4 |
| D3C89O2+D3CO2_O4i3 → D3C18H28_O5 | 1E-13 | R4 |
| D3C810O2+D3CO2_O4i3 → D3C18H28_O6 | 1E-13 | R4 |
| D3C811O2+D3CO2_O4i3 → D3C18H28_O6 | 1E-13 | R4 |
| D3C812O2+D3CO2_O4i3 → D3C18H28_O7 | 1E-13 | R4 |
| D3C813O2+D3CO2_O4i3 → D3C18H28_O8 | 1E-13 | R4 |
| D3C85O2+D3CO2_O4i3 → D3C18H28_O5 | 1E-13 | R4 |
| D3C86O2+D3CO2_O4i3 → D3C18H28_O6 | 1E-13 | R4 |
| D3C721CO3+D3CO2_O4i3 → D3C18H26_O7 | 1E-13 | R4 |
| | | |
| D3C1O2+D3CO2_C9_O4 → D3C19H30_O5 | 1E-13 | R4 |
| D3C2O2+D3CO2_C9_O4 → D3C19H30_O5 | 1E-13 | R4 |
| D3C96CO3+D3CO2_C9_O4 → D3C19H28_O6 | 1E-13 | R4 |
| D3CALO2+D3CO2_C9_O4 → D3C19H28_O6 | 1E-13 | R4 |
| D3C106O2+D3CO2_C9_O4 → D3C19H28_O7 | 1E-13 | R4 |
| D3C107O2+D3CO2_C9_O4 → D3C19H28_O6 | 1E-13 | R4 |
| D3C108O2+D3CO2_C9_O4 → D3C19H28_O7 | 1E-13 | R4 |
| D3C109O2+D3CO2_C9_O4 → D3C19H28_O6 | 1E-13 | R4 |
| D3C920CO3+D3CO2_C9_O4 → D3C19H28_O7 | 1E-13 | R4 |
| D3C96O2+D3CO2_C9_O4 → D3C18H28_O5 | 1E-13 | R4 |
| D3C89CO3+D3CO2_C9_O4 → D3C18H26_O6 | 1E-13 | R4 |
| D3C920O2+D3CO2_C9_O4 → D3C18H28_O6 | 1E-13 | R4 |
| D3C811CO3+D3CO2_C9_O4 → D3C18H26_O7 | 1E-13 | R4 |
| D3C921O2+D3CO2_C9_O4 → D3C18H28_O7 | 1E-13 | R4 |
| D3C922O2+D3CO2_C9_O4 → D3C18H28_O8 | 1E-13 | R4 |
| D3C97O2+D3CO2_C9_O4 → D3C18H28_O6 | 1E-13 | R4 |
| D3C98O2+D3CO2_C9_O4 → D3C18H28_O7 | 1E-13 | R4 |
| D3C89O2+D3CO2_C9_O4 → D3C17H26_O5 | 1E-13 | R4 |
| D3C810O2+D3CO2_C9_O4 → D3C17H26_O6 | 1E-13 | R4 |
| D3C811O2+D3CO2_C9_O4 → D3C17H26_O6 | 1E-13 | R4 |
| D3C812O2+D3CO2_C9_O4 → D3C17H26_O7 | 1E-13 | R4 |
| D3C813O2+D3CO2_C9_O4 → D3C17H26_O8 | 1E-13 | R4 |
| D3C85O2+D3CO2_C9_O4 → D3C17H26_O5 | 1E-13 | R4 |
| D3C86O2+D3CO2_C9_O4 → D3C17H26_O6 | 1E-13 | R4 |
| D3C721CO3+D3CO2_C9_O4 → D3C17H24_O7 | 1E-13 | R4 |
| | | |
| D3C1O2+D3CO2_O5i1 → D3C20H32_O6 | 2E-13 | R4 |
| D3C2O2+D3CO2_O5i1 → D3C20H32_O6 | 2E-13 | R4 |
| D3C96CO3+D3CO2_O5i1 → D3C20H30_O7 | 2E-13 | R4 |
| D3CALO2+D3CO2_O5i1 → D3C20H30_O7 | 2E-13 | R4 |

| | | |
|---|---|---|
| D3C106O2+D3CO2_O5i1 → D3C20H30_O8 | 2E-13 | R4 |
| D3C107O2+D3CO2_O5i1 → D3C20H30_O7 | 2E-13 | R4 |
| D3C108O2+D3CO2_O5i1 → D3C20H30_O8 | 2E-13 | R4 |
| D3C109O2+D3CO2_O5i1 → D3C20H30_O7 | 2E-13 | R4 |
| D3C920CO3+D3CO2_O5i1 → D3C20H30_O8 | 2E-13 | R4 |
| D3C96O2+D3CO2_O5i1 → D3C19H30_O6 | 2E-13 | R4 |
| D3C89CO3+D3CO2_O5i1 → D3C19H28_O7 | 2E-13 | R4 |
| D3C920O2+D3CO2_O5i1 → D3C19H30_O7 | 2E-13 | R4 |
| D3C811CO3+D3CO2_O5i1 → D3C19H28_O8 | 2E-13 | R4 |
| D3C921O2+D3CO2_O5i1 → D3C19H30_O8 | 2E-13 | R4 |
| D3C922O2+D3CO2_O5i1 → D3C19H30_O9 | 2E-13 | R4 |
| D3C97O2+D3CO2_O5i1 → D3C19H30_O7 | 2E-13 | R4 |
| D3C98O2+D3CO2_O5i1 → D3C19H30_O8 | 2E-13 | R4 |
| D3C89O2+D3CO2_O5i1 → D3C18H28_O6 | 2E-13 | R4 |
| D3C810O2+D3CO2_O5i1 → D3C18H28_O7 | 2E-13 | R4 |
| D3C811O2+D3CO2_O5i1 → D3C18H28_O7 | 2E-13 | R4 |
| D3C812O2+D3CO2_O5i1 → D3C18H28_O8 | 2E-13 | R4 |
| D3C813O2+D3CO2_O5i1 → D3C18H28_O9 | 2E-13 | R4 |
| D3C85O2+D3CO2_O5i1 → D3C18H28_O6 | 2E-13 | R4 |
| D3C86O2+D3CO2_O5i1 → D3C18H28_O7 | 2E-13 | R4 |
| D3C721CO3+D3CO2_O5i1 → D3C18H26_O8 | 2E-13 | R4 |
| | | |
| D3C1O2+D3CO2_O5i2 → D3C20H32_O6 | 2E-13 | R4 |
| D3C2O2+D3CO2_O5i2 → D3C20H32_O6 | 2E-13 | R4 |
| D3C96CO3+D3CO2_O5i2 → D3C20H30_O7 | 2E-13 | R4 |
| D3CALO2+D3CO2_O5i2 → D3C20H30_O7 | 2E-13 | R4 |
| D3C106O2+D3CO2_O5i2 → D3C20H30_O8 | 2E-13 | R4 |
| D3C107O2+D3CO2_O5i2 → D3C20H30_O7 | 2E-13 | R4 |
| D3C108O2+D3CO2_O5i2 → D3C20H30_O8 | 2E-13 | R4 |
| D3C109O2+D3CO2_O5i2 → D3C20H30_O7 | 2E-13 | R4 |
| D3C920CO3+D3CO2_O5i2 → D3C20H30_O8 | 2E-13 | R4 |
| D3C96O2+D3CO2_O5i2 → D3C19H30_O6 | 2E-13 | R4 |
| D3C89CO3+D3CO2_O5i2 → D3C19H28_O7 | 2E-13 | R4 |
| D3C920O2+D3CO2_O5i2 → D3C19H30_O7 | 2E-13 | R4 |
| D3C811CO3+D3CO2_O5i2 → D3C19H28_O8 | 2E-13 | R4 |
| D3C921O2+D3CO2_O5i2 → D3C19H30_O8 | 2E-13 | R4 |
| D3C922O2+D3CO2_O5i2 → D3C19H30_O9 | 2E-13 | R4 |
| D3C97O2+D3CO2_O5i2 → D3C19H30_O7 | 2E-13 | R4 |
| D3C98O2+D3CO2_O5i2 → D3C19H30_O8 | 2E-13 | R4 |
| D3C89O2+D3CO2_O5i2 → D3C18H28_O6 | 2E-13 | R4 |

| | | |
|---|---|---|
| D3C810O2+D3CO2_O5i2 → D3C18H28_O7 | 2E-13 | R4 |
| D3C811O2+D3CO2_O5i2 → D3C18H28_O7 | 2E-13 | R4 |
| D3C812O2+D3CO2_O5i2 → D3C18H28_O8 | 2E-13 | R4 |
| D3C813O2+D3CO2_O5i2 → D3C18H28_O9 | 2E-13 | R4 |
| D3C85O2+D3CO2_O5i2 → D3C18H28_O6 | 2E-13 | R4 |
| D3C86O2+D3CO2_O5i2 → D3C18H28_O7 | 2E-13 | R4 |
| D3C721CO3+D3CO2_O5i2 → D3C18H26_O8 | 2E-13 | R4 |
| | | |
| D3C1O2+D3CO2_O5i3 → D3C20H32_O6 | 2E-13 | R4 |
| D3C2O2+D3CO2_O5i3 → D3C20H32_O6 | 2E-13 | R4 |
| D3C96CO3+D3CO2_O5i3 → D3C20H30_O7 | 2E-13 | R4 |
| D3CALO2+D3CO2_O5i3 → D3C20H30_O7 | 2E-13 | R4 |
| D3C106O2+D3CO2_O5i3 → D3C20H30_O8 | 2E-13 | R4 |
| D3C107O2+D3CO2_O5i3 → D3C20H30_O7 | 2E-13 | R4 |
| D3C108O2+D3CO2_O5i3 → D3C20H30_O8 | 2E-13 | R4 |
| D3C109O2+D3CO2_O5i3 → D3C20H30_O7 | 2E-13 | R4 |
| D3C920CO3+D3CO2_O5i3 → D3C20H30_O8 | 2E-13 | R4 |
| D3C96O2+D3CO2_O5i3 → D3C19H30_O6 | 2E-13 | R4 |
| D3C89CO3+D3CO2_O5i3 → D3C19H28_O7 | 2E-13 | R4 |
| D3C920O2+D3CO2_O5i3 → D3C19H30_O7 | 2E-13 | R4 |
| D3C811CO3+D3CO2_O5i3 → D3C19H28_O8 | 2E-13 | R4 |
| D3C921O2+D3CO2_O5i3 → D3C19H30_O8 | 2E-13 | R4 |
| D3C922O2+D3CO2_O5i3 → D3C19H30_O9 | 2E-13 | R4 |
| D3C97O2+D3CO2_O5i3 → D3C19H30_O7 | 2E-13 | R4 |
| D3C98O2+D3CO2_O5i3 → D3C19H30_O8 | 2E-13 | R4 |
| D3C89O2+D3CO2_O5i3 → D3C18H28_O6 | 2E-13 | R4 |
| D3C810O2+D3CO2_O5i3 → D3C18H28_O7 | 2E-13 | R4 |
| D3C811O2+D3CO2_O5i3 → D3C18H28_O7 | 2E-13 | R4 |
| D3C812O2+D3CO2_O5i3 → D3C18H28_O8 | 2E-13 | R4 |
| D3C813O2+D3CO2_O5i3 → D3C18H28_O9 | 2E-13 | R4 |
| D3C85O2+D3CO2_O5i3 → D3C18H28_O6 | 2E-13 | R4 |
| D3C86O2+D3CO2_O5i3 → D3C18H28_O7 | 2E-13 | R4 |
| D3C721CO3+D3CO2_O5i3 → D3C18H26_O8 | 2E-13 | R4 |
| | | |
| D3C1O2+D3CO2_C9_O5 → D3C19H30_O6 | 2E-13 | R4 |
| D3C2O2+D3CO2_C9_O5 → D3C19H30_O6 | 2E-13 | R4 |
| D3C96CO3+D3CO2_C9_O5 → D3C19H28_O7 | 2E-13 | R4 |
| D3CALO2+D3CO2_C9_O5 → D3C19H28_O7 | 2E-13 | R4 |
| D3C106O2+D3CO2_C9_O5 → D3C19H28_O8 | 2E-13 | R4 |
| D3C107O2+D3CO2_C9_O5 → D3C19H28_O7 | 2E-13 | R4 |

| | | |
|---|---|---|
| D3C108O2+D3CO2_C9_O5 → D3C19H28_O8 | 2E-13 | R4 |
| D3C109O2+D3CO2_C9_O5 → D3C19H28_O7 | 2E-13 | R4 |
| D3C920CO3+D3CO2_C9_O5 → D3C19H28_O8 | 2E-13 | R4 |
| D3C96O2+D3CO2_C9_O5 → D3C18H28_O6 | 2E-13 | R4 |
| D3C89CO3+D3CO2_C9_O5 → D3C18H26_O7 | 2E-13 | R4 |
| D3C920O2+D3CO2_C9_O5 → D3C18H28_O7 | 2E-13 | R4 |
| D3C811CO3+D3CO2_C9_O5 → D3C18H26_O8 | 2E-13 | R4 |
| D3C921O2+D3CO2_C9_O5 → D3C18H28_O8 | 2E-13 | R4 |
| D3C922O2+D3CO2_C9_O5 → D3C18H28_O9 | 2E-13 | R4 |
| D3C97O2+D3CO2_C9_O5 → D3C18H28_O7 | 2E-13 | R4 |
| D3C98O2+D3CO2_C9_O5 → D3C18H28_O8 | 2E-13 | R4 |
| D3C89O2+D3CO2_C9_O5 → D3C17H26_O6 | 2E-13 | R4 |
| D3C810O2+D3CO2_C9_O5 → D3C17H26_O7 | 2E-13 | R4 |
| D3C811O2+D3CO2_C9_O5 → D3C17H26_O7 | 2E-13 | R4 |
| D3C812O2+D3CO2_C9_O5 → D3C17H26_O8 | 2E-13 | R4 |
| D3C813O2+D3CO2_C9_O5 → D3C17H26_O9 | 2E-13 | R4 |
| D3C85O2+D3CO2_C9_O5 → D3C17H26_O6 | 2E-13 | R4 |
| D3C86O2+D3CO2_C9_O5 → D3C17H26_O7 | 2E-13 | R4 |
| D3C721CO3+D3CO2_C9_O5 → D3C17H24_O8 | 2E-13 | R4 |
| | | |
| D3C1O2+D3CO2_O6i1 → D3C20H32_O7 | 1.2E-12 | R4 |
| D3C2O2+D3CO2_O6i1 → D3C20H32_O7 | 1.2E-12 | R4 |
| D3C96CO3+D3CO2_O6i1 → D3C20H30_O8 | 1.2E-12 | R4 |
| D3CALO2+D3CO2_O6i1 → D3C20H30_O8 | 1.2E-12 | R4 |
| D3C106O2+D3CO2_O6i1 → D3C20H30_O9 | 1.2E-12 | R4 |
| D3C107O2+D3CO2_O6i1 → D3C20H30_O8 | 1.2E-12 | R4 |
| D3C108O2+D3CO2_O6i1 → D3C20H30_O9 | 1.2E-12 | R4 |
| D3C109O2+D3CO2_O6i1 → D3C20H30_O8 | 1.2E-12 | R4 |
| D3C920CO3+D3CO2_O6i1 → D3C20H30_O9 | 1.2E-12 | R4 |
| D3C96O2+D3CO2_O6i1 → D3C19H30_O7 | 1.2E-12 | R4 |
| D3C89CO3+D3CO2_O6i1 → D3C19H28_O8 | 1.2E-12 | R4 |
| D3C920O2+D3CO2_O6i1 → D3C19H30_O8 | 1.2E-12 | R4 |
| D3C811CO3+D3CO2_O6i1 → D3C19H28_O9 | 1.2E-12 | R4 |
| D3C921O2+D3CO2_O6i1 → D3C19H30_O9 | 1.2E-12 | R4 |
| D3C922O2+D3CO2_O6i1 → D3C19H30_O10 | 1.2E-12 | R4 |
| D3C97O2+D3CO2_O6i1 → D3C19H30_O8 | 1.2E-12 | R4 |
| D3C98O2+D3CO2_O6i1 → D3C19H30_O9 | 1.2E-12 | R4 |
| D3C89O2+D3CO2_O6i1 → D3C18H28_O7 | 1.2E-12 | R4 |
| D3C810O2+D3CO2_O6i1 → D3C18H28_O8 | 1.2E-12 | R4 |
| D3C811O2+D3CO2_O6i1 → D3C18H28_O8 | 1.2E-12 | R4 |

| | | |
|---|---|---|
| D3C812O2+D3CO2_O6i1 → D3C18H28_O9 | 1.2E-12 | R4 |
| D3C813O2+D3CO2_O6i1 → D3C18H28_O10 | 1.2E-12 | R4 |
| D3C85O2+D3CO2_O6i1 → D3C18H28_O7 | 1.2E-12 | R4 |
| D3C86O2+D3CO2_O6i1 → D3C18H28_O8 | 1.2E-12 | R4 |
| D3C721CO3+D3CO2_O6i1 → D3C18H26_O9 | 1.2E-12 | R4 |
| | | |
| D3C1O2+D3CO2_O6i2 → D3C20H32_O7 | 1.2E-12 | R4 |
| D3C2O2+D3CO2_O6i2 → D3C20H32_O7 | 1.2E-12 | R4 |
| D3C96CO3+D3CO2_O6i2 → D3C20H30_O8 | 1.2E-12 | R4 |
| D3CALO2+D3CO2_O6i2 → D3C20H30_O8 | 1.2E-12 | R4 |
| D3C106O2+D3CO2_O6i2 → D3C20H30_O9 | 1.2E-12 | R4 |
| D3C107O2+D3CO2_O6i2 → D3C20H30_O8 | 1.2E-12 | R4 |
| D3C108O2+D3CO2_O6i2 → D3C20H30_O9 | 1.2E-12 | R4 |
| D3C109O2+D3CO2_O6i2 → D3C20H30_O8 | 1.2E-12 | R4 |
| D3C920CO3+D3CO2_O6i2 → D3C20H30_O9 | 1.2E-12 | R4 |
| D3C96O2+D3CO2_O6i2 → D3C19H30_O7 | 1.2E-12 | R4 |
| D3C89CO3+D3CO2_O6i2 → D3C19H28_O8 | 1.2E-12 | R4 |
| D3C920O2+D3CO2_O6i2 → D3C19H30_O8 | 1.2E-12 | R4 |
| D3C811CO3+D3CO2_O6i2 → D3C19H28_O9 | 1.2E-12 | R4 |
| D3C921O2+D3CO2_O6i2 → D3C19H30_O9 | 1.2E-12 | R4 |
| D3C922O2+D3CO2_O6i2 → D3C19H30_O10 | 1.2E-12 | R4 |
| D3C97O2+D3CO2_O6i2 → D3C19H30_O8 | 1.2E-12 | R4 |
| D3C98O2+D3CO2_O6i2 → D3C19H30_O9 | 1.2E-12 | R4 |
| D3C89O2+D3CO2_O6i2 → D3C18H28_O7 | 1.2E-12 | R4 |
| D3C810O2+D3CO2_O6i2 → D3C18H28_O8 | 1.2E-12 | R4 |
| D3C811O2+D3CO2_O6i2 → D3C18H28_O8 | 1.2E-12 | R4 |
| D3C812O2+D3CO2_O6i2 → D3C18H28_O9 | 1.2E-12 | R4 |
| D3C813O2+D3CO2_O6i2 → D3C18H28_O10 | 1.2E-12 | R4 |
| D3C85O2+D3CO2_O6i2 → D3C18H28_O7 | 1.2E-12 | R4 |
| D3C86O2+D3CO2_O6i2 → D3C18H28_O8 | 1.2E-12 | R4 |
| D3C721CO3+D3CO2_O6i2 → D3C18H26_O9 | 1.2E-12 | R4 |
| | | |
| D3C1O2+D3CO2_O6i3 → D3C20H32_O7 | 1.2E-12 | R4 |
| D3C2O2+D3CO2_O6i3 → D3C20H32_O7 | 1.2E-12 | R4 |
| D3C96CO3+D3CO2_O6i3 → D3C20H30_O8 | 1.2E-12 | R4 |
| D3CALO2+D3CO2_O6i3 → D3C20H30_O8 | 1.2E-12 | R4 |
| D3C106O2+D3CO2_O6i3 → D3C20H30_O9 | 1.2E-12 | R4 |
| D3C107O2+D3CO2_O6i3 → D3C20H30_O8 | 1.2E-12 | R4 |
| D3C108O2+D3CO2_O6i3 → D3C20H30_O9 | 1.2E-12 | R4 |
| D3C109O2+D3CO2_O6i3 → D3C20H30_O8 | 1.2E-12 | R4 |

| | | |
|---|---|---|
| D3C920CO3+D3CO2_O6i3 → D3C20H30_O9 | 1.2E-12 | R4 |
| D3C96O2+D3CO2_O6i3 → D3C19H30_O7 | 1.2E-12 | R4 |
| D3C89CO3+D3CO2_O6i3 → D3C19H28_O8 | 1.2E-12 | R4 |
| D3C920O2+D3CO2_O6i3 → D3C19H30_O8 | 1.2E-12 | R4 |
| D3C811CO3+D3CO2_O6i3 → D3C19H28_O9 | 1.2E-12 | R4 |
| D3C921O2+D3CO2_O6i3 → D3C19H30_O9 | 1.2E-12 | R4 |
| D3C922O2+D3CO2_O6i3 → D3C19H30_O10 | 1.2E-12 | R4 |
| D3C97O2+D3CO2_O6i3 → D3C19H30_O8 | 1.2E-12 | R4 |
| D3C98O2+D3CO2_O6i3 → D3C19H30_O9 | 1.2E-12 | R4 |
| D3C89O2+D3CO2_O6i3 → D3C18H28_O7 | 1.2E-12 | R4 |
| D3C810O2+D3CO2_O6i3 → D3C18H28_O8 | 1.2E-12 | R4 |
| D3C811O2+D3CO2_O6i3 → D3C18H28_O8 | 1.2E-12 | R4 |
| D3C812O2+D3CO2_O6i3 → D3C18H28_O9 | 1.2E-12 | R4 |
| D3C813O2+D3CO2_O6i3 → D3C18H28_O10 | 1.2E-12 | R4 |
| D3C85O2+D3CO2_O6i3 → D3C18H28_O7 | 1.2E-12 | R4 |
| D3C86O2+D3CO2_O6i3 → D3C18H28_O8 | 1.2E-12 | R4 |
| D3C721CO3+D3CO2_O6i3 → D3C18H26_O9 | 1.2E-12 | R4 |
| | | |
| D3C1O2+D3CO2_C9_O6 → D3C19H30_O7 | 1.2E-12 | R4 |
| D3C2O2+D3CO2_C9_O6 → D3C19H30_O7 | 1.2E-12 | R4 |
| D3C96CO3+D3CO2_C9_O6 → D3C19H28_O8 | 1.2E-12 | R4 |
| D3CALO2+D3CO2_C9_O6 → D3C19H28_O8 | 1.2E-12 | R4 |
| D3C106O2+D3CO2_C9_O6 → D3C19H28_O9 | 1.2E-12 | R4 |
| D3C107O2+D3CO2_C9_O6 → D3C19H28_O8 | 1.2E-12 | R4 |
| D3C108O2+D3CO2_C9_O6 → D3C19H28_O9 | 1.2E-12 | R4 |
| D3C109O2+D3CO2_C9_O6 → D3C19H28_O8 | 1.2E-12 | R4 |
| D3C920CO3+D3CO2_C9_O6 → D3C19H28_O9 | 1.2E-12 | R4 |
| D3C96O2+D3CO2_C9_O6 → D3C18H28_O7 | 1.2E-12 | R4 |
| D3C89CO3+D3CO2_C9_O6 → D3C18H26_O8 | 1.2E-12 | R4 |
| D3C920O2+D3CO2_C9_O6 → D3C18H28_O8 | 1.2E-12 | R4 |
| D3C811CO3+D3CO2_C9_O6 → D3C18H26_O9 | 1.2E-12 | R4 |
| D3C921O2+D3CO2_C9_O6 → D3C18H28_O9 | 1.2E-12 | R4 |
| D3C922O2+D3CO2_C9_O6 → D3C18H28_O10 | 1.2E-12 | R4 |
| D3C97O2+D3CO2_C9_O6 → D3C18H28_O8 | 1.2E-12 | R4 |
| D3C98O2+D3CO2_C9_O6 → D3C18H28_O9 | 1.2E-12 | R4 |
| D3C89O2+D3CO2_C9_O6 → D3C17H26_O7 | 1.2E-12 | R4 |
| D3C810O2+D3CO2_C9_O6 → D3C17H26_O8 | 1.2E-12 | R4 |
| D3C811O2+D3CO2_C9_O6 → D3C17H26_O8 | 1.2E-12 | R4 |
| D3C812O2+D3CO2_C9_O6 → D3C17H26_O9 | 1.2E-12 | R4 |
| D3C813O2+D3CO2_C9_O6 → D3C17H26_O10 | 1.2E-12 | R4 |

| | | |
|---|---|---|
| D3C85O2+D3CO2_C9_O6 → D3C17H26_O7 | 1.2E-12 | R4 |
| D3C86O2+D3CO2_C9_O6 → D3C17H26_O8 | 1.2E-12 | R4 |
| D3C721CO3+D3CO2_C9_O6 → D3C17H24_O9 | 1.2E-12 | R4 |
| | | |
| D3C1O2+D3CO2_O7i1 → D3C20H32_O8 | 1.6E-12 | R4 |
| D3C2O2+D3CO2_O7i1 → D3C20H32_O8 | 1.6E-12 | R4 |
| D3C96CO3+D3CO2_O7i1 → D3C20H30_O9 | 1.6E-12 | R4 |
| D3CALO2+D3CO2_O7i1 → D3C20H30_O9 | 1.6E-12 | R4 |
| D3C106O2+D3CO2_O7i1 → D3C20H30_O10 | 1.6E-12 | R4 |
| D3C107O2+D3CO2_O7i1 → D3C20H30_O9 | 1.6E-12 | R4 |
| D3C108O2+D3CO2_O7i1 → D3C20H30_O10 | 1.6E-12 | R4 |
| D3C109O2+D3CO2_O7i1 → D3C20H30_O9 | 1.6E-12 | R4 |
| D3C920CO3+D3CO2_O7i1 → D3C20H30_O10 | 1.6E-12 | R4 |
| D3C96O2+D3CO2_O7i1 → D3C19H30_O8 | 1.6E-12 | R4 |
| D3C89CO3+D3CO2_O7i1 → D3C19H28_O9 | 1.6E-12 | R4 |
| D3C920O2+D3CO2_O7i1 → D3C19H30_O9 | 1.6E-12 | R4 |
| D3C811CO3+D3CO2_O7i1 → D3C19H28_O10 | 1.6E-12 | R4 |
| D3C921O2+D3CO2_O7i1 → D3C19H30_O10 | 1.6E-12 | R4 |
| D3C922O2+D3CO2_O7i1 → D3C19H30_O11 | 1.6E-12 | R4 |
| D3C97O2+D3CO2_O7i1 → D3C19H30_O9 | 1.6E-12 | R4 |
| D3C98O2+D3CO2_O7i1 → D3C19H30_O10 | 1.6E-12 | R4 |
| D3C89O2+D3CO2_O7i1 → D3C18H28_O8 | 1.6E-12 | R4 |
| D3C810O2+D3CO2_O7i1 → D3C18H28_O9 | 1.6E-12 | R4 |
| D3C811O2+D3CO2_O7i1 → D3C18H28_O9 | 1.6E-12 | R4 |
| D3C812O2+D3CO2_O7i1 → D3C18H28_O10 | 1.6E-12 | R4 |
| D3C813O2+D3CO2_O7i1 → D3C18H28_O11 | 1.6E-12 | R4 |
| D3C85O2+D3CO2_O7i1 → D3C18H28_O8 | 1.6E-12 | R4 |
| D3C86O2+D3CO2_O7i1 → D3C18H28_O9 | 1.6E-12 | R4 |
| D3C721CO3+D3CO2_O7i1 → D3C18H26_O10 | 1.6E-12 | R4 |
| | | |
| D3C1O2+D3CO2_O7i2 → D3C20H32_O8 | 1.6E-12 | R4 |
| D3C2O2+D3CO2_O7i2 → D3C20H32_O8 | 1.6E-12 | R4 |
| D3C96CO3+D3CO2_O7i2 → D3C20H30_O9 | 1.6E-12 | R4 |
| D3CALO2+D3CO2_O7i2 → D3C20H30_O9 | 1.6E-12 | R4 |
| D3C106O2+D3CO2_O7i2 → D3C20H30_O10 | 1.6E-12 | R4 |
| D3C107O2+D3CO2_O7i2 → D3C20H30_O9 | 1.6E-12 | R4 |
| D3C108O2+D3CO2_O7i2 → D3C20H30_O10 | 1.6E-12 | R4 |
| D3C109O2+D3CO2_O7i2 → D3C20H30_O9 | 1.6E-12 | R4 |
| D3C920CO3+D3CO2_O7i2 → D3C20H30_O10 | 1.6E-12 | R4 |
| D3C96O2+D3CO2_O7i2 → D3C19H30_O8 | 1.6E-12 | R4 |

| | | |
|---|---|---|
| D3C89CO3+D3CO2_O7i2 → D3C19H28_O9 | 1.6E-12 | R4 |
| D3C920O2+D3CO2_O7i2 → D3C19H30_O9 | 1.6E-12 | R4 |
| D3C811CO3+D3CO2_O7i2 → D3C19H28_O10 | 1.6E-12 | R4 |
| D3C921O2+D3CO2_O7i2 → D3C19H30_O10 | 1.6E-12 | R4 |
| D3C922O2+D3CO2_O7i2 → D3C19H30_O11 | 1.6E-12 | R4 |
| D3C97O2+D3CO2_O7i2 → D3C19H30_O9 | 1.6E-12 | R4 |
| D3C98O2+D3CO2_O7i2 → D3C19H30_O10 | 1.6E-12 | R4 |
| D3C89O2+D3CO2_O7i2 → D3C18H28_O8 | 1.6E-12 | R4 |
| D3C810O2+D3CO2_O7i2 → D3C18H28_O9 | 1.6E-12 | R4 |
| D3C811O2+D3CO2_O7i2 → D3C18H28_O9 | 1.6E-12 | R4 |
| D3C812O2+D3CO2_O7i2 → D3C18H28_O10 | 1.6E-12 | R4 |
| D3C813O2+D3CO2_O7i2 → D3C18H28_O11 | 1.6E-12 | R4 |
| D3C85O2+D3CO2_O7i2 → D3C18H28_O8 | 1.6E-12 | R4 |
| D3C86O2+D3CO2_O7i2 → D3C18H28_O9 | 1.6E-12 | R4 |
| D3C721CO3+D3CO2_O7i2 → D3C18H26_O10 | 1.6E-12 | R4 |
| | | |
| D3C1O2+D3CO2_O7i3 → D3C20H32_O8 | 1.6E-12 | R4 |
| D3C2O2+D3CO2_O7i3 → D3C20H32_O8 | 1.6E-12 | R4 |
| D3C96CO3+D3CO2_O7i3 → D3C20H30_O9 | 1.6E-12 | R4 |
| D3CALO2+D3CO2_O7i3 → D3C20H30_O9 | 1.6E-12 | R4 |
| D3C106O2+D3CO2_O7i3 → D3C20H30_O10 | 1.6E-12 | R4 |
| D3C107O2+D3CO2_O7i3 → D3C20H30_O9 | 1.6E-12 | R4 |
| D3C108O2+D3CO2_O7i3 → D3C20H30_O10 | 1.6E-12 | R4 |
| D3C109O2+D3CO2_O7i3 → D3C20H30_O9 | 1.6E-12 | R4 |
| D3C920CO3+D3CO2_O7i3 → D3C20H30_O10 | 1.6E-12 | R4 |
| D3C96O2+D3CO2_O7i3 → D3C19H30_O8 | 1.6E-12 | R4 |
| D3C89CO3+D3CO2_O7i3 → D3C19H28_O9 | 1.6E-12 | R4 |
| D3C920O2+D3CO2_O7i3 → D3C19H30_O9 | 1.6E-12 | R4 |
| D3C811CO3+D3CO2_O7i3 → D3C19H28_O10 | 1.6E-12 | R4 |
| D3C921O2+D3CO2_O7i3 → D3C19H30_O10 | 1.6E-12 | R4 |
| D3C922O2+D3CO2_O7i3 → D3C19H30_O11 | 1.6E-12 | R4 |
| D3C97O2+D3CO2_O7i3 → D3C19H30_O9 | 1.6E-12 | R4 |
| D3C98O2+D3CO2_O7i3 → D3C19H30_O10 | 1.6E-12 | R4 |
| D3C89O2+D3CO2_O7i3 → D3C18H28_O8 | 1.6E-12 | R4 |
| D3C810O2+D3CO2_O7i3 → D3C18H28_O9 | 1.6E-12 | R4 |
| D3C811O2+D3CO2_O7i3 → D3C18H28_O9 | 1.6E-12 | R4 |
| D3C812O2+D3CO2_O7i3 → D3C18H28_O10 | 1.6E-12 | R4 |
| D3C813O2+D3CO2_O7i3 → D3C18H28_O11 | 1.6E-12 | R4 |
| D3C85O2+D3CO2_O7i3 → D3C18H28_O8 | 1.6E-12 | R4 |
| D3C86O2+D3CO2_O7i3 → D3C18H28_O9 | 1.6E-12 | R4 |

| | | |
|---|---|---|
| D3C721CO3+D3CO2_O7i3 → D3C18H26_O10 | 1.6E-12 | R4 |
| | | |
| D3C1O2+D3CO2_C9_O7 → D3C19H30_O8 | 1.6E-12 | R4 |
| D3C2O2+D3CO2_C9_O7 → D3C19H30_O8 | 1.6E-12 | R4 |
| D3C96CO3+D3CO2_C9_O7 → D3C19H28_O9 | 1.6E-12 | R4 |
| D3CALO2+D3CO2_C9_O7 → D3C19H28_O9 | 1.6E-12 | R4 |
| D3C106O2+D3CO2_C9_O7 → D3C19H28_O10 | 1.6E-12 | R4 |
| D3C107O2+D3CO2_C9_O7 → D3C19H28_O9 | 1.6E-12 | R4 |
| D3C108O2+D3CO2_C9_O7 → D3C19H28_O10 | 1.6E-12 | R4 |
| D3C109O2+D3CO2_C9_O7 → D3C19H28_O9 | 1.6E-12 | R4 |
| D3C920CO3+D3CO2_C9_O7 → D3C19H28_O10 | 1.6E-12 | R4 |
| D3C96O2+D3CO2_C9_O7 → D3C18H28_O8 | 1.6E-12 | R4 |
| D3C89CO3+D3CO2_C9_O7 → D3C18H28_O9 | 1.6E-12 | R4 |
| D3C920O2+D3CO2_C9_O7 → D3C18H28_O9 | 1.6E-12 | R4 |
| D3C811CO3+D3CO2_C9_O7 → D3C18H28_O10 | 1.6E-12 | R4 |
| D3C921O2+D3CO2_C9_O7 → D3C18H28_O10 | 1.6E-12 | R4 |
| D3C922O2+D3CO2_C9_O7 → D3C18H28_O11 | 1.6E-12 | R4 |
| D3C97O2+D3CO2_C9_O7 → D3C18H28_O9 | 1.6E-12 | R4 |
| D3C98O2+D3CO2_C9_O7 → D3C18H28_O10 | 1.6E-12 | R4 |
| D3C89O2+D3CO2_C9_O7 → D3C17H26_O8 | 1.6E-12 | R4 |
| D3C810O2+D3CO2_C9_O7 → D3C17H26_O9 | 1.6E-12 | R4 |
| D3C811O2+D3CO2_C9_O7 → D3C17H26_O9 | 1.6E-12 | R4 |
| D3C812O2+D3CO2_C9_O7 → D3C17H26_O10 | 1.6E-12 | R4 |
| D3C813O2+D3CO2_C9_O7 → D3C17H26_O11 | 1.6E-12 | R4 |
| D3C85O2+D3CO2_C9_O7 → D3C17H26_O8 | 1.6E-12 | R4 |
| D3C86O2+D3CO2_C9_O7 → D3C17H26_O9 | 1.6E-12 | R4 |
| D3C721CO3+D3CO2_C9_O7 → D3C17H24_O10 | 1.6E-12 | R4 |
| | | |
| D3C1O2+D3CO2_O8i1 → D3C20H32_O9 | 1.6E-12 | R4 |
| D3C2O2+D3CO2_O8i1 → D3C20H32_O9 | 1.6E-12 | R4 |
| D3C96CO3+D3CO2_O8i1 → D3C20H30_O10 | 1.6E-12 | R4 |
| D3CALO2+D3CO2_O8i1 → D3C20H30_O10 | 1.6E-12 | R4 |
| D3C106O2+D3CO2_O8i1 → D3C20H30_O11 | 1.6E-12 | R4 |
| D3C107O2+D3CO2_O8i1 → D3C20H30_O10 | 1.6E-12 | R4 |
| D3C108O2+D3CO2_O8i1 → D3C20H30_O11 | 1.6E-12 | R4 |
| D3C109O2+D3CO2_O8i1 → D3C20H30_O10 | 1.6E-12 | R4 |
| D3C920CO3+D3CO2_O8i1 → D3C20H30_O11 | 1.6E-12 | R4 |
| D3C96O2+D3CO2_O8i1 → D3C19H30_O9 | 1.6E-12 | R4 |
| D3C89CO3+D3CO2_O8i1 → D3C19H28_O10 | 1.6E-12 | R4 |
| D3C920O2+D3CO2_O8i1 → D3C19H30_O10 | 1.6E-12 | R4 |

| | | |
|---|---|---|
| D3C811CO3+D3CO2_O8i1 → D3C19H28_O11 | 1.6E-12 | R4 |
| D3C921O2+D3CO2_O8i1 → D3C19H30_O11 | 1.6E-12 | R4 |
| D3C922O2+D3CO2_O8i1 → D3C19H30_O12 | 1.6E-12 | R4 |
| D3C97O2+D3CO2_O8i1 → D3C19H30_O10 | 1.6E-12 | R4 |
| D3C98O2+D3CO2_O8i1 → D3C19H30_O11 | 1.6E-12 | R4 |
| D3C89O2+D3CO2_O8i1 → D3C18H28_O9 | 1.6E-12 | R4 |
| D3C810O2+D3CO2_O8i1 → D3C18H28_O10 | 1.6E-12 | R4 |
| D3C811O2+D3CO2_O8i1 → D3C18H28_O10 | 1.6E-12 | R4 |
| D3C812O2+D3CO2_O8i1 → D3C18H28_O11 | 1.6E-12 | R4 |
| D3C813O2+D3CO2_O8i1 → D3C18H28_O12 | 1.6E-12 | R4 |
| D3C85O2+D3CO2_O8i1 → D3C18H28_O9 | 1.6E-12 | R4 |
| D3C86O2+D3CO2_O8i1 → D3C18H28_O10 | 1.6E-12 | R4 |
| D3C721CO3+D3CO2_O8i1 → D3C18H26_O11 | 1.6E-12 | R4 |
| | | |
| D3C1O2+D3CO2_O8i2 → D3C20H32_O9 | 1.6E-12 | R4 |
| D3C2O2+D3CO2_O8i2 → D3C20H32_O9 | 1.6E-12 | R4 |
| D3C96CO3+D3CO2_O8i2 → D3C20H30_O10 | 1.6E-12 | R4 |
| D3CALO2+D3CO2_O8i2 → D3C20H30_O10 | 1.6E-12 | R4 |
| D3C106O2+D3CO2_O8i2 → D3C20H30_O11 | 1.6E-12 | R4 |
| D3C107O2+D3CO2_O8i2 → D3C20H30_O10 | 1.6E-12 | R4 |
| D3C108O2+D3CO2_O8i2 → D3C20H30_O11 | 1.6E-12 | R4 |
| D3C109O2+D3CO2_O8i2 → D3C20H30_O10 | 1.6E-12 | R4 |
| D3C920CO3+D3CO2_O8i2 → D3C20H30_O11 | 1.6E-12 | R4 |
| D3C96O2+D3CO2_O8i2 → D3C19H30_O9 | 1.6E-12 | R4 |
| D3C89CO3+D3CO2_O8i2 → D3C19H28_O10 | 1.6E-12 | R4 |
| D3C920O2+D3CO2_O8i2 → D3C19H30_O10 | 1.6E-12 | R4 |
| D3C811CO3+D3CO2_O8i2 → D3C19H28_O11 | 1.6E-12 | R4 |
| D3C921O2+D3CO2_O8i2 → D3C19H30_O11 | 1.6E-12 | R4 |
| D3C922O2+D3CO2_O8i2 → D3C19H30_O12 | 1.6E-12 | R4 |
| D3C97O2+D3CO2_O8i2 → D3C19H30_O10 | 1.6E-12 | R4 |
| D3C98O2+D3CO2_O8i2 → D3C19H30_O11 | 1.6E-12 | R4 |
| D3C89O2+D3CO2_O8i2 → D3C18H28_O9 | 1.6E-12 | R4 |
| D3C810O2+D3CO2_O8i2 → D3C18H28_O10 | 1.6E-12 | R4 |
| D3C811O2+D3CO2_O8i2 → D3C18H28_O10 | 1.6E-12 | R4 |
| D3C812O2+D3CO2_O8i2 → D3C18H28_O11 | 1.6E-12 | R4 |
| D3C813O2+D3CO2_O8i2 → D3C18H28_O12 | 1.6E-12 | R4 |
| D3C85O2+D3CO2_O8i2 → D3C18H28_O9 | 1.6E-12 | R4 |
| D3C86O2+D3CO2_O8i2 → D3C18H28_O10 | 1.6E-12 | R4 |
| D3C721CO3+D3CO2_O8i2 → D3C18H26_O11 | 1.6E-12 | R4 |

| | | |
|---|---|---|
| D3C1O2+D3CO2_O8i3 → D3C20H32_O9 | 1.6E-12 | R4 |
| D3C2O2+D3CO2_O8i3 → D3C20H32_O9 | 1.6E-12 | R4 |
| D3C96CO3+D3CO2_O8i3 → D3C20H30_O10 | 1.6E-12 | R4 |
| D3CALO2+D3CO2_O8i3 → D3C20H30_O10 | 1.6E-12 | R4 |
| D3C106O2+D3CO2_O8i3 → D3C20H30_O11 | 1.6E-12 | R4 |
| D3C107O2+D3CO2_O8i3 → D3C20H30_O10 | 1.6E-12 | R4 |
| D3C108O2+D3CO2_O8i3 → D3C20H30_O11 | 1.6E-12 | R4 |
| D3C109O2+D3CO2_O8i3 → D3C20H30_O10 | 1.6E-12 | R4 |
| D3C920CO3+D3CO2_O8i3 → D3C20H30_O11 | 1.6E-12 | R4 |
| D3C96O2+D3CO2_O8i3 → D3C19H30_O9 | 1.6E-12 | R4 |
| D3C89CO3+D3CO2_O8i3 → D3C19H28_O10 | 1.6E-12 | R4 |
| D3C920O2+D3CO2_O8i3 → D3C19H30_O10 | 1.6E-12 | R4 |
| D3C811CO3+D3CO2_O8i3 → D3C19H28_O11 | 1.6E-12 | R4 |
| D3C921O2+D3CO2_O8i3 → D3C19H30_O11 | 1.6E-12 | R4 |
| D3C922O2+D3CO2_O8i3 → D3C19H30_O12 | 1.6E-12 | R4 |
| D3C97O2+D3CO2_O8i3 → D3C19H30_O10 | 1.6E-12 | R4 |
| D3C98O2+D3CO2_O8i3 → D3C19H30_O11 | 1.6E-12 | R4 |
| D3C89O2+D3CO2_O8i3 → D3C18H28_O9 | 1.6E-12 | R4 |
| D3C810O2+D3CO2_O8i3 → D3C18H28_O10 | 1.6E-12 | R4 |
| D3C811O2+D3CO2_O8i3 → D3C18H28_O10 | 1.6E-12 | R4 |
| D3C812O2+D3CO2_O8i3 → D3C18H28_O11 | 1.6E-12 | R4 |
| D3C813O2+D3CO2_O8i3 → D3C18H28_O12 | 1.6E-12 | R4 |
| D3C85O2+D3CO2_O8i3 → D3C18H28_O9 | 1.6E-12 | R4 |
| D3C86O2+D3CO2_O8i3 → D3C18H28_O10 | 1.6E-12 | R4 |
| D3C721CO3+D3CO2_O8i3 → D3C18H26_O11 | 1.6E-12 | R4 |
| | | |
| D3C1O2+D3CO2_C9_O8 → D3C19H30_O9 | 1.6E-12 | R4 |
| D3C2O2+D3CO2_C9_O8 → D3C19H30_O9 | 1.6E-12 | R4 |
| D3C96CO3+D3CO2_C9_O8 → D3C19H28_O10 | 1.6E-12 | R4 |
| D3CALO2+D3CO2_C9_O8 → D3C19H28_O10 | 1.6E-12 | R4 |
| D3C106O2+D3CO2_C9_O8 → D3C19H28_O11 | 1.6E-12 | R4 |
| D3C107O2+D3CO2_C9_O8 → D3C19H28_O10 | 1.6E-12 | R4 |
| D3C108O2+D3CO2_C9_O8 → D3C19H28_O11 | 1.6E-12 | R4 |
| D3C109O2+D3CO2_C9_O8 → D3C19H28_O10 | 1.6E-12 | R4 |
| D3C920CO3+D3CO2_C9_O8 → D3C19H28_O11 | 1.6E-12 | R4 |
| D3C96O2+D3CO2_C9_O8 → D3C18H28_O9 | 1.6E-12 | R4 |
| D3C89CO3+D3CO2_C9_O8 → D3C18H26_O10 | 1.6E-12 | R4 |
| D3C920O2+D3CO2_C9_O8 → D3C18H28_O10 | 1.6E-12 | R4 |
| D3C811CO3+D3CO2_C9_O8 → D3C18H26_O11 | 1.6E-12 | R4 |
| D3C921O2+D3CO2_C9_O8 → D3C18H28_O11 | 1.6E-12 | R4 |

| | | |
|---|---|---|
| D3C922O2+D3CO2_C9_O8 → D3C18H28_O12 | 1.6E-12 | R4 |
| D3C97O2+D3CO2_C9_O8 → D3C18H28_O10 | 1.6E-12 | R4 |
| D3C98O2+D3CO2_C9_O8 → D3C18H28_O11 | 1.6E-12 | R4 |
| D3C89O2+D3CO2_C9_O8 → D3C17H26_O9 | 1.6E-12 | R4 |
| D3C810O2+D3CO2_C9_O8 → D3C17H26_O10 | 1.6E-12 | R4 |
| D3C811O2+D3CO2_C9_O8 → D3C17H26_O10 | 1.6E-12 | R4 |
| D3C812O2+D3CO2_C9_O8 → D3C17H26_O11 | 1.6E-12 | R4 |
| D3C813O2+D3CO2_C9_O8 → D3C17H26_O12 | 1.6E-12 | R4 |
| D3C85O2+D3CO2_C9_O8 → D3C17H26_O9 | 1.6E-12 | R4 |
| D3C86O2+D3CO2_C9_O8 → D3C17H26_O10 | 1.6E-12 | R4 |
| D3C721CO3+D3CO2_C9_O8 → D3C17H24_O11 | 1.6E-12 | R4 |
| | | |
| D3C1O2+D3CO2_O9i1 → D3C20H32_O10 | 1.6E-12 | R4 |
| D3C2O2+D3CO2_O9i1 → D3C20H32_O10 | 1.6E-12 | R4 |
| D3C96CO3+D3CO2_O9i1 → D3C20H30_O11 | 1.6E-12 | R4 |
| D3CALO2+D3CO2_O9i1 → D3C20H30_O11 | 1.6E-12 | R4 |
| D3C106O2+D3CO2_O9i1 → D3C20H30_O12 | 1.6E-12 | R4 |
| D3C107O2+D3CO2_O9i1 → D3C20H30_O11 | 1.6E-12 | R4 |
| D3C108O2+D3CO2_O9i1 → D3C20H30_O12 | 1.6E-12 | R4 |
| D3C109O2+D3CO2_O9i1 → D3C20H30_O11 | 1.6E-12 | R4 |
| D3C920CO3+D3CO2_O9i1 → D3C20H30_O12 | 1.6E-12 | R4 |
| D3C96O2+D3CO2_O9i1 → D3C19H30_O10 | 1.6E-12 | R4 |
| D3C89CO3+D3CO2_O9i1 → D3C19H28_O11 | 1.6E-12 | R4 |
| D3C920O2+D3CO2_O9i1 → D3C19H30_O11 | 1.6E-12 | R4 |
| D3C811CO3+D3CO2_O9i1 → D3C19H28_O12 | 1.6E-12 | R4 |
| D3C921O2+D3CO2_O9i1 → D3C19H30_O12 | 1.6E-12 | R4 |
| D3C922O2+D3CO2_O9i1 → D3C19H30_O13 | 1.6E-12 | R4 |
| D3C97O2+D3CO2_O9i1 → D3C19H30_O11 | 1.6E-12 | R4 |
| D3C98O2+D3CO2_O9i1 → D3C19H30_O12 | 1.6E-12 | R4 |
| D3C89O2+D3CO2_O9i1 → D3C18H28_O10 | 1.6E-12 | R4 |
| D3C810O2+D3CO2_O9i1 → D3C18H28_O11 | 1.6E-12 | R4 |
| D3C811O2+D3CO2_O9i1 → D3C18H28_O11 | 1.6E-12 | R4 |
| D3C812O2+D3CO2_O9i1 → D3C18H28_O12 | 1.6E-12 | R4 |
| D3C813O2+D3CO2_O9i1 → D3C18H28_O13 | 1.6E-12 | R4 |
| D3C85O2+D3CO2_O9i1 → D3C18H28_O10 | 1.6E-12 | R4 |
| D3C86O2+D3CO2_O9i1 → D3C18H28_O11 | 1.6E-12 | R4 |
| D3C721CO3+D3CO2_O9i1 → D3C18H26_O12 | 1.6E-12 | R4 |
| | | |
| D3C1O2+D3CO2_O9i2 → D3C20H32_O10 | 1.6E-12 | R4 |
| D3C2O2+D3CO2_O9i2 → D3C20H32_O10 | 1.6E-12 | R4 |

| | | |
|---|---|---|
| D3C96CO3+D3CO2_O9i2 → D3C20H30_O11 | 1.6E-12 | R4 |
| D3CALO2+D3CO2_O9i2 → D3C20H30_O11 | 1.6E-12 | R4 |
| D3C106O2+D3CO2_O9i2 → D3C20H30_O12 | 1.6E-12 | R4 |
| D3C107O2+D3CO2_O9i2 → D3C20H30_O11 | 1.6E-12 | R4 |
| D3C108O2+D3CO2_O9i2 → D3C20H30_O12 | 1.6E-12 | R4 |
| D3C109O2+D3CO2_O9i2 → D3C20H30_O11 | 1.6E-12 | R4 |
| D3C920CO3+D3CO2_O9i2 → D3C20H30_O12 | 1.6E-12 | R4 |
| D3C96O2+D3CO2_O9i2 → D3C19H30_O10 | 1.6E-12 | R4 |
| D3C89CO3+D3CO2_O9i2 → D3C19H28_O11 | 1.6E-12 | R4 |
| D3C920O2+D3CO2_O9i2 → D3C19H30_O11 | 1.6E-12 | R4 |
| D3C811CO3+D3CO2_O9i2 → D3C19H28_O12 | 1.6E-12 | R4 |
| D3C921O2+D3CO2_O9i2 → D3C19H30_O12 | 1.6E-12 | R4 |
| D3C922O2+D3CO2_O9i2 → D3C19H30_O13 | 1.6E-12 | R4 |
| D3C97O2+D3CO2_O9i2 → D3C19H30_O11 | 1.6E-12 | R4 |
| D3C98O2+D3CO2_O9i2 → D3C19H30_O12 | 1.6E-12 | R4 |
| D3C89O2+D3CO2_O9i2 → D3C18H28_O10 | 1.6E-12 | R4 |
| D3C810O2+D3CO2_O9i2 → D3C18H28_O11 | 1.6E-12 | R4 |
| D3C811O2+D3CO2_O9i2 → D3C18H28_O11 | 1.6E-12 | R4 |
| D3C812O2+D3CO2_O9i2 → D3C18H28_O12 | 1.6E-12 | R4 |
| D3C813O2+D3CO2_O9i2 → D3C18H28_O13 | 1.6E-12 | R4 |
| D3C85O2+D3CO2_O9i2 → D3C18H28_O10 | 1.6E-12 | R4 |
| D3C86O2+D3CO2_O9i2 → D3C18H28_O11 | 1.6E-12 | R4 |
| D3C721CO3+D3CO2_O9i2 → D3C18H26_O12 | 1.6E-12 | R4 |
| | | |
| D3C1O2+D3CO2_O9i3 → D3C20H32_O10 | 1.6E-12 | R4 |
| D3C2O2+D3CO2_O9i3 → D3C20H32_O10 | 1.6E-12 | R4 |
| D3C96CO3+D3CO2_O9i3 → D3C20H30_O11 | 1.6E-12 | R4 |
| D3CALO2+D3CO2_O9i3 → D3C20H30_O11 | 1.6E-12 | R4 |
| D3C106O2+D3CO2_O9i3 → D3C20H30_O12 | 1.6E-12 | R4 |
| D3C107O2+D3CO2_O9i3 → D3C20H30_O11 | 1.6E-12 | R4 |
| D3C108O2+D3CO2_O9i3 → D3C20H30_O12 | 1.6E-12 | R4 |
| D3C109O2+D3CO2_O9i3 → D3C20H30_O11 | 1.6E-12 | R4 |
| D3C920CO3+D3CO2_O9i3 → D3C20H30_O12 | 1.6E-12 | R4 |
| D3C96O2+D3CO2_O9i3 → D3C19H30_O10 | 1.6E-12 | R4 |
| D3C89CO3+D3CO2_O9i3 → D3C19H28_O11 | 1.6E-12 | R4 |
| D3C920O2+D3CO2_O9i3 → D3C19H30_O11 | 1.6E-12 | R4 |
| D3C811CO3+D3CO2_O9i3 → D3C19H28_O12 | 1.6E-12 | R4 |
| D3C921O2+D3CO2_O9i3 → D3C19H30_O12 | 1.6E-12 | R4 |
| D3C922O2+D3CO2_O9i3 → D3C19H30_O13 | 1.6E-12 | R4 |
| D3C97O2+D3CO2_O9i3 → D3C19H30_O11 | 1.6E-12 | R4 |

| | | |
|---|---|---|
| D3C98O2+D3CO2_O9i3 → D3C19H30_O12 | 1.6E-12 | R4 |
| D3C89O2+D3CO2_O9i3 → D3C18H28_O10 | 1.6E-12 | R4 |
| D3C810O2+D3CO2_O9i3 → D3C18H28_O11 | 1.6E-12 | R4 |
| D3C811O2+D3CO2_O9i3 → D3C18H28_O11 | 1.6E-12 | R4 |
| D3C812O2+D3CO2_O9i3 → D3C18H28_O12 | 1.6E-12 | R4 |
| D3C813O2+D3CO2_O9i3 → D3C18H28_O13 | 1.6E-12 | R4 |
| D3C85O2+D3CO2_O9i3 → D3C18H28_O10 | 1.6E-12 | R4 |
| D3C86O2+D3CO2_O9i3 → D3C18H28_O11 | 1.6E-12 | R4 |
| D3C721CO3+D3CO2_O9i3 → D3C18H26_O12 | 1.6E-12 | R4 |
| | | |
| D3C1O2+D3CO2_C9_O9 → D3C19H30_O10 | 1.6E-12 | R4 |
| D3C2O2+D3CO2_C9_O9 → D3C19H30_O10 | 1.6E-12 | R4 |
| D3C96CO3+D3CO2_C9_O9 → D3C19H28_O11 | 1.6E-12 | R4 |
| D3CALO2+D3CO2_C9_O9 → D3C19H28_O11 | 1.6E-12 | R4 |
| D3C106O2+D3CO2_C9_O9 → D3C19H28_O12 | 1.6E-12 | R4 |
| D3C107O2+D3CO2_C9_O9 → D3C19H28_O11 | 1.6E-12 | R4 |
| D3C108O2+D3CO2_C9_O9 → D3C19H28_O12 | 1.6E-12 | R4 |
| D3C109O2+D3CO2_C9_O9 → D3C19H28_O11 | 1.6E-12 | R4 |
| D3C920CO3+D3CO2_C9_O9 → D3C19H28_O12 | 1.6E-12 | R4 |
| D3C96O2+D3CO2_C9_O9 → D3C18H28_O10 | 1.6E-12 | R4 |
| D3C89CO3+D3CO2_C9_O9 → D3C18H26_O11 | 1.6E-12 | R4 |
| D3C920O2+D3CO2_C9_O9 → D3C18H28_O11 | 1.6E-12 | R4 |
| D3C811CO3+D3CO2_C9_O9 → D3C18H26_O12 | 1.6E-12 | R4 |
| D3C921O2+D3CO2_C9_O9 → D3C18H28_O12 | 1.6E-12 | R4 |
| D3C922O2+D3CO2_C9_O9 → D3C18H28_O13 | 1.6E-12 | R4 |
| D3C97O2+D3CO2_C9_O9 → D3C18H28_O11 | 1.6E-12 | R4 |
| D3C98O2+D3CO2_C9_O9 → D3C18H28_O12 | 1.6E-12 | R4 |
| D3C89O2+D3CO2_C9_O9 → D3C17H26_O10 | 1.6E-12 | R4 |
| D3C810O2+D3CO2_C9_O9 → D3C17H26_O11 | 1.6E-12 | R4 |
| D3C811O2+D3CO2_C9_O9 → D3C17H26_O11 | 1.6E-12 | R4 |
| D3C812O2+D3CO2_C9_O9 → D3C17H26_O12 | 1.6E-12 | R4 |
| D3C813O2+D3CO2_C9_O9 → D3C17H26_O13 | 1.6E-12 | R4 |
| D3C85O2+D3CO2_C9_O9 → D3C17H26_O10 | 1.6E-12 | R4 |
| D3C86O2+D3CO2_C9_O9 → D3C17H26_O11 | 1.6E-12 | R4 |
| D3C721CO3+D3CO2_C9_O9 → D3C17H24_O13 | 1.6E-12 | R4 |
| | | |
| D3C1O2+D3CO2_O10i1 → D3C20H32_O11 | 1.6E-12 | R4 |
| D3C2O2+D3CO2_O10i1 → D3C20H32_O11 | 1.6E-12 | R4 |
| D3C96CO3+D3CO2_O10i1 → D3C20H30_O12 | 1.6E-12 | R4 |
| D3CALO2+D3CO2_O10i1 → D3C20H30_O12 | 1.6E-12 | R4 |

| | | |
|---|---|---|
| D3C106O2+D3CO2_O10i1 → D3C20H30_O13 | 1.6E-12 | R4 |
| D3C107O2+D3CO2_O10i1 → D3C20H30_O12 | 1.6E-12 | R4 |
| D3C108O2+D3CO2_O10i1 → D3C20H30_O13 | 1.6E-12 | R4 |
| D3C109O2+D3CO2_O10i1 → D3C20H30_O12 | 1.6E-12 | R4 |
| D3C920CO3+D3CO2_O10i1 → D3C20H30_O13 | 1.6E-12 | R4 |
| D3C96O2+D3CO2_O10i1 → D3C19H30_O11 | 1.6E-12 | R4 |
| D3C89CO3+D3CO2_O10i1 → D3C19H28_O12 | 1.6E-12 | R4 |
| D3C920O2+D3CO2_O10i1 → D3C19H30_O12 | 1.6E-12 | R4 |
| D3C811CO3+D3CO2_O10i1 → D3C19H28_O13 | 1.6E-12 | R4 |
| D3C921O2+D3CO2_O10i1 → D3C19H30_O13 | 1.6E-12 | R4 |
| D3C922O2+D3CO2_O10i1 → D3C19H30_O14 | 1.6E-12 | R4 |
| D3C97O2+D3CO2_O10i1 → D3C19H30_O12 | 1.6E-12 | R4 |
| D3C98O2+D3CO2_O10i1 → D3C19H30_O13 | 1.6E-12 | R4 |
| D3C89O2+D3CO2_O10i1 → D3C18H28_O11 | 1.6E-12 | R4 |
| D3C810O2+D3CO2_O10i1 → D3C18H28_O12 | 1.6E-12 | R4 |
| D3C811O2+D3CO2_O10i1 → D3C18H28_O12 | 1.6E-12 | R4 |
| D3C812O2+D3CO2_O10i1 → D3C18H28_O13 | 1.6E-12 | R4 |
| D3C813O2+D3CO2_O10i1 → D3C18H28_O14 | 1.6E-12 | R4 |
| D3C85O2+D3CO2_O10i1 → D3C18H28_O11 | 1.6E-12 | R4 |
| D3C86O2+D3CO2_O10i1 → D3C18H28_O12 | 1.6E-12 | R4 |
| D3C721CO3+D3CO2_O10i1 → D3C18H26_O13 | 1.6E-12 | R4 |
| | | |
| D3C1O2+D3CO2_O10i3 → D3C20H32_O11 | 1.6E-12 | R4 |
| D3C2O2+D3CO2_O10i3 → D3C20H32_O11 | 1.6E-12 | R4 |
| D3C96CO3+D3CO2_O10i3 → D3C20H30_O12 | 1.6E-12 | R4 |
| D3CALO2+D3CO2_O10i3 → D3C20H30_O12 | 1.6E-12 | R4 |
| D3C106O2+D3CO2_O10i3 → D3C20H30_O13 | 1.6E-12 | R4 |
| D3C107O2+D3CO2_O10i3 → D3C20H30_O12 | 1.6E-12 | R4 |
| D3C108O2+D3CO2_O10i3 → D3C20H30_O13 | 1.6E-12 | R4 |
| D3C109O2+D3CO2_O10i3 → D3C20H30_O12 | 1.6E-12 | R4 |
| D3C920CO3+D3CO2_O10i3 → D3C20H30_O13 | 1.6E-12 | R4 |
| D3C96O2+D3CO2_O10i3 → D3C19H30_O11 | 1.6E-12 | R4 |
| D3C89CO3+D3CO2_O10i3 → D3C19H28_O12 | 1.6E-12 | R4 |
| D3C920O2+D3CO2_O10i3 → D3C19H30_O12 | 1.6E-12 | R4 |
| D3C811CO3+D3CO2_O10i3 → D3C19H28_O13 | 1.6E-12 | R4 |
| D3C921O2+D3CO2_O10i3 → D3C19H30_O13 | 1.6E-12 | R4 |
| D3C922O2+D3CO2_O10i3 → D3C19H30_O14 | 1.6E-12 | R4 |
| D3C97O2+D3CO2_O10i3 → D3C19H30_O12 | 1.6E-12 | R4 |
| D3C98O2+D3CO2_O10i3 → D3C19H30_O13 | 1.6E-12 | R4 |
| D3C89O2+D3CO2_O10i3 → D3C18H28_O11 | 1.6E-12 | R4 |

| | | |
|---|---|---|
| D3C810O2+D3CO2_O10i3 → D3C18H28_O12 | 1.6E-12 | R4 |
| D3C811O2+D3CO2_O10i3 → D3C18H28_O12 | 1.6E-12 | R4 |
| D3C812O2+D3CO2_O10i3 → D3C18H28_O13 | 1.6E-12 | R4 |
| D3C813O2+D3CO2_O10i3 → D3C18H28_O14 | 1.6E-12 | R4 |
| D3C85O2+D3CO2_O10i3 → D3C18H28_O11 | 1.6E-12 | R4 |
| D3C86O2+D3CO2_O10i3 → D3C18H28_O12 | 1.6E-12 | R4 |
| D3C721CO3+D3CO2_O10i3 → D3C18H26_O13 | 1.6E-12 | R4 |
| | | |
| D3C1O2+D3CO2_C9_O10 → D3C19H30_O11 | 1.6E-12 | R4 |
| D3C2O2+D3CO2_C9_O10 → D3C19H30_O11 | 1.6E-12 | R4 |
| D3C96CO3+D3CO2_C9_O10 → D3C19H28_O12 | 1.6E-12 | R4 |
| D3CALO2+D3CO2_C9_O10 → D3C19H28_O12 | 1.6E-12 | R4 |
| D3C106O2+D3CO2_C9_O10 → D3C19H28_O13 | 1.6E-12 | R4 |
| D3C107O2+D3CO2_C9_O10 → D3C19H28_O12 | 1.6E-12 | R4 |
| D3C108O2+D3CO2_C9_O10 → D3C19H28_O13 | 1.6E-12 | R4 |
| D3C109O2+D3CO2_C9_O10 → D3C19H28_O12 | 1.6E-12 | R4 |
| D3C920CO3+D3CO2_C9_O10 → D3C19H28_O13 | 1.6E-12 | R4 |
| D3C96O2+D3CO2_C9_O10 → D3C18H28_O11 | 1.6E-12 | R4 |
| D3C89CO3+D3CO2_C9_O10 → D3C18H26_O12 | 1.6E-12 | R4 |
| D3C920O2+D3CO2_C9_O10 → D3C18H28_O12 | 1.6E-12 | R4 |
| D3C811CO3+D3CO2_C9_O10 → D3C18H26_O13 | 1.6E-12 | R4 |
| D3C921O2+D3CO2_C9_O10 → D3C18H28_O13 | 1.6E-12 | R4 |
| D3C922O2+D3CO2_C9_O10 → D3C18H28_O14 | 1.6E-12 | R4 |
| D3C97O2+D3CO2_C9_O10 → D3C18H28_O12 | 1.6E-12 | R4 |
| D3C98O2+D3CO2_C9_O10 → D3C18H28_O13 | 1.6E-12 | R4 |
| D3C89O2+D3CO2_C9_O10 → D3C17H26_O11 | 1.6E-12 | R4 |
| D3C810O2+D3CO2_C9_O10 → D3C17H26_O12 | 1.6E-12 | R4 |
| D3C811O2+D3CO2_C9_O10 → D3C17H26_O12 | 1.6E-12 | R4 |
| D3C812O2+D3CO2_C9_O10 → D3C17H26_O13 | 1.6E-12 | R4 |
| D3C813O2+D3CO2_C9_O10 → D3C17H26_O14 | 1.6E-12 | R4 |
| D3C85O2+D3CO2_C9_O10 → D3C17H26_O11 | 1.6E-12 | R4 |
| D3C86O2+D3CO2_C9_O10 → D3C17H26_O12 | 1.6E-12 | R4 |
| D3C721CO3+D3CO2_C9_O10 → D3C17H24_O14 | 1.6E-12 | R4 |
| | | |
| D3C1O2+D3CO2_O11i1 → D3C20H32_O12 | 1.6E-12 | R4 |
| D3C2O2+D3CO2_O11i1 → D3C20H32_O12 | 1.6E-12 | R4 |
| D3C96CO3+D3CO2_O11i1 → D3C20H30_O13 | 1.6E-12 | R4 |
| D3CALO2+D3CO2_O11i1 → D3C20H30_O13 | 1.6E-12 | R4 |
| D3C106O2+D3CO2_O11i1 → D3C20H30_O14 | 1.6E-12 | R4 |
| D3C107O2+D3CO2_O11i1 → D3C20H30_O13 | 1.6E-12 | R4 |

| | | |
|---|---|---|
| D3C108O2+D3CO2_O11i1 → D3C20H30_O14 | 1.6E-12 | R4 |
| D3C109O2+D3CO2_O11i1 → D3C20H30_O13 | 1.6E-12 | R4 |
| D3C920CO3+D3CO2_O11i1 → D3C20H30_O14 | 1.6E-12 | R4 |
| D3C96O2+D3CO2_O11i1 → D3C19H30_O12 | 1.6E-12 | R4 |
| D3C89CO3+D3CO2_O11i1 → D3C19H28_O13 | 1.6E-12 | R4 |
| D3C920O2+D3CO2_O11i1 → D3C19H30_O13 | 1.6E-12 | R4 |
| D3C811CO3+D3CO2_O11i1 → D3C19H28_O14 | 1.6E-12 | R4 |
| D3C921O2+D3CO2_O11i1 → D3C19H30_O14 | 1.6E-12 | R4 |
| D3C922O2+D3CO2_O11i1 → D3C19H30_O15 | 1.6E-12 | R4 |
| D3C97O2+D3CO2_O11i1 → D3C19H30_O13 | 1.6E-12 | R4 |
| D3C98O2+D3CO2_O11i1 → D3C19H30_O14 | 1.6E-12 | R4 |
| D3C89O2+D3CO2_O11i1 → D3C18H28_O12 | 1.6E-12 | R4 |
| D3C810O2+D3CO2_O11i1 → D3C18H28_O13 | 1.6E-12 | R4 |
| D3C811O2+D3CO2_O11i1 → D3C18H28_O13 | 1.6E-12 | R4 |
| D3C812O2+D3CO2_O11i1 → D3C18H28_O14 | 1.6E-12 | R4 |
| D3C813O2+D3CO2_O11i1 → D3C18H28_O15 | 1.6E-12 | R4 |
| D3C85O2+D3CO2_O11i1 → D3C18H28_O12 | 1.6E-12 | R4 |
| D3C86O2+D3CO2_O11i1 → D3C18H28_O13 | 1.6E-12 | R4 |
| D3C721CO3+D3CO2_O11i1 → D3C18H26_O14 | 1.6E-12 | R4 |
| | | |
| D3C1O2+D3CO2_O11i2 → D3C20H32_O12 | 1.6E-12 | R4 |
| D3C2O2+D3CO2_O11i2 → D3C20H32_O12 | 1.6E-12 | R4 |
| D3C96CO3+D3CO2_O11i2 → D3C20H30_O13 | 1.6E-12 | R4 |
| D3CALO2+D3CO2_O11i2 → D3C20H30_O13 | 1.6E-12 | R4 |
| D3C106O2+D3CO2_O11i2 → D3C20H30_O14 | 1.6E-12 | R4 |
| D3C107O2+D3CO2_O11i2 → D3C20H30_O13 | 1.6E-12 | R4 |
| D3C108O2+D3CO2_O11i2 → D3C20H30_O14 | 1.6E-12 | R4 |
| D3C109O2+D3CO2_O11i2 → D3C20H30_O13 | 1.6E-12 | R4 |
| D3C920CO3+D3CO2_O11i2 → D3C20H30_O14 | 1.6E-12 | R4 |
| D3C96O2+D3CO2_O11i2 → D3C19H30_O12 | 1.6E-12 | R4 |
| D3C89CO3+D3CO2_O11i2 → D3C19H28_O13 | 1.6E-12 | R4 |
| D3C920O2+D3CO2_O11i2 → D3C19H30_O13 | 1.6E-12 | R4 |
| D3C811CO3+D3CO2_O11i2 → D3C19H28_O14 | 1.6E-12 | R4 |
| D3C921O2+D3CO2_O11i2 → D3C19H30_O14 | 1.6E-12 | R4 |
| D3C922O2+D3CO2_O11i2 → D3C19H30_O15 | 1.6E-12 | R4 |
| D3C97O2+D3CO2_O11i2 → D3C19H30_O13 | 1.6E-12 | R4 |
| D3C98O2+D3CO2_O11i2 → D3C19H30_O14 | 1.6E-12 | R4 |
| D3C89O2+D3CO2_O11i2 → D3C18H28_O12 | 1.6E-12 | R4 |
| D3C810O2+D3CO2_O11i2 → D3C18H28_O13 | 1.6E-12 | R4 |
| D3C811O2+D3CO2_O11i2 → D3C18H28_O13 | 1.6E-12 | R4 |

| | | |
|---|---|---|
| D3C812O2+D3CO2_O11i2 → D3C18H28_O14 | 1.6E-12 | R4 |
| D3C813O2+D3CO2_O11i2 → D3C18H28_O15 | 1.6E-12 | R4 |
| D3C85O2+D3CO2_O11i2 → D3C18H28_O12 | 1.6E-12 | R4 |
| D3C86O2+D3CO2_O11i2 → D3C18H28_O13 | 1.6E-12 | R4 |
| D3C721CO3+D3CO2_O11i2 → D3C18H26_O14 | 1.6E-12 | R4 |
| | | |
| D3C1O2+D3CO2_O12 → D3C20H32_O13 | 1.6E-12 | R4 |
| D3C2O2+D3CO2_O12 → D3C20H32_O13 | 1.6E-12 | R4 |
| D3C96CO3+D3CO2_O12 → D3C20H30_O14 | 1.6E-12 | R4 |
| D3CALO2+D3CO2_O12 → D3C20H30_O14 | 1.6E-12 | R4 |
| D3C106O2+D3CO2_O12 → D3C20H30_O15 | 1.6E-12 | R4 |
| D3C107O2+D3CO2_O12 → D3C20H30_O14 | 1.6E-12 | R4 |
| D3C108O2+D3CO2_O12 → D3C20H30_O15 | 1.6E-12 | R4 |
| D3C109O2+D3CO2_O12 → D3C20H30_O14 | 1.6E-12 | R4 |
| D3C920CO3+D3CO2_O12 → D3C20H30_O15 | 1.6E-12 | R4 |
| D3C96O2+D3CO2_O12 → D3C19H30_O13 | 1.6E-12 | R4 |
| D3C89CO3+D3CO2_O12 → D3C19H28_O14 | 1.6E-12 | R4 |
| D3C920O2+D3CO2_O12 → D3C19H30_O14 | 1.6E-12 | R4 |
| D3C811CO3+D3CO2_O12 → D3C19H28_O15 | 1.6E-12 | R4 |
| D3C921O2+D3CO2_O12 → D3C19H30_O15 | 1.6E-12 | R4 |
| D3C922O2+D3CO2_O12 → D3C19H30_O16 | 1.6E-12 | R4 |
| D3C97O2+D3CO2_O12 → D3C19H30_O14 | 1.6E-12 | R4 |
| D3C98O2+D3CO2_O12 → D3C19H30_O15 | 1.6E-12 | R4 |
| D3C89O2+D3CO2_O12 → D3C18H28_O13 | 1.6E-12 | R4 |
| D3C810O2+D3CO2_O12 → D3C18H28_O14 | 1.6E-12 | R4 |
| D3C811O2+D3CO2_O12 → D3C18H28_O14 | 1.6E-12 | R4 |
| D3C812O2+D3CO2_O12 → D3C18H28_O15 | 1.6E-12 | R4 |
| D3C813O2+D3CO2_O12 → D3C18H28_O16 | 1.6E-12 | R4 |
| D3C85O2+D3CO2_O12 → D3C18H28_O13 | 1.6E-12 | R4 |
| D3C86O2+D3CO2_O12 → D3C18H28_O14 | 1.6E-12 | R4 |
| D3C721CO3+D3CO2_O12 → D3C18H26_O15 | 1.6E-12 | R4 |

## References


Chen, H., Ren, Y., Cazaunau, M., Daële, V., Hu, Y., Chen, J., and Mellouki, A.: Rate coefficients for the reaction of ozone with 2- and 3-carene, Chemical Physics Letters, 621, 71-77, 10.1016/j.cplett.2014.12.056, 2015.

DeCarlo, P. F., Kimmel, J. R., Trimborn, A., Northway, M. J., Jayne, J. T., Aiken, A. C., Gonin, M., Fuhrer, K., Horvath, T., Docherty, K. S., Worsnop, D. R., and Jimenez, J. L.: Field-Deployable, High-Resolution, Time-of-Flight Aerosol Mass Spectrometer, Analytical Chemistry, 78, 8281-8289, 10.1021/ac061249n, 2006.

Dillon, T. J., Dulitz, K., Groß, C. B. M., and Crowley, J. N.: Temperature-dependent rate coefficients for the reactions of the hydroxyl radical with the atmospheric biogenics isoprene, alpha-pinene and delta-3-carene, Atmospheric Chemistry and Physics, 17, 15137-15150, 10.5194/acp-17-15137-2017, 2017.

Ehn, M., Thornton, J. A., Kleist, E., Sipilä, M., Junninen, H., Pullinen, I., Springer, M., Rubach, F., Tillmann, R., and Lee, B.: A large source of low-volatility secondary organic aerosol, Nature, 506, 476-479, 2014.

Eiguren-Fernandez, A., Lewis, G. S., Spielman, S. R., and Hering, S. V.: Time-resolved characterization of particle associated polycyclic aromatic hydrocarbons using a newly-developed sequential spot sampler with automated extraction and analysis, Atmospheric Environment, 96, 125-134, https://doi.org/10.1016/j.atmosenv.2014.07.031, 2014.

Eiguren Fernandez, A., Lewis, G. S., and Hering, S. V.: Design and Laboratory Evaluation of a Sequential Spot Sampler for Time-Resolved Measurement of Airborne Particle Composition, Aerosol Science and Technology, 48, 655-663, 10.1080/02786826.2014.911409, 2014.

Hantschke, L., Novelli, A., Bohn, B., Cho, C., Reimer, D., Rohrer, F., Tillmann, R., Glowania, M., Hofzumahaus, A., Kiendler-Scharr, A., Wahner, A., and Fuchs, H.: Atmospheric photooxidation and ozonolysis of $\Delta$3-carene and 3-caronaldehyde: rate constants and product yields, Atmospheric Chemistry and Physics, 21, 12665-12685, 10.5194/acp-21-12665-2021, 2021.

Jokinen, T., Sipilä, M., Junninen, H., Ehn, M., Lönn, G., Hakala, J., Petäjä, T., Mauldin, R. L., Kulmala, M., and Worsnop, D. R.: Atmospheric sulphuric acid and neutral cluster measurements using CI-APi-TOF, Atmospheric Chemistry and Physics, 12, 4117-4125, 10.5194/acp-12-4117-2012, 2012.

Jokinen, T., Sipila, M., Richters, S., Kerminen, V. M., Paasonen, P., Stratmann, F., Worsnop, D., Kulmala, M., Ehn, M., Herrmann, H., and Berndt, T.: Rapid autoxidation forms highly oxidized $RO_2$ radicals in the atmosphere, Angewandte Chemie International Edition, 53, 14596-14600, 10.1002/anie.201408566, 2014.

Jordan, A., Haidacher, S., Hanel, G., Hartungen, E., Märk, L., Seehauser, H., Schottkowsky, R., Sulzer, P., and Märk, T. D.: A high resolution and high sensitivity proton-transfer-reaction time-of-flight mass spectrometer (PTR-TOF-MS), International Journal of Mass Spectrometry, 286, 122-128, 10.1016/j.ijms.2009.07.005, 2009.

Kristensen, K., Jensen, L., Glasius, M., and Bilde, M.: The effect of sub-zero temperature on the formation and composition of secondary organic aerosol from ozonolysis of alpha-pinene, Environmental Science: Processes & Impacts, 19, 1220-1234, 2017.

Li, L., Thomsen, D., Wu, C., Priestley, M., Iversen, E. M., Tygesen Skønager, J., Luo, Y., Ehn, M., Roldin, P., Pedersen, H. B., Bilde, M., Glasius, M., and Hallquist, M.: Gas-to-Particle Partitioning of Products from Ozonolysis of $\Delta$3-Carene and the Effect of Temperature and Relative Humidity, The Journal of Physical Chemistry A, 128, 918-928, 10.1021/acs.jpca.3c07316, 2024.

Lopez-Hilfiker, F. D., Mohr, C., Ehn, M., Rubach, F., Kleist, E., Wildt, J., Mentel, T. F., Lutz, A., Hallquist, M., Worsnop, D., and Thornton, J. A.: A novel method for online analysis of gas and particle composition: description and evaluation of a Filter Inlet for Gases and AEROsols (FIGAERO), Atmospheric Measurement Techniques, 7, 983-1001, 10.5194/amt-7-983-2014, 2014.

Peräkylä, O., Riva, M., Heikkinen, L., Quéléver, L., Roldin, P., and Ehn, M.: Experimental investigation into the volatilities of highly oxygenated organic molecules (HOMs), Atmospheric Chemistry and Physics, 20, 649-669, 10.5194/acp-20-649-2020, 2020.

Quéléver, L. L. J., Kristensen, K., Normann Jensen, L., Rosati, B., Teiwes, R., Daellenbach, K. R., Peräkylä, O., Roldin, P., Bossi, R., Pedersen, H. B., Glasius, M., Bilde, M., and Ehn, M.: Effect of temperature on the formation of highly oxygenated organic molecules (HOMs) from alpha-pinene ozonolysis, Atmospheric Chemistry and Physics, 19, 7609-7625, 10.5194/acp-19-7609-2019, 2019.

Riva, M., Rantala, P., Krechmer, J. E., Peräkylä, O., Zhang, Y., Heikkinen, L., Garmash, O., Yan, C., Kulmala, M., Worsnop, D., and Ehn, M.: Evaluating the performance of five different chemical ionization techniques for detecting gaseous oxygenated organic species, Atmospheric Measurement Techniques, 12, 2403-2421, 10.5194/amt-12-2403-2019, 2019.

Thomsen, D., Iversen, E. M., Skønager, J. T., Luo, Y., Li, L., Roldin, P., Priestley, M., Pedersen, H. B., Hallquist, M., and Ehn, M.: The effect of temperature and relative humidity on secondary organic aerosol formation from ozonolysis of $\Delta$3-carene, Environmental Science: Atmospheres, 4, 88-103, 2024.

Tuovinen, S., Kontkanen, J., Cai, R., and Kulmala, M.: Condensation sink of atmospheric vapors: the effect of vapor properties and the resulting uncertainties, Environmental Science: Atmospheres, 1, 543-557, 2021.

Wang, L., Liu, Y., and Wang, L.: Ozonolysis of 3-carene in the atmosphere. Formation mechanism of hydroxyl radical and secondary ozonides, Physical Chemistry Chemical Physics, 21, 8081-8091, 10.1039/c8cp07195k, 2019.